SYNAPTIC VESICLE RECYCLING BY CLATHRIN-MEDIATED ENDOCYTOSIS

by

Mingyu Gu

A dissertation submitted to the faculty of
the University of Utah
in partial fulfillment of the requirements for the degree of

Doctor of Philosophy

Department of Biology

The University of Utah

December 2010

The University of Utah Graduate School

STATEMENT OF DISSERTATION APPROVAL

The dissertation of **Mingyu Gu**

has been approved by the following supervisory committee members:

Erik M. Jorgensen	, Chair	**10/15/2010** Date Approved
Markus Babst	, Member	**10/19/2010** Date Approved
Michael J. Bastiani	, Member	**10/15/2010** Date Approved
A. Villu Maricq	, Member	**10/15/2010** Date Approved
Lawrence M. Okun	, Member	**10/15/2010** Date Approved

and by **Neil J. Vickers** , Chair of the Department of **Biology**

and by Charles A. Wight, Dean of The Graduate School.

ABSTRACT

Synapses are the places where neurons communicate with their targets. At chemical synapses, neurotransmitters are contained in synaptic vesicles and are released into the synaptic cleft upon fusion with the plasma membrane. This event happens at high frequency at synapses and thus synaptic vesicles need to be regenerated locally to prevent vesicle depletion. The popular model for synaptic vesicle endocytosis is to re-sort vesicle proteins left in the plasma membrane into an invaginated vesicle by clathrin-mediated endocytosis. However, some pieces of evidence suggest that clathrin-independent endocytosis might also contribute to synaptic vesicle recycling.

In this dissertation, we present the studies on endocytic accessory proteins from clathrin-mediated endocytosis and focus primarily on their potential roles in neurotransmission by using the genetic model organism *Caenorhabditis elegans*. The proteins investigated include the major adaptor complex AP2, the synaptotagmin adaptor UNC-41 and the membrane bending protein, Epsin. We demonstrate that, one; AP2 is responsible for 70% synaptic vesicle recycling in *C. elegans*. Second, synaptic recycling of synaptotagmin requires UNC-41. Third, Epsin is not required for curvature acquisition in clathrin-mediated endocytosis at synapses. Thus these studies push forward our understanding towards synaptic vesicle recycling at synapses and demonstrate clathrin-mediated endocytosis is likely the major mechanism for synaptic vesicle endocytosis in *C. elegans.*

CONTENTS

LIST OF FIGURES

ACKNOWLEDGEMENTS

I would like to thank people who helped me and supported me during my study in graduate school. Erik Jorgensen for wonderful scientific thoughts, discussion, advice and the great care during my sickness. The entire Jorgensen lab for ideas and the nice working environment. Especially, I would like to thank Kim Schuske, Qiang Liu, Shigeki Watanabe for their direct contribution to my projects. I would also like to thank Wayne Davis, Glen Ernstrom, Robbert Hobson, Michael Ailion, Gunther Hollopeter and Ewa Bednarek for their useful inputs and help. I would like to thank my thesis committee: Mike Bastiani, Markus Babst, Larry Okun and Villu Maricq for their bright suggestions and guidance. At last I would like to thank for my parents Qin, Jinrong and Gu, Huitao for being supportive all the time and my lovely wife Fan.

CHAPTER 1

INTRODUCTION

Neurons communicate with their targets via a specialized structure called the synapse. There are two kinds of synapses: electrical synapses and chemical synapses. At an electrical synapse, a channel that allows electrical charges to flow through connects two cells and the signal is transmitted in the form of electrical currents. At a chemical synapse, neurons release neurotransmitters, such as acetylcholine or glutamate into an extracelluar space called the synaptic cleft. The neurotransmitter diffuses across the cleft and binds its receptor on the plasma membrane of the postsynaptic cell. One kind of receptors is ligand-gated ion channels. Binding with the corresponding neurotransmitter opens the channel, allowing ions to flow through it and across the plasma membrane. This in turn alters the activity of the postsynaptic cell. My research focuses on chemical synapses in *Caenorhabditis elegans*. In this dissertation, synapse refers to the chemical synapse.

At the synapse, there are up to hundreds of membrane-bound organelles called synaptic vesicles. These vesicles are acidified by the vacuolar type H^+-ATPase. The pH gradient can be used to exchange protons for neurotransmitters through neurotransmitter transporters. A synaptic vesicle is always filled with a fixed amount of neurotransmitter. Voltage-gated calcium channels at the plasma membrane control the release of filled

vesicles. Upon calcium influx, the calcium sensor on the synaptic vesicle senses the elevated calcium level at the synapse and then triggers the fusion machinery, SNARE complexes, to form. SNARE complexes are helical bundles formed by t-SNARE from the plasma membrane and v-SNARE from the synaptic vesicle. These helical bundles can bring a synaptic vesicle close to the plasma membrane. Finally fusion occurs and neurotransmitters are released into the synaptic cleft.

Synaptic vesicle release can happen at a very high frequency. After vesicle exocytosis, vesicle numbers are dramatically reduced. To sustain neurotransmission, cells can use two strategies. One, the cell can synthesize vesicle proteins and form new vesicles or vesicle precursors in the soma and then transport them through the axon all the way down to the synapse. However, this process is slow. Synthesizing new proteins takes at least half an hour. Vesicular transport velocity is only a couple micrometers per second, but the length of an axon in humans can reach up to 1 meter; therefore, this *de novo* pathway is necessary but not sufficient to maintain the release of synaptic vesicles at the synapse. The second strategy is to recycle synaptic vesicle locally, called synaptic vesicle endocytosis. When a synaptic vesicle fuses with the plasma membrane, the contents of the vesicle are released into the synaptic cleft and vesicle proteins, such as the V-ATPase and SNAREs, are left in the pre-synaptic plasma membrane. Synaptic vesicle endocytosis retrieves vesicle proteins from the plasma membrane and sorts the proper amount of these proteins into a vesicle-sized vacuole to generate a new vesicle. These recycled vesicles can then load neurotransmitters and once again join the queue for vesicle exocytosis. Compared to the first strategy, recycling is more efficient and is likely the major strategy used at active synapses.

Three potential mechanisms of synaptic vesicle endocytosis

Synaptic vesicle endocytosis is a basic but critical step in neurotransmission. There are three potential mechanisms for a synapse to recycle synaptic vesicles: clathrin-mediated endocytosis, kiss-and-run and bulk endocytosis. The following section will introduce these three mechanisms respectively.

Clathrin-mediated endocytosis

John Heuser and Tom Reese first discovered this mechanism in 1973. They used electron microscopy to visualize frog neuromuscular junction and saw synaptic vesicles with clathrin coats (Heuser and Reese, 1973). The clathrin-mediated endocytosis is required in almost every single cell of a living organism. This endocytosis pathway can be divided into four steps. First transmembrane cargo proteins are enriched at the site of endocytosis. Second, clathrin forms a soccer-ball shaped coat on the invaginated membrane. Third, a GTPase called dynamin pinches off the coated vesicle from the membrane. And last, the clathrin-coat is removed to free the newly formed vesicle. Numerous studies after Heuser have confirmed the importance of clathrin in synaptic vesicle endocytosis. For example, when clathrin is pulled down from rat brain homogenate, synaptic vesicle proteins are co-immunoprecipitated (Maycox et al., 1992). Disrupting other accessory proteins in the same pathway with clathrin, such as dynamin, endophilin or synaptojanin, severely compromises neurotransmission (De Camilli et al., 1995; Verstreken et al., 2002; Verstreken et al., 2003). It is almost certain that clathrin is involved in synaptic vesicle endocytosis. However, it is extremely difficult to completely block clathrin-mediated endocytosis at synapses due to lethality after the elimination of clathrin or other central components in the same pathway. Therefore, new techniques and

further studies are still required in order to fully understand the importance of the clathrin-mediated pathway in neurotransmission.

Kiss-and-run

This model was first proposed in 1973 by B. Ceccareli, who thought synaptic vesicles can release their neurotransmitters by forming a transient fusion pore with the plasma membrane. After releasing, the synaptic vesicle will back off and seal the fusion pore. The vesicle will then wait to be refilled with neurotransmitters for the next round of exocytosis. Throughout this entire process the synaptic vesicle identity is maintained. This is also a completely clathrin-independent mechanism for synaptic vesicle recycling. The existence of kiss-and-run was first observed in mast cells (Spruce et al., 1990) by capacitance measurement. Several different approaches were subsequently used to detect this releasing mechanism, such as amperometry (Alvarez de Toledo et al., 1993), FM dye (Aravanis et al., 2003) and synaptophluorin (Gandhi and Stevens, 2003). From all these studies, a fast endocytosis mode can be detected with the τ about 1 second or less. Because the τ for clathrin dependent endocytosis is more than 10 s (Smith et al., 2008), this fast mode of endocytosis fits the idea of kiss-and-run. However the importance of kiss-and-run may vary between different kinds of synapses. In addition the proteins specifically involved in kiss-and-run are still unknown.

Bulk endocytosis

In this mode of endocytosis, a large portion of plasma membrane is internalized and forms an endosome in the cytoplasm. This mechanism of endocytosis was noted at frog neuromuscular junction under moderate to heavy stimulation protocol (Heuser and

Reese, 1973). This process is thought of as a slow endocytosis and not the major mechanism used by synapses to recycle synaptic vesicles under regular conditions; however, it could function as a compensatory pathway when synapses are under stress. This form of endocytosis may also have an intimate connection with clathrin-mediated endocytosis. First of all, both types of endocytosis may share proteins for membrane bending and vesicle scission. Second, newly formed synaptic vesicles likely bud from this endosomal structure through clathrin-mediated endocytosis (Takei et al., 1996). From these points of view, this endocytosis method helps prevent cell surface expansion at heavily stimulated synapses and also facilitates vesicle biogenesis from an endosomal intermediate, which is probably dependent on a clathrin adaptor complex AP3 (Danglot and Galli, 2007).

Clathrin adaptors and membrane-bending proteins

Of the three models for synaptic vesicle endocytosis, the easiest one to be tested is clathrin-mediated endocytosis, which has basically four steps: clathrin recruitment, membrane invagination, vesicle scission and clathrin uncoating. Clathrin requires help from other proteins to complete this four-step endocytosis; thus, each step of this pathway can be blocked by eliminating the corresponding proteins. My research focuses on the proteins for clathrin recruitment and membrane invagination, which will be introduced in more detail below.

Clathrin adaptors

This group of proteins has two functions: clathrin recruitment and cargo trapping. On its own, clathrin cannot interact with lipids. It relies on its interaction with different

types of clathrin adaptors to localize to various membrane-bound organelles. The organelles have different lipid compositions which attract unique clathrin adaptors. By doing this, clathrin can be specifically recruited to whichever place needs vesicle budding. The other function of the adaptors is to bind with transmembrane cargo proteins. This interaction occurs at the other side of the protein, thus the cargoes are trapped and enriched at the budding place. Of all the clathrin adaptors, one of the most important types is called adaptor protein (AP) complex. There are four AP complexes, AP1-AP4, in mammalian cells and three AP complexes, AP1-3 in *Caenorhabditis elegans* (Robinson, 2004). A common feature of these AP complexes is that they have four different subunits, two large ones, a medium one and a small one. AP2 is the only complex that primarily localizes on the plasma membrane by interacting with PI(4,5)P2 (Gaidarov and Keen, 1999), making it the obvious candidate for clathrin-mediated endocytosis of synaptic vesicles.

The medium subunit of AP2 is called μ2 adaptin and its major function is to recruit cargoes into clathrin-coated pits (Owen and Evans, 1998). Knocking-out μ2 in mice causes embryonic lethality (Mitsunari et al., 2005), but in *C. elegans* μ2 adaptin mutants can survive until adulthood. The corresponding gene in the worm is named *apm-2*. In Chapter 2, we investigate the function of μ2 in synaptic vesicle recycling. We found that in the absence of μ2, there is a 40% reduction in synaptic vesicles and that the motility of the mutant animal is close to wild type after skin-specific rescue. Therefore we concluded that μ2 facilitates but is not absolutely required for synaptic vesicle endocytosis.

Based on our previous study on μ2 adaptin, we realized that AP2 function is

probably not completely eliminated in *apm-2* mutants, so we aimed at knocking out the entire AP2 in order to fully understand its function in synaptic vesicle endocytosis. One of the big subunits of AP2 is called α adaptin. Its functions are binding with PI(4,5)P2 and interacting with other accessory proteins in clathrin-mediated endocytosis (Owen et al., 1999; Traub et al., 1999). In *C. elegans,* the gene name of α adaptin is *apa-2*. We conducted a noncomplementation screen and isolated a null allele of this gene. In Chapter 3 we discuss our investigation of the role of α adaptin in synaptic vesicle endocytosis. We found that *apa-2* mutants have a 50% reduction in synaptic vesicle and nearly wild-type motility. We further built *apm-2 apa-2* double mutants. In this case the mutations are almost lethal with survival rate of about 10%. The double mutant has 30% of the normal amount of synaptic vesicles and is more impaired for movement than the *apa-2* mutant. However, skin-rescued double mutants can still move fairly well. Based on these results we concluded that AP2 contributes to the majority of synaptic vesicle recycling at *C. elegans* motor-neuron synapses. But AP2-independent endocytosis, either clathrin dependent or not, exists to support neurotransmission in the absence of AP2.

Neuronal-specific clathrin adaptors

Synaptic vesicle endocytosis is a specialized endocytic event and neurons have evolved some neuronal-specific adaptors to assist clathrin for synaptic vesicle endocytosis. Two of these adaptors have been characterized, AP180 and stonin2. AP180 is the adaptor for a SNARE protein, synaptobrevin (Nonet et al., 1999) and is also involved in regulating the size of synaptic vesicles (Zhang et al., 1998). Stonin2 has been identified as the adaptor for another vesicle protein, synaptotagmin I, in *Drosophila* and mammals (Fergestad and Broadie, 2001; Fergestad et al., 1999; Jung et al., 2007). In

Chapter 4 we discuss our characterization of the orthologue of stonin2 in *C. elegans*, *unc-41*. We found UNC-41 is also required for recruiting synaptotagmin I at synapses in *C. elegans.* The synaptotagmin-binding motif in UNC-41 is essential for UNC-41 synaptic localization. UNC-41 also has a μ- homologous domain at its C-terminus that is similar to the signal-binding domain of the μ adaptins. We studied the potential functional redundancy between UNC-41 and APM-2 in synaptic vesicle endocytosis by ultrastructural analysis. We found that UNC-41 and APM-2 do not function redundantly but rather in the same pathway.

Membrane-bending proteins

Vesicle invagination during clathrin-mediated endocytosis is accomplished by a highly organized protein-protein network. Clathrin is most likely acting to maintain the shape of invaginated vesicles by forming a clathrin coat at the surface. But how is the membrane curvature generated at the beginning? And how does the cell sense that curvature to know the proper time for terminating vesicle growth? These functions are accomplished by N-BAR and ENTH domain proteins. Both types of proteins have the ability to generate membrane curvature by inserting an amphipathic N-terminal helix into the cytosolic leaflet of the lipid bilayer (Itoh and De Camilli, 2006). The representative N-BAR domain protein is amphiphysin. Its N-BAR domain can generate and sense the curvature at the neck of the invaginated membrane. The middle portion of the protein contains the clathrin and AP2 binding sites (Slepnev et al., 2000). Finally the C-terminal SH3 domain binds dynamin and synaptojanin for vesicle scission and clathrin uncoating (David et al., 1996; McPherson et al., 1996). Thus amphiphysin probably functions at the end of clathrin-mediated endocytosis by coupling the scission neck formation with

vesicle release. The representative ENTH domain protein is epsin. It has an ENTH domain at its N-terminus, which can bind PI(4,5)P2 and cause membrane invagination in a similar way as amphiphysin (Itoh and De Camilli, 2006). The rest of the protein contains clathrin, AP2, eps15 and ubiquitin binding sites (Chen et al., 1998; Polo et al., 2002; Rosenthal et al., 1999). Epsin was shown to be essential for clathrin to generate invaginated pits on a lipid monolayer (Ford et al., 2002); thus it was proposed that Epsin functions at the beginning of clathrin-mediated endocytosis for curvature acquisition. In Chapter 5, we characterize a deletion allele of *epn-1*, the orthologue of epsin in *C. elegans*. In the absence of EPN-1, worms are embryonic lethal suggesting a broad requirement for this protein for worm viability. To study the potential role of EPN-1 in synaptic vesicle endocytosis, we first examined the expression pattern of *epn-1* by tagging the protein with a fluorescent marker, GFP. We found that *epn-1* is expressed in almost every tissue. However, to our surprise, when EPN-1 is expressed exclusively in neurons, the protein does not localize to synapses. This is a piece of strong evidence that EPN-1 is not required for synaptic vesicle endocytosis, but further characterization of this protein in other types of endocytosis should still be interesting.

Dissertation outline and summary

This dissertation summarizes all of my graduate work on the importance of clathrin-mediated endocytosis for synaptic vesicle recycling in the nematode, *Caenorhabditis elegans.* To block clathrin-mediated endocytosis, I removed pathway components such as clathrin adaptors and membrane bending proteins. Each chapter of this dissertation details the findings for a particular component. Chapter 2 presents a published paper about the function of μ2 adaptin in synaptic vesicle endocytosis. Chapter

3 discusses the endocytic defects of α adaptin and AP2 deficient synapses. Chapter 4 contains the study of *C. elegans* stonin-2 and its relationship with synaptotagmin recycling at synapses. The final chapter is the preliminary characterization of an ENTH-domain protein, Epsin, in clathrin-mediated endocytosis.

References

Alvarez de Toledo, G., R. Fernandez-Chacon, and J.M. Fernandez. 1993. Release of secretory products during transient vesicle fusion. *Nature*. 363:554-8.

Aravanis, A.M., J.L. Pyle, and R.W. Tsien. 2003. Single synaptic vesicles fusing transiently and successively without loss of identity. *Nature*. 423:643-7.

Chen, H., S. Fre, V.I. Slepnev, M.R. Capua, K. Takei, M.H. Butler, P.P. Di Fiore, and P. De Camilli. 1998. Epsin is an EH-domain-binding protein implicated in clathrin-mediated endocytosis. *Nature*. 394:793-7.

Danglot, L., and T. Galli. 2007. What is the function of neuronal AP-3? *Biol Cell*. 99:349-61.

David, C., P.S. McPherson, O. Mundigl, and P. de Camilli. 1996. A role of amphiphysin in synaptic vesicle endocytosis suggested by its binding to dynamin in nerve terminals. *Proc Natl Acad Sci U S A*. 93:331-5.

De Camilli, P., K. Takei, and P.S. McPherson. 1995. The function of dynamin in endocytosis. *Curr Opin Neurobiol*. 5:559-65.

Fergestad, T., and K. Broadie. 2001. Interaction of stoned and synaptotagmin in synaptic vesicle endocytosis. *J Neurosci*. 21:1218-27.

Fergestad, T., W.S. Davis, and K. Broadie. 1999. The stoned proteins regulate synaptic vesicle recycling in the presynaptic terminal. *J Neurosci*. 19:5847-60.

Ford, M.G., I.G. Mills, B.J. Peter, Y. Vallis, G.J. Praefcke, P.R. Evans, and H.T. McMahon. 2002. Curvature of clathrin-coated pits driven by epsin. *Nature*. 419:361-6.

Gaidarov, I., and J.H. Keen. 1999. Phosphoinositide-AP-2 interactions required for targeting to plasma membrane clathrin-coated pits. *J Cell Biol*. 146:755-64.

Gandhi, S.P., and C.F. Stevens. 2003. Three modes of synaptic vesicular recycling revealed by single-vesicle imaging. *Nature*. 423:607-13.

Heuser, J.E., and T.S. Reese. 1973. Evidence for recycling of synaptic vesicle membrane during transmitter release at the frog neuromuscular junction. *J Cell Biol*. 57:315-44.

Itoh, T., and P. De Camilli. 2006. BAR, F-BAR (EFC) and ENTH/ANTH domains in the regulation of membrane-cytosol interfaces and membrane curvature. *Biochim Biophys Acta*. 1761:897-912.

Jung, N., M. Wienisch, M. Gu, J.B. Rand, S.L. Muller, G. Krause, E.M. Jorgensen, J. Klingauf, and V. Haucke. 2007. Molecular basis of synaptic vesicle cargo recognition by the endocytic sorting adaptor stonin 2. *J Cell Biol*. 179:1497-510.

Maycox, P.R., E. Link, A. Reetz, S.A. Morris, and R. Jahn. 1992. Clathrin-coated vesicles in nervous tissue are involved primarily in synaptic vesicle recycling. *J Cell Biol*. 118:1379-88.

McPherson, P.S., E.P. Garcia, V.I. Slepnev, C. David, X. Zhang, D. Grabs, W.S. Sossin, R. Bauerfeind, Y. Nemoto, and P. De Camilli. 1996. A presynaptic inositol-5-phosphatase. *Nature*. 379:353-7.

Mitsunari, T., F. Nakatsu, N. Shioda, P.E. Love, A. Grinberg, J.S. Bonifacino, and H. Ohno. 2005. Clathrin adaptor AP-2 is essential for early embryonal development. *Mol Cell Biol*. 25:9318-23.

Nonet, M.L., A.M. Holgado, F. Brewer, C.J. Serpe, B.A. Norbeck, J. Holleran, L. Wei, E. Hartwieg, E.M. Jorgensen, and A. Alfonso. 1999. UNC-11, a Caenorhabditis elegans AP180 homologue, regulates the size and protein composition of synaptic vesicles. *Mol Biol Cell*. 10:2343-60.

Owen, D.J., and P.R. Evans. 1998. A structural explanation for the recognition of tyrosine-based endocytotic signals. *Science*. 282:1327-32.

Owen, D.J., Y. Vallis, M.E. Noble, J.B. Hunter, T.R. Dafforn, P.R. Evans, and H.T. McMahon. 1999. A structural explanation for the binding of multiple ligands by the alpha-adaptin appendage domain. *Cell*. 97:805-15.

Polo, S., S. Sigismund, M. Faretta, M. Guidi, M.R. Capua, G. Bossi, H. Chen, P. De Camilli, and P.P. Di Fiore. 2002. A single motif responsible for ubiquitin recognition and monoubiquitination in endocytic proteins. *Nature*. 416:451-5.

Robinson, M.S. 2004. Adaptable adaptors for coated vesicles. *Trends Cell Biol*. 14:167-74.

Rosenthal, J.A., H. Chen, V.I. Slepnev, L. Pellegrini, A.E. Salcini, P.P. Di Fiore, and P. De Camilli. 1999. The epsins define a family of proteins that interact with components of the clathrin coat and contain a new protein module. *J Biol Chem*.

274:33959-65.

Slepnev, V.I., G.C. Ochoa, M.H. Butler, and P. De Camilli. 2000. Tandem arrangement of the clathrin and AP-2 binding domains in amphiphysin 1 and disruption of clathrin coat function by amphiphysin fragments comprising these sites. *J Biol Chem*. 275:17583-9.

Smith, S.M., R. Renden, and H. von Gersdorff. 2008. Synaptic vesicle endocytosis: fast and slow modes of membrane retrieval. *Trends Neurosci*. 31:559-68.

Spruce, A.E., L.J. Breckenridge, A.K. Lee, and W. Almers. 1990. Properties of the fusion pore that forms during exocytosis of a mast cell secretory vesicle. *Neuron*. 4:643-54.

Takei, K., O. Mundigl, L. Daniell, and P. De Camilli. 1996. The synaptic vesicle cycle: a single vesicle budding step involving clathrin and dynamin. *J Cell Biol*. 133:1237-50.

Traub, L.M., M.A. Downs, J.L. Westrich, and D.H. Fremont. 1999. Crystal structure of the alpha appendage of AP-2 reveals a recruitment platform for clathrin-coat assembly. *Proc Natl Acad Sci U S A*. 96:8907-12.

Verstreken, P., O. Kjaerulff, T.E. Lloyd, R. Atkinson, Y. Zhou, I.A. Meinertzhagen, and H.J. Bellen. 2002. Endophilin mutations block clathrin-mediated endocytosis but not neurotransmitter release. *Cell*. 109:101-12.

Verstreken, P., T.W. Koh, K.L. Schulze, R.G. Zhai, P.R. Hiesinger, Y. Zhou, S.Q. Mehta, Y. Cao, J. Roos, and H.J. Bellen. 2003. Synaptojanin is recruited by endophilin to promote synaptic vesicle uncoating. *Neuron*. 40:733-48.

Zhang, B., Y.H. Koh, R.B. Beckstead, V. Budnik, B. Ganetzky, and H.J. Bellen. 1998. Synaptic vesicle size and number are regulated by a clathrin adaptor protein required for endocytosis. *Neuron*. 21:1465-75.

CHAPTER 2

μ2 ADAPTIN FACILITATES BUT IS NOT ESSENTIAL FOR SYNAPTIC VESICLE RECYCLING IN *CAENORHABDITIS ELEGANS*

Reprinted with permission from the Rockefeller University Press

Gu et al., 2008. Originally published in *Journal of Cell Biology.* VOL.185: 881-897

My contribution to this work including the following:

1. Outcrossing mutant alleles of *apm-2*, which encodes the orthologue of μ2 adaptin in *C. elegans.*
2. Cuticle defect analysis of *apm-2* mutants.
3. Investigating the expression pattern of *apm-2*.
4. Investigating the pre-synaptic localization of APM-2.
5. Examining the distribution of vesicle proteins in the dorsal nerve cord from *apm-2* mutants.
6. Tissue-specific rescue of *apm-2* mutants.
7. Aldicarb assay on *apm-2* mutants and tissue-specific rescued animals.
8. Thrashing assay on *apm-2* mutants and tissue-specific rescued animals.

Paul Baum (University of California, San Francisco) contributed to the following:
Isolating and characterizing *apm-2* alleles.

Shigeki Watanabe (University of Utah, Salt Lake City) contributed to the following:
Characterizing *apm-2* mutants and tissue-specific rescued animals by electron microscopy.

Qiang Liu (University of Utah, Salt Lake City) contributed to the following:
Characterizing *apm-2* mutants and tissue-specific rescued animals by electrophysiology.

Published December 1, 2008

JCB: ARTICLE

THE JOURNAL OF CELL BIOLOGY

μ2 adaptin facilitates but is not essential for synaptic vesicle recycling in *Caenorhabditis elegans*

Mingyu Gu,[1] Kim Schuske,[1] Shigeki Watanabe,[1] Qiang Liu,[1] Paul Baum,[2,3] Gian Garriga,[2] and Erik M. Jorgensen[1]

[1]Howard Hughes Medical Institute and Department of Biology, University of Utah, Salt Lake City, UT 84112
[2]Department of Molecular and Cell Biology, Helen Wills Neuroscience Institute, University of California, Berkeley, Berkeley, CA 94720
[3]Division of Experimental Medicine, Department of Medicine, San Francisco General Hospital, University of California, San Francisco, San Francisco, CA 94110

Synaptic vesicles must be recycled to sustain neurotransmission, in large part via clathrin-mediated endocytosis. Clathrin is recruited to endocytic sites on the plasma membrane by the AP2 adaptor complex. The medium subunit (μ2) of AP2 binds to cargo proteins and phosphatidylinositol-4,5-bisphosphate on the cell surface. Here, we characterize the *apm-2* gene (also called *dpy-23*), which encodes the only μ2 subunit in the nematode *Caenorhabditis elegans*. APM-2 is highly expressed in the nervous system and is localized to synapses; yet specific loss of APM-2 in neurons does not affect locomotion. In *apm-2* mutants, clathrin is mislocalized at synapses, and synaptic vesicle numbers and evoked responses are reduced to 60 and 65%, respectively. Collectively, these data suggest AP2 μ2 facilitates but is not essential for synaptic vesicle recycling.

Introduction

After synaptic vesicle fusion, vesicle proteins are retrieved from the plasma membrane and recycled into new synaptic vesicles to sustain neuronal transmission. Recycling is thought to be initiated by the recruitment of clathrin to patches of membrane containing synaptic vesicle proteins. The reformed vesicle with a geodesic coat is budded into the cytoplasm. This model is supported by extensive associative and functional evidence. In electron micrographs of the frog neuromuscular junction, invaginating vesicles at presynaptic terminals are enveloped by a coat (Heuser and Reese, 1973). Purification of vesicles from rat brain indicate that clathrin is associated with synaptic vesicle proteins (Maycox et al., 1992). Genetic disruption of clathrin-associated endocytic proteins such as AP180, synaptojanin, dynamin, and endophilin leads to a depletion of synaptic vesicles (De Camilli et al., 1995; Nonet et al., 1999; Harris et al., 2000; Verstreken et al., 2002, 2003; Schuske et al., 2003; Newton et al., 2006). Finally, specific disruption of clathrin interactions with the adaptor protein AP180 disrupts synaptic vesicle recycling (Augustine et al., 2006; Granseth et al., 2006). These data suggest that clathrin-mediated endocytosis is the main mechanism used by synapses to recycle vesicles after exocytosis.

Clathrin is linked to cargo and membranes by the clathrin adaptor complex (Keen, 1987). Four different adaptor omplexes have been identified in mammals: AP1, AP2, AP3, and AP4 (Keen, 1987; Simpson et al., 1997; Dell'Angelica et al., 1999). These adaptor protein complexes localize to different membranes in the cell and coordinate cargo selection and vesicle biogenesis (Lewin and Mellman, 1998; Robinson and Bonifacino, 2001; Robinson, 2004). AP2 is the adaptor complex functioning during endocytosis at the plasma membrane (Mahaffey et al., 1990; Traub, 2003). There are four different subunits in the AP2 complex: α (large), β2 (large), μ2 (medium), and σ2 (small; Matsui and Kirchhausen, 1990), and each subunit serves a specific function. In particular, the μ2 subunit recruits cargo proteins containing the tyrosine-based Yxxϕ motif (Owen and Evans, 1998) and mediates in part the association of the AP2 complex to membranes (Gaidarov and Keen, 1999; Rohde et al., 2002; Honing et al., 2005).

Here, we characterize mutants that lack μ2 adaptin, encoded by the *apm-2* gene (also called *dpy-23*), in the nematode *Caenorhabditis elegans*. We demonstrate that μ2 is partially required for synaptic localization of clathrin and for the stability of the AP2 complex. However, synaptic vesicles are still recycled in the absence of μ2. Our data suggest that despite previous predictions, μ2 is not absolutely required for synaptic vesicle endocytosis. Moreover, the decrease in synaptic vesicle number

Correspondence to Erik M. Jorgensen: jorgensen@biology.utah.edu

Abbreviations used in this paper: CHC, clathrin heavy chain; ePSC, evoked postsynaptic current; mPSC, miniature postsynaptic current; ORF, open reading frame.

The online version of this article contains supplemental material.

Supplemental Material can be found at:
http://jcb.rupress.org/content/suppl/2008/11/25/jcb.200806088.DC1.html

The Rockefeller University Press $30.00
J. Cell Biol. Vol. 183 No. 5 881–892
www.jcb.org/cgi/doi/10.1083/jcb.200806088

Published December 1, 2008

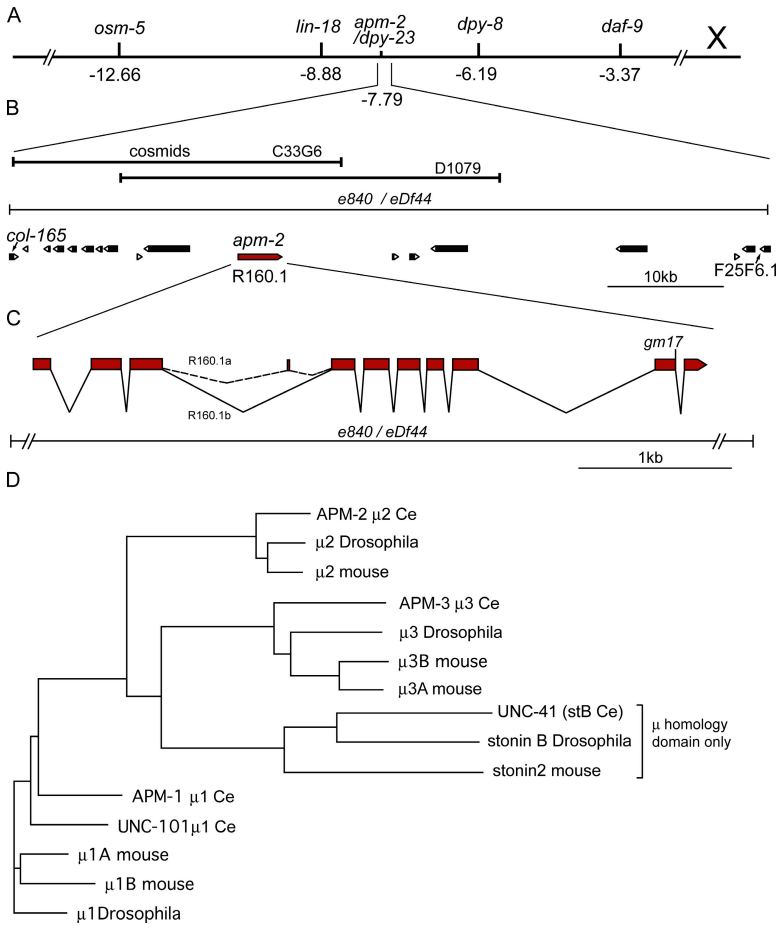

Figure 1. ***apm-2* cloning.** (A) Genetic map position of *apm-2* on chromosome X. (B) Either of two overlapping cosmids, C33G6 and D1079, rescue *apm-2(gm17)*. Below, the mutation *e840* (also called *eDf44*) is a deletion of 100 kb that removes 18 ORFs from *col-165* to F25F6.1. (C) Genomic structure of *apm-2* gene. The *e840* allele deletes the entire ORF; *gm17* is a G to A transition at the donor site of the last intron. The splice form R160.1a (Lee et al., 1994) includes an exon encoding six amino acids. This splice form is not essential because it is not required for rescue of *apm-2* mutant phenotypes (see Fig. 6 B) and is also not conserved in other species. (D) Phylogenetic tree of μ subunits from mouse, *Drosophila*, and *C. elegans*. For stonin B, only the μ homology domains were used in the alignment. See Materials and methods for accession numbers.

does not cause a locomotion defect in μ2 knockout mutants, so a smaller reserve pool might be adequate for *C. elegans* under normal condition.

Results

dpy-23/apm-2 encodes μ2 adaptin in *C. elegans*

Two mutant alleles for the locus *dpy-23 (e840* and *gm17*) have been identified. Both mutants have a variable dumpy (Dpy) phenotype in which animals vary from almost wild-type length to approximately half the size (Fig. S1 A, available at http://www.jcb.org/cgi/content/full/jcb.200806088/DC1). The dumpy phenotype is likely caused by defects in cuticle morphology. Specific defects in the cuticle are observed in the head and along the body. About 5% of the animals have "jowls" or protrusions on either side of the head (Fig. S1 B). The cuticular ridges along the body, called alae, are distorted and have multiple breaks along their length (Fig. S1 C). In addition, mutant worms are slightly uncoordinated (Unc) and have a strong egg-laying defect suggesting a role for *dpy-23* in the nervous system.

The *dpy-23* mutant phenotype was mapped to the interval between –7.91 to –7.55 on chromosome X (Fig. 1 A). The gene encoding μ2 adaptin, called *apm-2*, maps to this interval, and RNA interference to this gene gave rise to a variable dumpy phenotype suggesting *dpy-23* is likely to encode μ2 (Grant and Hirsh, 1999). We cloned the *dpy-23* gene and demonstrated that the mutated gene is *apm-2*. Two overlapping cosmids, D1079 and C33G6, in the region rescued the *dpy-23* mutant phenotype. A 12-kb genomic PCR fragment (5 kb upstream, 5 kb coding sequence of μ2 adaptin, and 2 kb downstream) could fully rescue the dumpy, uncoordinated, and egg-laying defects of *dpy-23(e840)* and *dpy-23(gm17)* (Fig. S1 A). Interestingly, overexpression of *dpy-23* in a wild-type background causes the same phenotypes as *dpy-23* loss-of-function mutations (Fig. S1 A). Because *dpy-23* encodes μ2 we will refer to the gene by its alternative name, *apm-2* (adaptor protein medium subunit 2), throughout the remainder of the manuscript.

apm-2 encodes the only μ2 subunit in *C. elegans* (Fig. 1 D). It is somewhat surprising that disruption of the single μ2 subunit in the worm gives rise to a viable animal. To determine whether μ2 adaptin is completely disrupted in the mutants, the lesions were identified. Genomic Southern analysis showed that *apm-2(e840)*

Published December 1, 2008

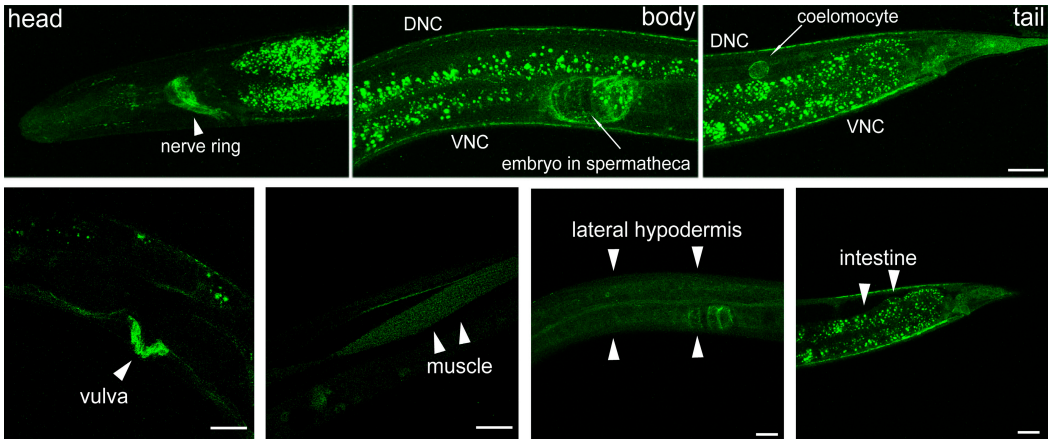

Figure 2. **APM-2 is expressed ubiquitously.** The expression pattern of translational fusion protein APM-2::GFP (Fig. S4, pMG4, available at http://www.jcb.org/cgi/content/full/jcb.200806088/DC1) in young adult hermaphrodites. Worms are oriented anterior left and dorsal up. The image of the muscle is from the transcriptional fusion of GFP driven by the *apm-2* promoter (Fig. S4, pMG3) in a young adult hermaphrodite. Muscle expression was not observed using GFP-tagged μ2, perhaps because of faint expression or synaptic localization, which overlaps strong APM-2 expression in the presynaptic terminals. The vulva and muscle expression figures are single-slice confocal images. The rest of the images are z-stack projections through the whole worm or the tissues of interest. The contrast for the image of the vulva was increased to show the outline of the worm. Bars, 20 μm. DNC, dorsal nerve cord; VNC, ventral nerve cord.

contains a deletion of ~100 kb that includes the entire coding sequence of μ2 adaptin. To identify the endpoints of the deletion, individual open reading frames (ORFs) were PCR amplified from *apm-2(e840)* mutant DNA and it was found that the deletion removes 17 additional ORFs from *col-165* to F25F6.1 (Fig. 1 B). *apm-2(gm17)* was found to contain a G to A point mutation in the splice donor site of the last intron (Fig. 1 C). Failure to splice at this intron would introduce a stop codon 27 nt downstream of the splice junction. If translated, 9 amino acids encoded by the intron would replace the 40 amino acids at the C terminus comprising β strands 15, 16, and 17. β16 has been shown to be critical for binding cargo containing the YXXϕ motif (Ohno et al., 1995; Owen and Evans, 1998). Although *apm-2(gm17)* appears to have a slightly dominant phenotype, the recessive phenotypes of *apm-2(e840)* and *apm-2(gm17)* are virtually identical, suggesting that *gm17* fully disrupts μ2 function.

μ2 is thought to be a critical component of the AP2 complex and should therefore be present in all tissues. To determine where μ2 is expressed, a construct fusing GFP to the APM-2 protein was expressed under the control of the endogenous *apm-2* promoter (Fig. S4, pMG4, available at http://www.jcb.org/cgi/content/full/jcb.200806088/DC1). Because the N terminus of μ2 adaptin is involved in assembly of the AP2 complex (Aguilar et al., 1997; Collins et al., 2002), GFP was fused to the C terminus of the APM-2 protein. The APM-2::GFP fusion protein fully rescues *apm-2* mutant phenotypes, suggesting the tagged protein is functional and is expressed in tissues that require μ2 function. Fluorescence is observed in the nervous system, coelomocyte, spermatheca, and vulva (Fig. 2). In addition, weaker expression is observed in the intestine and the hypodermis. Although fluorescence is not detected in body muscles of animals expressing the tagged protein, muscle expression is observed in animals expressing a transcriptional reporter (Fig. 2 and Fig. S4, pMG3). Thus, *apm-2* is expressed in all tissues examined, which confirms and extends a previous paper claiming that *apm-2* is expressed in neurons and some hypodermal cells (Shim and Lee, 2000).

μ2 is not essential for synaptic vesicle recycling in *C. elegans*

AP2 is thought to recruit synaptic vesicle proteins and clathrin to the endocytic zone. If μ2 is required for synaptic vesicle recycling, then several predictions can be made. First, μ2 should be localized to synapses. Second, μ2 should contribute to clathrin localization at the synapse. Third, the focus of the uncoordinated phenotype should be the nervous system. Fourth, *apm-2* mutants will have a depletion of synaptic vesicles as assayed by electron microscopy. Fifth, *apm-2* mutants will have impaired synaptic transmission as assayed by electrophysiology because of an inability to recycle vesicles.

Because *apm-2* is expressed in virtually all tissues, it is not possible to assay synaptic localization with the rescuing GFP construct, the fluorescence signal is simply too high. To look at a small subset of neurons, the *apm-2* cDNA (R160.1b) was placed under the control of a GABA neuron–specific promoter and GFP was fused at the C terminus. APM-2::GFP is localized at synapses and colocalizes with the synaptic vesicle protein synaptobrevin/VAMP (Fig. 3 A). In addition, APM-2::GFP colocalizes with C-terminal RFP-tagged clathrin heavy chain (CHC) at the synapse (Fig. 3 B). Interestingly, synaptic localization of APM-2::GFP is not dependent on AP180 (*unc-11*), synaptojanin (*unc-26*), synaptotagmin (*snt-1*), or stonin (*unc-41*) (Fig. S2 A, available at http://www.jcb.org/cgi/content/full/jcb.200806088/DC1). These data indicate that μ2 associates with synaptic varicosities as predicted, but this localization is independent of other endocytosis proteins.

Published December 1, 2008

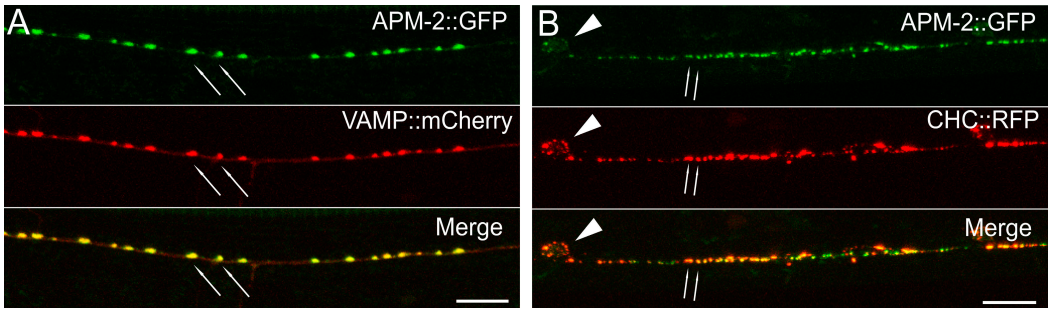

Figure 3. **APM-2 colocalizes with synaptic proteins and clathrin.** Young adult hermaphrodites were used for imaging. (A) APM-2 is localized to synapses. (top) GFP-tagged APM-2 in the GABA neuron processes in the dorsal nerve cord. (middle) mCherry-tagged synaptobrevin in the GABA neuron processes in the dorsal nerve cord. Synaptobrevin is localized to synaptic regions. The fluorescent puncta corresponds to synaptic varicosities along the dorsal muscles (arrows). (bottom) Merged image demonstrates that APM-2::GFP colocalizes with synaptobrevin at synapses. (B) APM-2 is colocalized with CHC. (top) GFP-tagged APM-2 in the GABA neuron processes in the ventral nerve cord. (middle) RFP-tagged CHC-1 in the GABA neuron processes in the ventral nerve cord. CHC is localized to both synaptic regions (arrows) and GABA neuron cell bodies (arrowhead). (bottom) Merged image demonstrates that APM-2::GFP colocalizes with CHC at synapses. Images are confocal z-stack projections through the worm nerve cord. Bars, 10 µm.

Clathrin interacts with AP2 via the appendage domain of the β2 subunit (Dell'Angelica et al., 1998). Thus, if *apm-2* mutations disrupt AP2 function, then it is possible that clathrin localization at the synapse should be altered. We analyzed the distribution of N-terminal GFP-tagged clathrin (GFP::CHC) in the dorsal and ventral nerve cords of GABA neurons in *apm-2* mutants. In the dorsal cord of *apm-2* mutants clathrin is diffuse compared with the wild type (Fig. 4; percentage of animals scored with diffuse clathrin in the dorsal cord: in the wild type, 31%, $n = 29$; in *dpy-23(e840)*, 80%, $n = 15$, $P < 0.01$; in *dpy-23(gm17)*, 70%, $n = 30$, $P < 0.01$). However, in the ventral nerve cord clathrin distribution is punctate, similar to wild-type animals (Fig. S2 B). It is possible clathrin localization near cell bodies in the ventral nerve cord is caused by AP1 function at the Golgi apparatus. Clathrin is still localized at dorsal synapses in 20–30% of the mutant animals; perhaps by other clathrin-binding proteins such as AP180, epsin, or amphiphysin. Thus, µ2 contributes to, but is not essential for, clathrin synaptic localization.

Defects in synaptic vesicle endocytosis cause the mislocalization of synaptic vesicle proteins. For example, in the absence of the endocytosis proteins, such as AP180 (Nonet et al., 1999), synaptojanin, and endophilin (Schuske et al., 2003), synaptic vesicle proteins are diffuse along the axon instead of clustering at synaptic varicosities. In contrast, the vesicle proteins synaptobrevin, synaptogyrin, and synaptotagmin are localized properly in the dorsal and lateral nerve cords of *apm-2* mutants (Fig. 4). These results suggest that µ2, unlike other endocytosis proteins, is not required to maintain vesicle proteins at the synapse.

Mutants with defects in synaptic vesicle endocytosis exhibit reduced synaptic transmission and are uncoordinated (Nonet et al., 1999; Harris et al., 2000; Schuske et al., 2003). *apm-2* mutants are also uncoordinated but the uncoordinated phenotype arises from defects in the hypodermis rather than the nervous system. When APM-2::GFP is expressed under the control of a ubiquitous promoter the tagged µ2 protein rescues all *apm-2(e840)* mutant phenotypes (Fig. 5, A and B). When µ2 protein is expressed under a pan-neuronal promoter, the *apm-2* mutants are still dumpy, uncoordinated, and egg-laying defective, effectively looking the same as the original *apm-2(e840)* mutants. In contrast, when µ2 protein is expressed under a hypodermal promoter, the *apm-2(e840)* transgenic animals are

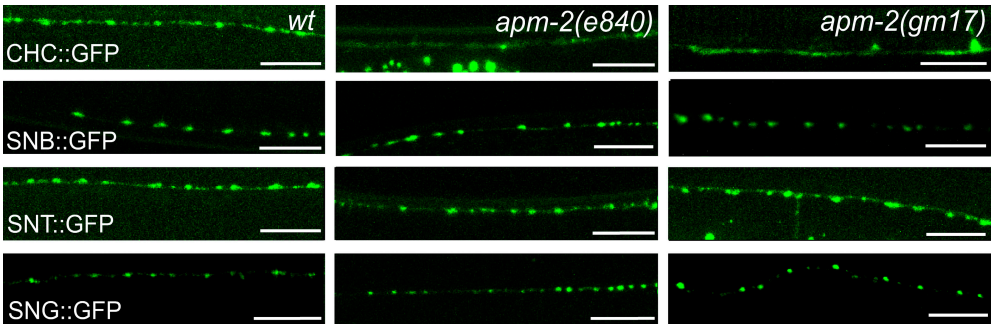

Figure 4. **Clathrin but not synaptic vesicle proteins are mislocalized in *apm-2* mutants.** For CHC, synaptobrevin (SNB), and synaptotagmin (SNT), GFP-tagged proteins were expressed in the GABA neurons and imaged in the dorsal nerve cord. Presynaptic varicosities of neuromuscular junctions along the dorsal nerve cord of an adult hermaphrodite are visible as fluorescent puncta. For synaptogyrin (SNG), GFP-tagged protein is expressed in all neurons under its own promoter and imaged in the lateral cord. Images are confocal z-stack projections through the worm nerve cord. Bars, 10 µm.

Published December 1, 2008

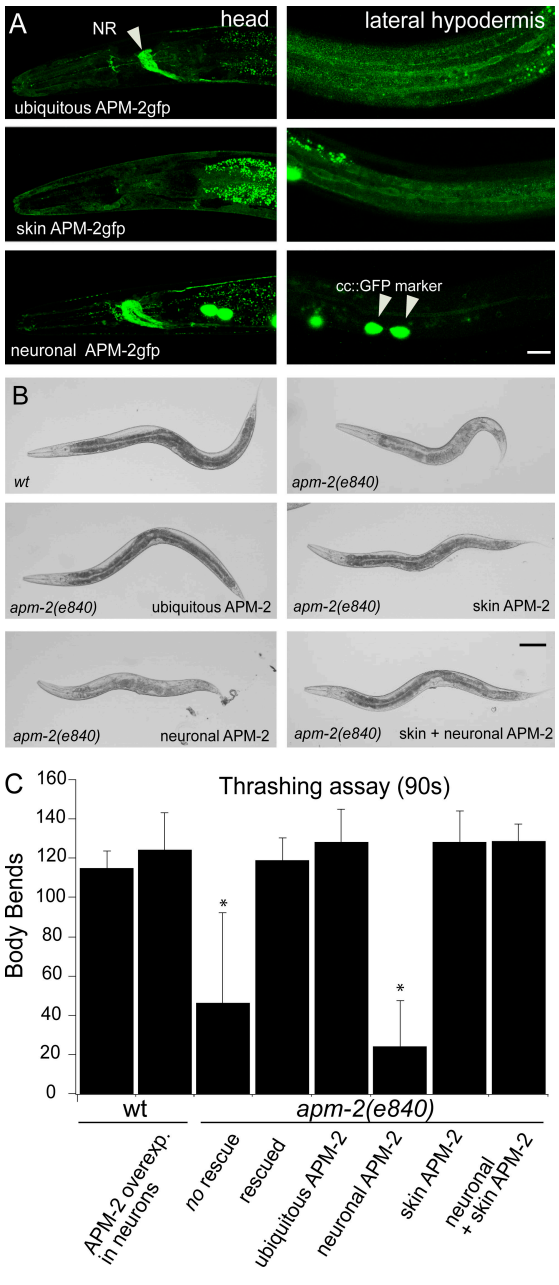

Figure 5. ***apm-2(e840)* tissue-specific rescue.** (A) APM-2::GFP expression pattern under different promoters. Ubiquitous expression is driven by the *dpy-30* promoter, hypodermal expression (skin) is driven by the *pdi-2* promoter, and neuronal expression is driven by the *rab-3* promoter (Fig S4, pMG10, pMG8, and pMG9, respectively; available at http://www.jcb.org/cgi/content/full/jcb.200806088/DC1). Worms are oriented anterior left and dorsal up. Images are confocal z-stack projections through the whole worm or the tissue of interest. All worms were imaged under identical conditions; the contrast for skin APM-2gfp panel was increased to show skin-specific expression. NR, nerve ring. Bar, 20 µm. (B) Expression of APM-2 in the skin rescues the dumpy phenotype. See Materials and methods for full genotypes. The injection concentration of *apm-2::GFP* DNA is at 1 ng/µl in all genotypes. Bar, 100 µm. (C) Thrashing assay. Expression of APM-2 in the skin rescues the locomotory phenotype. Worms were placed in buffer and body bends were counted for 90 s. Overexpression of APM-2::GFP in the nervous system (EG4017) does not create a dominant-negative phenotype (*, $P < 0.01$.). Expression of APM-2 under its own promoter (EG1616), a ubiquitous promoter (EG4015), or a skin promoter (EG4029 and EG4030) rescues thrashing. Expression of APM-2 in neurons alone does not rescue thrashing (EG4213). The data are presented as mean ± SD.

not dumpy (Fig. 5 B, skin APM-2); moreover, the jerky uncoordinated phenotype is also rescued. Previous studies have demonstrated that the µ2 functions in the skin rescue developmental defects in the nervous system (Pan et al., 2008); our data suggest that these nonautonomous defects might extend to development or function of motor neurons as well. However, skin-rescued animals are egg-laying defective and the body bends are increased in amplitude, suggesting neuronal function is somewhat altered. To quantify locomotion in the mosaic strains, animals were placed in a drop of liquid and body bends were counted for 90 s for each strain (Fig. 5 C). Thrashing rates of the hypodermal rescued strains are the same as in the wild type; whereas neuronal expression of µ2 does not rescue thrashing. The reduced thrashing is not due to a dominant-negative effect because overexpression of µ2 in the neurons does not impair locomotion in the wild type. Collectively, these data suggest the uncoordinated phenotype of *apm-2* mutants is almost exclusively caused by hypodermal defects rather than defects in the nervous system.

To directly visualize synaptic vesicles, we characterized *apm-2* mutant synapses using electron microscopy. In AP180 mutants the diameter of synaptic vesicles is increased, implicating a role for this adaptin in the control of the diameter of the reforming vesicles (Zhang et al., 1998; Nonet et al., 1999). In *apm-2(e840)* mutants, however, the diameters of synaptic vesicles are the same as in the wild type (Fig. 6 and Fig. 7 A), suggesting µ2 adaptin, unlike AP180, is not required for regulating the size of synaptic vesicles. In *apm-2(e840)* mutants, the number of remaining vesicles are 58% in acetylcholine neurons and 64% in GABA neurons compared with the wild type (Fig. 6 and Fig. 7 B). Similar vesicle reductions relative to the wild type were also observed in *apm-2(gm17)* (unpublished data). Vesicle number is rescued in *apm-2(e840)* animals containing the neuron-specific AMP-2::GFP construct but not in animals that contain the hypodermal specific APM-2::GFP, indicating that the defect is caused by a loss of neuronal APM-2 function (Fig. 6 and Fig. 7 B). The decrease in synaptic vesicle number in *apm-2* mutants suggests µ2 has a significant role in synaptic vesicle recycling. Other mutants lacking endocytosis proteins such as synaptojanin and endophilin have only 38 and 30% the normal number of vesicles, respectively (Harris et al., 2000; Schuske et al., 2003). Thus the endocytosis defect in the absence of µ2 is less severe than other endocytosis mutants. Interestingly, the reduced vesicle pool in *apm-2* mutants is able to sustain neuronal transmission because animals lacking µ2 in the nervous system are not uncoordinated. Consistent with this observation, the number of docked vesicles in *apm-2* mutants is only slightly decreased in GABA neurons and is almost normal in acetylcholine neurons (Fig. 7 C).

Published December 1, 2008

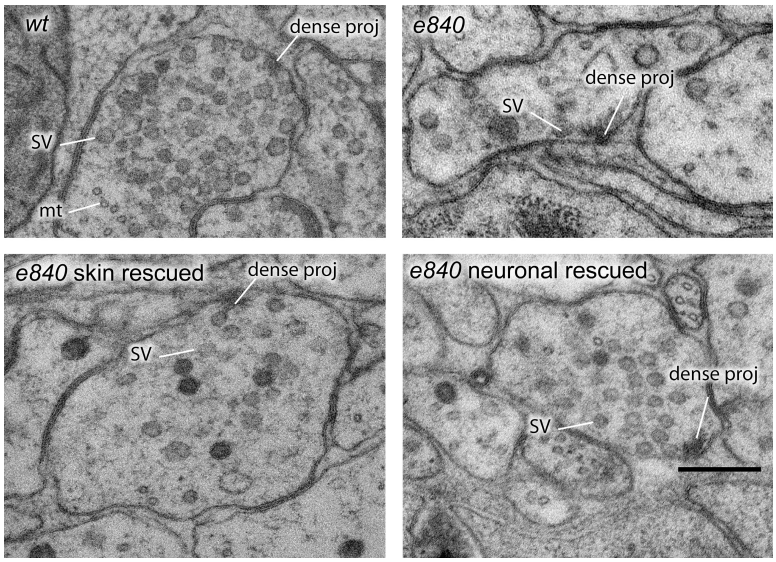

Figure 6. ***apm-2(e840)* neuromuscular junction ultrastructure.** Representative images of neuromuscular junctions in the ventral nerve cord from wild-type, EG3622 *dpy-23(e840)*, EG4029 *dpy-23(e840) Ex[Ppdi-2::APM-2::GFP]*, and EG4213 *dpy-23(e840) Ex[Prab-3::APM-2::GFP]* adult hermaphrodites. *apm-2(e840)* shows reduced numbers of synaptic vesicles. Vesicle number is restored in the neuronal-rescued animals but not in the skin-rescued animals. Bar, 200 nm. SV, synaptic vesicle; mt, microtubule; dense proj, dense projection.

To assay neurotransmitter release, animals were tested for sensitivity to the acetylcholinesterase inhibitor aldicarb (Nguyen et al., 1995). *apm-2* mutants are slightly hypersensitive to aldicarb (Fig. S3 A, available at http://www.jcb.org/cgi/content/full/jcb.200806088/DC1), and the neuronally rescued worms exhibit an identical hypersensitivity to the *apm-2* strain. Expression of *apm-2* in the hypodermis rescued the hypersensitivity to a wild-type level (Fig. S3 B), suggesting that the hypersensitivity could be caused by defects in the cuticle. To directly measure synaptic transmission, we recorded currents at neuromuscular junctions. In the *apm-2* mutants, the miniature frequency and the evoked amplitude are reduced to 60 and 82% of the wild-type levels, respectively (Fig. 8, skin rescue). These values correlate fairly well with the 55 and 69% levels of synaptic vesicles observed at GABA and acetylcholine synapses (Fig. 7 B, skin rescue). Full rescue of synaptic transmission is only observed when *apm-2* is simultaneously expressed in both the hypodermis and neurons (Fig. 8). Collectively, our data demonstrate that μ2 has a detectable role in synaptic vesicle recycling, although this role is not visible in locomotion assays.

Knocking out μ2 is not equal to knocking down AP2

Residual function from the AP2 complex could still remain in the absence of the medium subunit. There are two lines of evidence: genetic and biochemical. First, α adaptin knockdowns are more severe than μ2 adaptin knockdowns in the yolk uptake assay (Grant and Hirsh, 1999). RNA interference against clathrin, α adaptin, or β2 adaptin each abolished uptake of a GFP-tagged vitellogenin (YP170-GFP) into oocytes. In contrast, RNA interference against either μ2 or σ2 adaptin did not disrupt uptake, suggesting that not all of the subunits of the AP2 complex are required for this process. Because RNA interference is not always fully penetrant we used our deletion allele to assay μ2 function in yolk uptake. Approximately 120 gonads of each genotype were assayed for the presence of YP170-GFP fluorescence in oocytes. Over 98% of the gonads in both *apm-2(e840)* and *apm-2(gm17)* mutants were scored as positive for yolk protein uptake (Fig. 9 A). However, the number of oocytes within each gonad containing YP170-GFP was reduced in both alleles of *apm-2* compared with the wild type (wild type: one oocyte, 7%; two or more, 93%; *apm-2(e840)*: one oocyte, 42%; two or more oocytes, 58%; *apm-2(gm17)*: one oocyte, 36%; two or more oocytes, 64%; Fig. 9 B). In all genotypes yolk accumulation is greatest in the oldest oocyte, which is found adjacent to the spermatheca. The defect is not as severe as that seen when the α or β2 subunits of the complex are depleted by RNA interference (Grant and Hirsh, 1999), suggesting that μ2 adaptin subunits are less important than the α adaptin or β2 adaptin subunits in this process.

Second, some α adaptin remains in a complex with σ2 adaptin in the μ2 adaptin mutants. Previous results suggested that each subunit is required for function and stability of the AP2 complex; e.g., RNA interference of the μ2 subunit in HeLaM cells greatly reduced the expression level of the α subunit (Motley et al., 2003). In addition, expression of any single AP2 subunit in bacteria produces an insoluble protein; only simultaneous expression of all subunits produces a soluble protein complex (Collins et al., 2002). To determine if the AP2 complex is stable in the absence of the μ2 subunit, we performed quantitative Western blot analysis of α adaptin. α adaptin is reduced to 60% in *apm-2(e840)* and to 12% in *amp-2(gm17)* (Fig. 9 C). Oddly, the reduction in α adaptin is more severe in the truncated allele of μ2 rather than in the null mutant; it is possible that incorporation of truncated μ2 leads to a destabilization of the whole complex. Consistent with this result, *apm-2(e840)/+* heterozygous animals are wild type, whereas *apm-2(gm17)/+* animals are slightly uncoordinated and have an egg-laying defect. The reduction in α adaptin levels in both alleles indicates that μ2 is required to stabilize the AP2 complex; however, some residual α adaptin remains in the absence of μ2.

Published December 1, 2008

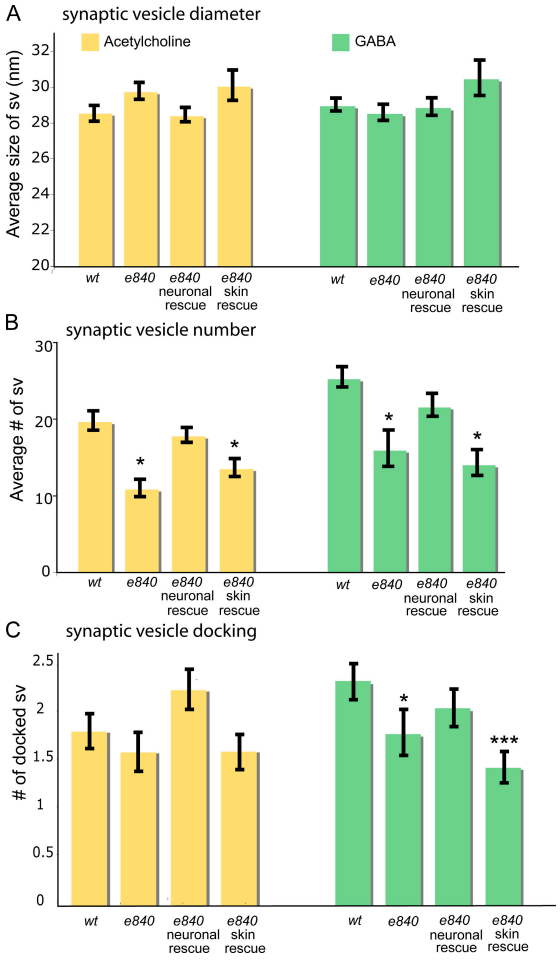

Figure 7. **Synaptic vesicle numbers are reduced in *apm-2(e840)* mutants.** The ventral nerve cord was reconstructed from serial electron micrographs and distribution of synaptic vesicles at neuromuscular junctions was measured from two young adult hermaphrodites for each genotype. (A) Vesicle diameters are identical in wild-type, *apm-2(e840)*, and *apm-2(e840)* tissue-specific rescued animals. Mean size of synaptic vesicles per profile containing a dense projection in nanometers ± SEM is as follows: wild-type acetylcholine, 28.52 ± 0.38, *n* = 734 vesicles; *apm-2(e840)* acetylcholine, 29.71 ± 0.47, *n* = 377 vesicles; neuronal-rescued *apm-2(e840)* acetylcholine, 28.38 ± 0.40, *n* = 744 vesicles; skin-rescued *apm-2(e840)* acetylcholine, 28.38 ± 0.85, *n* = 675 vesicles; wild-type GABA, 28.70 ± 0.35, *n* = 904 vesicles; *apm-2(e840)* GABA 28.27 ± 0.44, *n* = 474 vesicles; neuronal-rescued *apm-2(e840)* GABA, 28.59 ± 0.48, *n* = 1073 vesicles; skin-rescued *apm-2(e840)* GABA, 30.15 ± 0.96, *n* = 700 vesicles. (B) The number of synaptic vesicles is reduced in neurons lacking APM-2. Mean number of synaptic vesicles per profile containing a dense projection ± SEM: wild-type acetylcholine, 19.63 ± 1.28, *n* = 38 synapses; *apm-2(e840)* acetylcholine, 10.83 ± 1.13, *n* = 35 synapses; neuronal-rescued *apm-2(e840)* acetylcholine, 17.74 ± 0.97, *n* = 42 synapses; skin-rescued *apm-2(e840)* acetylcholine, 13.5 ± 1.18, *n* = 50 synapses; wild-type GABA, 25.11 ± 1.17, *n* = 36 synapses; *apm-2(e840)* GABA, 15.83 ± 2.23, *n* = 30 synapse; neuronal-rescued *apm-2(e840)* GABA, 21.46 ± 1.34, *n* = 50 synapses; skin-rescued *apm-2(e840)* GABA, 13.92 ± 1.51, *n* = 50 synapses. (C) The number of docked synaptic vesicles is slightly reduced in neurons lacking APM-2. Mean number of docked synaptic vesicles per profile containing a dense projection ± SEM: wild-type acetylcholine, 1.82 ± 0.13; *apm-2(e840)* acetylcholine, 1.60 ± 0.19; neuronal-rescued *apm-2(e840)* acetylcholine, 2.24 ± 0.20; skin-rescued *apm-2(e840)* acetylcholine, 1.60 ± 0.16; wild-type GABA, 2.36 ± 0.17; *apm-2(e840)* GABA, 1.8 ± 0.22; neuronal-rescued *apm-2(e840)* GABA, 2.06 ± 0.18; skin-rescued *apm-2(e840)* GABA, 1.44 ± 0.14. The number of synapses is the same as in B. *, $P < 0.05$; ***, $P < 0.001$.

The residual α adaptin remains bound to σ2 adaptin. α adaptin tagged with GFP was immunoprecipitated from the wild type and *apm-2* mutants. β adaptin coimmunoprecipitated from the wild-type animals but not from μ2 mutant animals (Fig. S5 A, available at http://www.jcb.org/cgi/content/full/jcb.200806088/DC1). In contrast, σ2 adaptin (HA tagged) coimmunoprecipitated from both the wild-type and μ2 mutant animals (Fig. S5, B and C). Moreover, residual α adaptin can still be localized in the absence of μ2. Coelomocytes are scavenger cells in *C. elegans* with high levels of endocytosis. N-Terminal tagged α adaptin is localized properly to the plasma membrane of mutant coelomocytes (Fig. 9 D). Similarly, tagged α adaptin is localized to synapses in *apm-2* mutants. These data suggest that the protein is folded and transported correctly in mutant cells. Thus, it is possible that AP2 is at least partially functional in *apm-2* mutants.

Discussion

In this study, we characterized the only AP2 μ2 adaptin subunit in *C. elegans* and its function in synaptic vesicle endocytosis. μ2 adaptin is encoded by the gene *dpy-23* (*apm-2*). It is expressed ubiquitously in adult worms and is highly expressed in the nervous system. Absence of μ2 impairs but does not eliminate synaptic vesicle endocytosis. Animals lacking μ2 have ∼60% of the normal number of vesicles at synaptic varicosities, and synaptic vesicle proteins are properly localized at the synapse. This phenotype is much less severe than worm mutants lacking other recycling proteins such as AP180 (*unc-11*), synaptojanin (*unc-26*), and endophilin (*unc-57*) (Nonet et al., 1999; Harris et al., 2000; Schuske et al., 2003). For example, the number of synaptic vesicles in synaptojanin and endophilin mutants is reduced to ∼35%, the normal number of synaptic vesicles found at neuromuscular junctions.

The conclusion that μ2 is not essential for synaptic vesicle recycling leads to several considerations. (a) Do other proteins recruit cargo? (b) Can other medium subunits stabilize AP2? (c) Do other proteins recruit clathrin?

The specific role of μ2 is in cargo recruitment, in particular, its interactions with synaptotagmin were thought to be essential for synaptic vesicle biogenesis (Zhang et al., 1994; Jorgensen et al., 1995; Haucke et al., 2000). However, our data indicate that μ2 is not required to recruit proteins to synaptic vesicles. The essential synaptic vesicle proteins are synaptobrevin, synaptotagmin, and the neurotransmitter transporters. Other ancillary proteins have been identified that recruit these synaptic vesicle proteins to sites of endocytosis. AP180 is required to recruit synaptobrevin to synaptic vesicles (Zhang et al., 1998; Nonet et al., 1999; Bao et al., 2005). Stonin, which is distantly related to μ2, is required for synaptotagmin recycling (Fergestad and Broadie, 2001; Martina et al., 2001; Walther et al., 2004). The vesicular GABA transporter is recruited by a

Published December 1, 2008

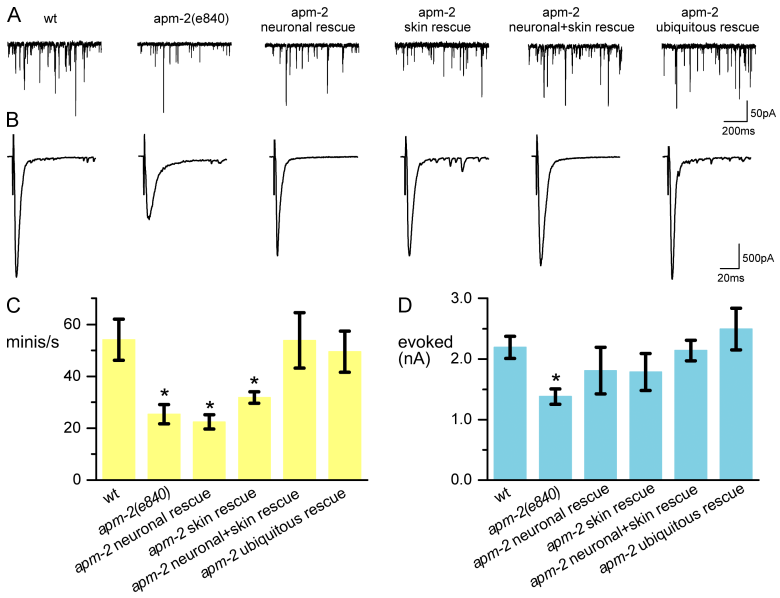

Figure 8. **Electrophysiological analysis at neuromuscular junctions of wild-type, *apm-2(e840)*, and various *apm-2(e840)* tissue-specific rescued worms.** (A) sample traces of mPSC recorded from wild-type, *apm-2(e840)*, neuronal-rescued *apm-2(e840)*, skin-rescued *apm-2(e840)*, neuronal- and skin-rescued *apm-2(e840)*, and ubiquitously rescued *apm-2(e840)* worms. (B) sample traces of ePSC recorded from the aforementioned animals. (C) Summary of mPSC frequencies (Hz ± SEM): wild type, 54.1 ± 8.0, n = 8; *apm-2(e840)*, 25.4 ± 3.7, n = 9; neuronal-rescued *apm-2(e840)*, 22.4 ± 2.7, n = 8; skin-rescued *apm-2(e840)*, 31.9 ± 2.2, n = 12; neuronal- and skin-rescued *apm-2(e840)*, 53.9 ± 10.7, n = 8; ubiquitously rescued *apm-2(e840)*, 49.5 ± 7.9, n = 8. (D) Summary of ePSC amplitudes (nA ± SEM): wild type, 2.19 ± 0.18, n = 8; *apm-2(e840)*, 1.38 ± 0.13, n = 7; neuronal-rescued *apm-2(e840)*, 1.81 ± 0.39, n = 7; skin-rescued *apm-2(e840)*, 1.79 ± 0.31, n = 8; neuronal- and skin-rescued *apm-2(e840)*, 2.14 ± 0.17, n = 6; ubiquitously rescued *apm-2(e840)*, 2.50 ± 0.34, n = 7. *, $P < 0.05$, compared with wild-type; unpaired t test.

LAMP-related protein called UNC-46 (Schuske et al., 2007). Because of these defects in cargo recruitment, all of these mutants are severely uncoordinated in worms. In contrast, mutants lacking μ2 in the nervous system are not uncoordinated and evoked responses are at 82% of the levels observed in the wild type, indicating that synaptic transmission is largely intact. Thus, if μ2 recruits cargo to recycling vesicles it is unlikely to be a component essential for neurotransmission.

The medium subunit μ2 is also known to stabilize the AP2 complex (Motley et al., 2003). One could imagine that medium subunits from the AP1 or AP3 complexes (there is no AP4 in *C. elegans*) could substitute for μ2 and provide AP2 complex function. However, adaptins from different complexes do not appear to be redundant in other organisms. For example, in yeast, overexpression of σ2 cannot substitute for the loss of σ1 (Phan et al., 1994). Similarly, we found that other medium subunits cannot substitute for μ2 in *C. elegans*. Mutants lacking μ1 (*unc-101*) are severely uncoordinated and exhibit defects in anterograde transport of olfactory receptors to olfactory cilia (Dwyer et al., 2001). Overexpression of μ2 cannot rescue the severely uncoordinated phenotype of the μ1 mutant in a thrashing assay (unpublished data). Moreover, *apm-2 unc-101* (μ1 μ2) double mutants exhibit an additive dumpy and uncoordinated phenotype rather than a synthetic phenotype, suggesting that these proteins are not acting redundantly. Mutants lacking μ3 (*apm-2(tm920)*) are outwardly wild type but slightly aldicarb resistant. Again, μ2 and μ3 mutations do not show synthetic interactions: *apm-2 apm-3* double mutants (with μ2 rescued in skin) exhibit similar aldicarb sensitivity as the μ3 mutant alone. In addition, our data show that AP2 is destabilized in the absence of μ2, suggesting μ2 is the only medium subunit used by AP2 in *C. elegans*.

Our data are consistent with a study in other systems suggesting that clathrin can be recruited by alternative adaptors (Traub, 2003). In particular, AP180 is required for normal synaptic vesicle endocytosis and it is likely that AP180 could recruit clathrin and form vesicles in the absence of AP2 (Zhang et al., 1998; Nonet et al., 1999). Our results for μ2 seem to conflict with previous studies that suggest that the AP2 subunit α adaptin is essential for synaptic vesicle recycling in *Drosophila melanogaster*. A weak mutation in the *Drosophila* α adaptin subunit *D-αAda*^{1} leads to slowly moving larvae, which die as pupae (Gonzalez-Gaitan and Jackle, 1997). The neurons of these animals are not efficient in taking up FM1-43 dye at boutons upon stimulation. The null mutants die before hatching and the electron microscopy data suggest that these animals are depleted of synaptic vesicles. However, in *C. elegans*, the behavioral defects of *apm-2*–null mutants are less pronounced. The hypodermal rescued mutants have almost normal movement and the evoked current upon stimulation is close to the wild type. Thus the neurotransmission defect in μ2 mutants in worms is less severe than that of α adaptin mutants in flies. Although it is possible that residual AP2 function accounts for vesicle recycling in μ2 mutants, it is also possible that AP2 is not essential for synaptic vesicle recycling at *C. elegans* neuromuscular junctions.

Materials and methods

Mapping and mutation analysis

The mutation *e840* was isolated in an x-ray mutagenesis by S. Brenner (Agency for Science, Technology, and Research, Biopolis, Singapore). The mutation *gm17* was isolated in an EMS screen for egg-laying defective animals. *gm17* was mapped between two polymorphisms on the X chromosome, *gmP'* and *pgP2*, and was successfully rescued by two overlapping cosmids, D1079 and C33G6. The sequence of *gm17* was determined by DNA sequencing. The molecular nature of *e840* was determined by genomic southern analysis and the break points of *e840* deletion were further characterized by PCR against *apm-2* neighboring ORFs. Because *e840* is a multigene deletion, an alternative name, *eDf44*, has been given by J. Hodgkin (University of Oxford, Oxford, England).

Published December 1, 2008

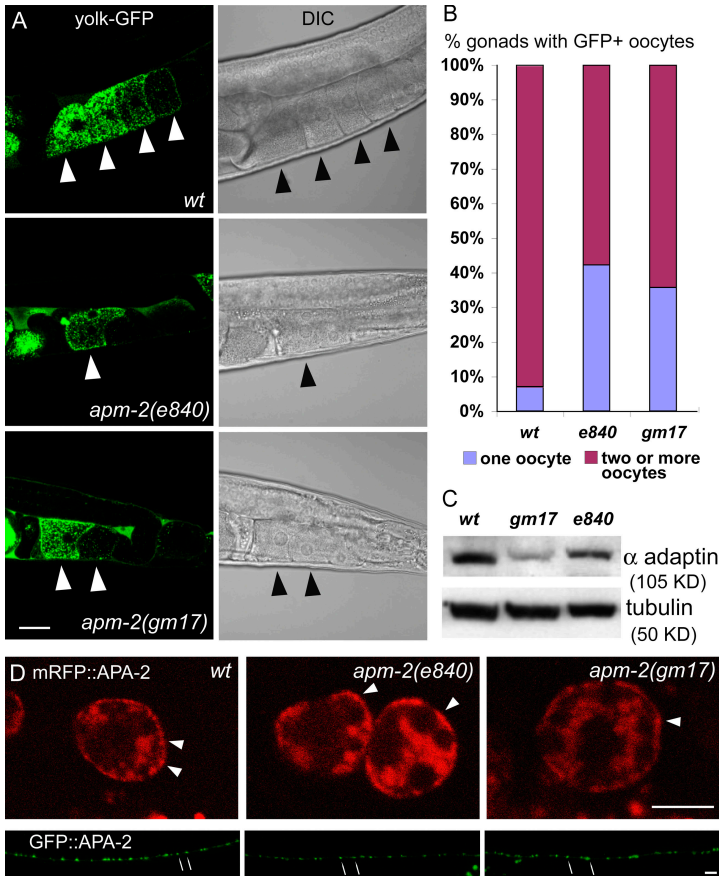

Figure 9. **Yolk protein endocytosis in *apm-2* mutants.** (A) Oocytes from adult worms expressing yolk protein YP170::GFP. Arrowheads indicate the GFP-positive oocytes. Figures are single-slice confocal images. Bar, 20 μm. (B) A bar graph showing the percentage of gonads with different numbers of GFP-positive oocytes. (C) A Western blot of the wild-type and *apm-2* mutant worm lysates probed with an antibody against α adaptin (APA-2). 200 μg of protein was loaded in each lane. (D) APA-2 localization in scavenger cell, coelomocytes, and GABA synapses. Images were taken from adult worms. Arrowheads indicate the RFP-positive plasma membrane of coelomocytes. Arrows indicate the GFP-positive synapses. Coelomocyte figures are single-slice confocal images. GABA synapse images are z-stack projections. Bars, 5 μm.

***C. elegans* strains**

The wild strain is Bristol N2. The reference strains for *e840* and *gm17* were outcrossed twice before phenotypic analysis. The outcrossed strains are EG2988 *apm-2(gm17)X* and EG3622 *apm-2(e840)X*.

The strains used in the synaptobrevin and clathrin colocalization assays were EG4052 *lin-15(n765ts)X; oxEx761[Punc-47:APM-2(cDNA)::GFP Punc-47:SNB::mCherry lin-15(+)]* and EG4051 *lin-15(n765ts)X; oxEx759[Punc-47:APM-2(cDNA)::GFP Punc-47:CHC-1::RFP lin-15(+)]*.

The strains used in the synaptic vesicle protein distribution assays were MT8247 *lin-15(n765ts) nIs52[Punc-25::SNB::GFP lin-15(+)]X*, EG3733 *apm-2(e840) nIs52[Punc-25::SNB::GFP lin-15(+)]X*, EG3229 *apm-2(gm17) nIs52[Punc-25::SNB::GFP lin-15(+)]X*, NM1233 *jsIs219[SNG-1::GFP rol-6(su1006)]II*, EG3563 *jsIs219[SNG-1::GFP rol-6(su1006)]II; apm-2(e840)X*, EG3736 *jsIs219[SNG-1::GFP rol-6(su1006)]II; apm-2(gm17)X*, EG3855 *lin-15(n765ts) oxIs224[Punc-47::GFP::SNT-1 lin-15(+)]X*, EG3889 *apm-2(e840) oxIs224[Punc-47::GFP::SNT-1,lin-15(+)]X*, and EG3891 *apm-2(gm17) oxIs224[Punc-47:GFP::SNT-1 lin-15(+)]X*.

The strains used in the clathrin distribution assays were EG3381 *oxIs-164[Punc-47::GFP::CHC-1 lin-15(+)]IV; lin-15(n765)X*, EG3735 *oxIs-164[Punc-47:GFP::CHC-1 lin-15(+)]IV; apm-2(e840)X* and EG3564 *oxIs164[Punc-47::GFP::CHC-1 lin-15(+)]IV; apm-2(gm17)X*.

The strains used in APM-2 distribution assays were EG4055 *snt-1(n2665)II; oxEx763[Punc-47::APM-2(cDNA)::GFP Pmyo-2::GFP]*, EG4091 *unc-41(n268)V; oxEx767[Punc-47::APm-2(cDNA)::GFP Pmyo-2::GFP]*, EG4103 *unc-11(e47)I; oxEx767[Punc-47::APM-2(cDNA)::GFP Pmyo-2::GFP]*, and EG4089 *unc-26(s1710)IV; oxEx767[Punc-47::APM-2(cDNA)::GFP Pmyo-2::GFP]*.

The strains used in APM-2 tissue-specific rescue assay were EG4017 *lin-15(n765)X; oxEx747[Prab-3::APM-2(cDNA)::GFP (pMG9) lin-15(+)]*, EG1616 *apm-2(e840)X; oxEx730[APM-2::GFP (pMG4) Punc-122::GFP]*, EG4213 *apm-2(e840)X; oxEx789[Prab-3::APM-2(cDNA)::GFP (pMG9) Punc-122::GFP]*, EG4015 *apm-2(e840)X; oxEx745[Pdpy-30::APM-2(cDNA)::GFP (pMG10) Punc-122::GFP]*, EG4029 *apm-2(e840)X; oxEx753[Ppdi-2::APM-2(cDNA)::GFP (pMG8) Punc-122::GFP]*, EG4030 *apm-2(e840)X; oxEx745[Ppdi-2::APM-2(cDNA)::GFP (pMG8) Prab-3::APM-2(cDNA)::GFP (pMG9) Punc-122::GFP]*, and EG4093 *apm-2(e840)X, oxEx773[Ppdi-2::APM-2(cDNA)::GFP (pMG8) Pmyo-2::GFP]*. *Punc-122* is the coelomocyte promoter.

The strains used in yolk uptake assay were DH1033 *sqt-1(sc103)II; bIs1[vit-2::GFP rol-6(su1006)]X*, EG4062 *apm-2(e840) bIs1[vit-2::GFP rol-6(su1006)]X*, EG4059 *apm-2(gm17) bIs1[vit-2::GFP rol-6(su1006)]X*.

The strain used in α adaptin coelomocyte plasma membrane localization assay were RT490 *unc-119(ed3) III; pwIs177[Punc-122:mRFP::apa-2; cb-unc-119(+)]*, EG4188 *apm-2(e840) X; pwIs177[Punc-122:mRFP::apa-2; cb-unc-119(+)]*, EG4189 *apm-2(gm17) X; pwIs177[Punc-122:mRFP::apa-2; cb-unc-119(+)]*. They were provided by B.D. Grant (Rutgers University, Piscataway, NJ)

The strains used in α adaptin GABA synaptic localization assay were GK275 *unc-119(ed3) III; dkIs160[Punc-25:GFP::apa-2,unc-119(+)]*, EG4203 *apm-2(e840) X; dkIs160[Punc-25:GFP::apa-2,unc-119(+)]*, and EG4204 *apm-2(gm17) X; dkIs160[Punc-25:GFP::apa-2,unc-119(+)]*. They were provided by K. Sato (Gunma University, Gunma, Japan).

The strains used in AP2 assembly immunoprecipitation were EG5264 *oxEx1275[Papa-2::apa-2::GFP Punc-122::GFP]*, EG5265 *apm-2(e840)X, oxEx1275[Papa-2::apa-2::GFP Punc-122::GFP]*, EG5266 *oxEx1276[Papa-2::apa-2::GFP Paps-2::aps-2::HA Punc-122::GFP]*, and EG5267 *apa-2(e840)X oxEx1276 [Papa-2::apa-2::GFP Paps-2::aps-2::HA Punc-122::GFP]*.

Phylogenetic analysis

The phylogenetic tree of μ adaptin was made by ClustalX (1.83.1 Mac) and Treeview X. The protein accession numbers are as follows: μ3A mouse (Q9JKC8); μ3B mouse (Q8R2R9); μ3 *Drosophila* (NP_788873); APM-3

Published December 1, 2008

(NP_508184); stB *Drosophila* (Q24212); APT-10 (stB Ce; NP_505566); stB mouse (NP_780576); μ2 *Drosophila* (NP_732744); μ2 mouse (NP_033809); APM-2 (NP_001024865); APM-1(NP_491572); UNC-101 (NP_001040675); μ1A mouse (AAF61814); μ1B mouse (AF067146); μ1 *Drosophila* (NP_649906).

GFP constructs

pMG1, *apm-2* genomic region. A 12-kb *apm-2* genomic PCR fragment was amplified from cosmid C33G6, including 5 kb upstream of the start codon, 5 kb of coding sequence, and 2 kb downstream of the stop codon, and was cloned between BamHI and PstI restriction sites in pGEM-3zf(+) (Promega). Primers used were 5′-ATTAGGATCCAGGTGGTGGTGGTGAAGA-3′ and 5′-AGATCTGCAGTCGGCTAACGGCTAATTCGGCTAA-3′.

pMG2, *apm-2* transcriptional GFP. The construct comprises the *apm-2* promoter only driving GFP. This construct does not show expression in neurons, suggesting that a neuronal enhancer is contained within an intron.

pMG3, *apm-2* transcriptional GFP. GFP with the *unc-54* 3′UTR was PCR amplified from the plasmid pPD95.77 (provided by A. Fire, Carnegie Institution of Washington, Baltimore, MD). The primers used were 5′-GGCTGAAATCACTCACAACGATGG-3′ and 5′-TACAGTCGACTACGGCCGACTAGTAGGAAACAGT-3′. This fragment contains SalI restriction sites at both ends and was inserted into the SalI site of pMG1, which is in the second exon of *apm-2*.

pMG4, *apm-2* translational GFP. *apm-2* 10-kb genomic PCR fragment, including 5 kb upstream of the start codon and 5 kb of coding sequence without the stop codon, was amplified from pMG1 and cloned between the BamHI and PstI restriction sites in pGEM-3zf(+). Primers used were 5′-ATTAGGATCCAGGTGGTGGTGGTGAAGA-3′ and 5′-ACAGCTGCAGGCATCTGGTTTCATACAGTCCCGA-3′. GFP with the *unc-54* 3′UTR was cloned from the plasmid pPD95.77 with a PstI site at one end and a HindIII site at the other end and was then inserted after the *apm-2* coding sequence to make a GFP fusion protein. Primers used were 5′-ACATCTGCAGTTGGCCAAAGGACCCAAAGGTATG-3′ and 5′-ACGCAAGCTTCGGCCGACTAGTAGGAAACAGTTA-3′.

Constructs for *apm-2* tissue-specific rescue assay

Multisite Gateway three-fragment construction vectors were used (Invitrogen). Promoter entry vectors, including pENTRY4-1 *Pdpy-30* and pENTRY4-1 *Ppdi-2*, were ordered from Open Biosystems. The *Ppdi-2* construct (Open Biosystems) lacks 373 nt (−808 to approximately −435 from the start codon of *pdi-2*) in the promoter region; however, skin expression was still observed using this construct. pENTRY4-1 *Prab-3* was generated by BP reaction. ORF entry vector pENTRY1-2 *apm-2* (ORF) was ordered from Open Biosystems. 3′UTR entry vector pENTRY2-3 GFP::*unc-54* 3′UTR was made by a Gateway BP reaction. The final constructs, *apm-2*::GFP fusion gene driven by different promoters, were generated by Gateway LR reactions.

Constructs for AP2: assembly immunoprecipitation

pMG16, *apa-2* translational GFP. *apa-2* 6-kb genomic sequence, including 2.3 kb of promoter and 3.7 kb of coding sequence without stop codon, was cloned between KpnI and XbaI sites in pGEM-3zf(+). Primers used were 5′-ACTCGGTACCGCATACTTGATGGAAAACCCGCTC-3′ and 5′-AGCCTCTAGAAAATTGGTTGCCCAATAAGTCTAC-3′.

GFP with the *unc-54* 3′UTR was cloned from Fire laboratory vector pPD 95.77 with an XbaI site at one end and a HindIII site at the other end. This fragment was inserted after the *apm-2* coding sequence to make a GFP fusion protein. Primers used were 5′-ACCGTCTAGAGGGGTAGAAAAAATGAGTAAAGGA-3′ and 5′-AGCGAAGCTTCGGCCGACTAGTAGGAAACAGTTA-3′.

pMG28, HA-tagged translational APS-2. *aps-2* 2-kb genomic sequence, including 1 kb of promoter and 1 kb of coding sequence (stop codon is replaced by HA tag), was cloned between EcoRI and PstI sites in pGEM-3zf(+). Primers used were 5′-AGCGGAATTCCGTTTAGTTCTTGAGTGGCTTG-3′ and 5′-ACAGCTGCAGAGCGTAATCTGGAACATCGTATGGGTATTCCAGGGAAGTAAGCATGAGCA-3′.

unc-54 3′UTR was cloned from Fire laboratory vector pPD 95.77 with a PstI site at one end and a HindIII site at the other end. This fragment was inserted after the *aps-2::HA* coding sequence. Primers used were 5′-AGGCCTGCAGTAGCATTCGTAGAATTCCAACTGA-3′ and 5′-AGGCAAGCTTCCCATAGACACTACTCCACTTTC-3′.

Microinjection

The total DNA concentration of injection mix is 100 ng/μl. The injection marker was 50 ng/μl *Punc-122::GFP*, if not specified. 1-kb DNA ladder (Fermentas) was used to make the injection mix final concentration 100 ng/μl.

Rescue experiment. 10 ng/μl of 12-kb *apm-2* genomic PCR fragment was injected into N2 to overexpress APM-2 in wild-type animals. 0.25 ng/μ of 12-kb *apm-2* genomic PCR fragment was injected into N2. The extrachromosomal array was then crossed into *apm-2(e840)* and *apm-2(gm17)* mutants to evaluate rescue.

Tissue-specific rescue. 1 ng/μl each of pMG10 *Pdpy-30::apm-2::GFP*, pMG8 *Ppdi-2::apm-2::GFP*, and pMG9 *Prab-3::apm-2::GFP* DNAs were injected, respectively, into *apm-2(e840)*. For the skin and nervous system double rescue experiment, 1 ng/μl each of pMG8 and pMG9 were injected together. 10 ng/μl pMG9 and 50 ng/μl *lin-15(+)* were coinjected into *lin-15(n765ts)* to overexpress APM-2::GFP only in the nervous system. 1 ng/μl pMG8 and 2 ng/μl *Pmyo-2::GFP* were coinjected into *apm-2(e840)* to rescue *apm-2* mutant in skin with a different injection marker.

AP2 complex immunoprecipitation. pMG16 was injected at 10 ng/μl into the wild type. The array was crossed into *apm-2(e840)*. pMG16 and pMG28 were coinjected at 10 ng/μl into the wild type and the same array was then crossed into *apm-2(e840)*.

Western blot analysis

Worm samples were prepared by boiling 1 vol of the worm pellet in 9 vol of 1× loading buffer for 5 min. Samples were run on a 10% SDS-PAGE gel then transferred to polyvinylidene fluoride transfer membrane (Immobilon). Primary antibody for α adaptin was a rabbit polyclonal APA-2 antibody at a dilution of 1:500 (provided by B. Grant). Primary antibody incubation was done in 1% milk at room temperature for 4 h. Primary antibody for the standard control tubulin was a 12G10 mouse monoclonal antibody (Developmental Studies Hybridoma Bank) at a dilution of 1:5,000. Primary antibody incubation was done in 1% milk at room temperature for 1 h, and then the membrane was washed three times in 10 ml of 1× PBS plus Tween 20 (PBST). Secondary antibodies were anti-rabbit and mouse IgG fragment conjugated with HRP (GE Healthcare). Secondary incubations were done in 10% milk at room temperature for 45 min, and then the membrane was washed five times in 10 ml of 1× PBST. Detection reagent used was Lumigen PS-3 (GE Healthcare).

AP2 complex immunoprecipitation

250 μl (± 50 μl) of worm pellet was harvested. The pellet was suspended in 2 ml of ice-cold lysis buffer (5% Triton X-100, 50 mM Hepes, pH 7.3, 50 mM NaCl, and 1 tablet of protease inhibitor cocktail [Roche]). The sample was lysed by a bead beater (NMB) for 10 s, three times, and was spun, and the supernatant was recovered. The supernatant was pushed through a 0.22-μm filter. 15 μl of agarose-conjugated rat anti-GFP IgG2a beads (MBL International) were added to the lysate. The mixture was incubated at 4°C for 2 h. Beads were harvested and washed with 1 ml of lysis buffer three times. 100 μl of loading buffer was added on the bead pellet and boiled for 15 min.

Samples were run on 7, 10, or 15% SDS-PAGE and transferred to a polyvinylidene fluoride membrane. Primary antibody for GFP was a mouse monoclonal antibody at a dilution of 1:5,000 (Clontech Laboratories, Inc.). Primary antibody for HA was a mouse monoclonal antibody (12CA5; Santa Cruz Biotechnology, Inc.) at a dilution of 1:5,000. Primary antibody for β adaptin was a mouse monoclonal antibody (Thermo Fisher Scientific) at a dilution of 1:5,000. Primary antibody incubation was performed in 5% BSA at 4°C overnight, and then the membrane was washed three times in 10 ml of 1× PBST. Secondary antibodies were goat anti–mouse IgG fragment conjugated with HRP (GE Healthcare). Secondary incubations were performed in 5% BSA at 22.5°C for 2 h, and then the membrane was washed five times in 10 ml of 1× PBST. Detection reagent was SuperSignal West Dura kit (Thermo Fisher Scientific).

Thrashing assay

A single worm was put into a 50-μl drop of M9 solution. The worm was allowed to adapt to the liquid environment for 2 min. The number of body bends was counted for 90 s for each genotype ($n = 7$). We analyzed lines of *apm-2(e840)* rescued by skin APM-2::GFP with two different injection markers (EG4029 *Punc-122::GFP* and EG4093 *Pmyo-2::GFP*). The results are the same.

Aldicarb resistance assay

Each agar plate was seeded with bacteria and weighed to top spread plates with the appropriate amount of aldicarb. Plates with six different aldicarb final concentrations were prepared (0.1, 0.3, 0.5, 0.7, 0.9, and 1.1 mM). Aldicarb was allowed to soak in overnight at room temperature.

Published December 1, 2008

For each genotype, 20 worms were put onto plates containing each different aldicarb concentration. The plates were blinded and the percentage of paralyzed worms were scored after 4 h of exposure to aldicarb. The same experiment was repeated five times for each genotype except *apm-2(e840) oxEx755[Prab-3::apm-2::GFP, Punc-122::GFP]*, which had only 10 worms on each plate and the experiment was repeated four times because of fewer transgenic animals.

Confocal microscopy

Worms are immobilized by using 2% phenoxy propanol and imaged on a confocal microscope (Pascal LSM5; Carl Zeiss, Inc.) with a plan-Neofluar 10x 0.3 NA, 20x 0.5 NA, or 40x 1.3 NA or plan-apochromat 63x 1.4 NA oil objectives (Carl Zeiss, Inc.).

Electron microscopy

Wild-type (N2), *apm-2(e840)*, EG4029 *apm-2(e840); oxEx753[Ppdi-2::apm-2::GFP, Punc-122::GFP]*, and EG4213 *apm-2(e840); oxEx789[Prab-3::apm-2::GFP, Punc-122::GFP]* adult nematodes were prepared in parallel for transmission electron microscopy as previously described (Hammarlund et al., 2007). In brief, 10 young adult hermaphrodites were placed onto a freeze chamber (100-µm well of type A specimen carrier) containing space-filling bacteria, covered with a type B specimen carrier flat side down, and frozen instantaneously in the HPM 010 (Leica). This step was repeated for animals of all genotypes. The frozen animals were fixed in the EM AFS system (Leica) with 1% osmium tetroxide and 0.1% uranyl acetate in anhydrous acetone for 2 d at –90°C and for 38.9 more hours with gradual temperature increase (6°C/h to −20°C over 11.7 h, constant temperature at −20°C for 16 h, and 10°C/h to 20°C over 4 h). The fixed animals were embedded in araldite resin following the infiltration series (30% araldite/acetone for 4 h, 70% araldite/acetone for 5 h, 90% araldite/acetone overnight, and pure araldite for 8 h). Mutant and control blocks were blinded. Ribbons of ultra-thin (33-nm) serial sections were collected using an Ultracut 6 microtome (Leica) at the level of the anterior reflex of the gonad. Images were obtained on an electron microscope (H-7100; Hitachi) using a digital camera (Gatan). 250 ultra-thin contiguous sections were cut, and the ventral nerve cord was reconstructed from two animals representing each genotype. Image analysis was performed using ImageJ software. The numbers of synaptic vesicles (~30 nm), dense-core vesicles (~40 nm), and large vesicles (>40 nm) in each synapse were counted and their distance from presynaptic specialization and plasma membrane as well as the diameter of each were measured from acetylcholine neurons VA and VB and the GABA neuron VD. A synapse was defined as the serial sections containing a dense projection as well as sections on either side of that density, which contain synaptic vesicle numbers above the mean number of synaptic vesicles per profile.

Electrophysiology

C. elegans were grown at room temperature (22–24°C) on agar plates with a layer of OP50 *Escherichia coli*. Adult hermaphrodite animals were used for electrophysiological analysis. Miniature and evoked postsynaptic currents (mPSCs and ePSCs) at the neuromuscular junction were recorded as previously described (Liu et al., 2007) using a technique originally developed by Richmond and Jorgensen (1999). In brief, an animal was immobilized on a sylgard-coated glass coverslip by applying a cyanoacrylate adhesive along the dorsal side. A longitudinal incision was made in the dorsolateral region. After clearing the viscera, the cuticle flap was folded back and glued to the coverslip, exposing the ventral nerve cord and two adjacent muscle quadrants. A microscope (Axioskop; Carl Zeiss, Inc.) equipped with a 40× water immersion lens and 15× eyepieces was used for viewing the preparation. Borosilicate glass pipettes with a tip resistance of ~3–5 MΩ were used as electrodes for voltage clamping. The classical whole-cell configuration was obtained by rupturing the patch membrane of a gigaohm seal formed between the recording electrode and a body wall muscle cell. The cell was voltage clamped at −60 mV to record mPSCs and ePSCs. ePSCs were evoked by applying a 0.5-ms square wave current pulse at a supramaximal voltage (25 V) through a stimulation electrode placed in close apposition to the ventral nerve cord. Postsynaptic currents were amplified (EP10; HEKA) and acquired with Patchmaster software (HEKA). Data were sampled at a rate of 10 kHz after filtering at 2 kHz. The recording pipette solution contained the following: 120 mM KCl, 20 mM KOH, 5 mM TES, 0.25 mM $CaCl_2$, 4 mM $MgCl_2$, 36 mM sucrose, 5 mM EGTA, and 4 mM Na_2ATP; pH adjusted to 7.2 with KOH and osmolarity at ~310–320 mosM. The standard external solution included the following: 150 mM NaCl, 5 mM KCl, 5 mM $CaCl_2$, 1 mM $MgCl_2$, 5 mM sucrose, 10 mM glucose, and 15 mM Hepes; pH adjusted to 7.35 with NaOH with osmolarity ~330–340 mosM.

Amplitude and frequency of mPSCs were analyzed using MiniAnalysis (Synaptosoft). A detection threshold of 10 pA was used in initial automatic analysis, followed by visual inspections to include missed events (≥5 pA) and to exclude false events resulting from baseline fluctuations. Amplitudes of ePSCs were measured with Fitmaster (HEKA). The amplitude of the largest peak of ePSCs from each experiment was used for statistical analysis. Data were imported into Origin, version 7.5 (OriginLab), for graphing and statistical analysis. Unpaired *t* test was used for statistical comparisons. A value of $P < 0.05$ is considered statistically significant. All values are expressed as mean ± SEM. *n* is the number of worms that were recorded.

Quantification

ImageJ 1.36b was used for the pixel intensity analysis of α adaptin Western blot.

Online supplemental material

Fig. S1 shows rescue of the *apm-2* mutant phenotype. Fig. S2 shows that APM-2 is not mislocalized in endocytic mutants. Fig. S3 shows *apm-2* aldicarb assay. Fig. S4 is a cartoon structure of *apm-2::GFP* DNA constructs. Fig. S5 depicts the assembly of AP2 with or without µ2. Online supplemental material is available at http://www.jcb.org/cgi/content/full/jcb.200806088/DC1.

We thank Barth Grant for kindly providing the APA-2 polyclonal antibody and coelomocyte mRFP::APA-2 strain. We also thank Ken Sato for providing CHC::GFP constructs and GABA neuron GFP::APA-2 strain. We thank Jim Rand and Kiely Grundahl for sharing unpublished information about *unc-41*.

This research was supported by National Institutes of Health grants 5R37NS034307-14 (to E.M. Jorgensen) and NS32057 (to G. Garriga). E.M. Jorgensen is a Howard Hughes Medical Institute Investigator.

Submitted: 13 June 2008
Accepted: 30 October 2008

References

Aguilar, R.C., H. Ohno, K.W. Roche, and J.S. Bonifacino. 1997. Functional domain mapping of the clathrin-associated adaptor medium chains mu1 and mu2. *J. Biol. Chem.* 272:27160–27166.

Augustine, G.J., J.R. Morgan, C.A. Villalba-Galea, S. Jin, K. Prasad, and E.M. Lafer. 2006. Clathrin and synaptic vesicle endocytosis: studies at the squid giant synapse. *Biochem. Soc. Trans.* 34:68–72.

Bao, H., R.W. Daniels, G.T. MacLeod, M.P. Charlton, H.L. Atwood, and B. Zhang. 2005. AP180 maintains the distribution of synaptic and vesicle proteins in the nerve terminal and indirectly regulates the efficacy of Ca2+-triggered exocytosis. *J. Neurophysiol.* 94:1888–1903.

Collins, B.M., A.J. McCoy, H.M. Kent, P.R. Evans, and D.J. Owen. 2002. Molecular architecture and functional model of the endocytic AP2 complex. *Cell.* 109:523–535.

De Camilli, P., K. Takei, and P.S. McPherson. 1995. The function of dynamin in endocytosis. *Curr. Opin. Neurobiol.* 5:559–565.

Dell'Angelica, E.C., J. Klumperman, W. Stoorvogel, and J.S. Bonifacino. 1998. Association of the AP-3 adaptor complex with clathrin. *Science.* 280:431–434.

Dell'Angelica, E.C., C. Mullins, and J.S. Bonifacino. 1999. AP-4, a novel protein complex related to clathrin adaptors. *J. Biol. Chem.* 274:7278–7285.

Dwyer, N.D., C.E. Adler, J.G. Crump, N.D. L'Etoile, and C.I. Bargmann. 2001. Polarized dendritic transport and the AP-1 mu1 clathrin adaptor UNC-101 localize odorant receptors to olfactory cilia. *Neuron.* 31:277–287.

Fergestad, T., and K. Broadie. 2001. Interaction of stoned and synaptotagmin in synaptic vesicle endocytosis. *J. Neurosci.* 21:1218–1227.

Gaidarov, I., and J.H. Keen. 1999. Phosphoinositide–AP-2 interactions required for targeting to plasma membrane clathrin-coated pits. *J. Cell Biol.* 146:755–764.

Gonzalez-Gaitan, M., and H. Jackle. 1997. Role of *Drosophila* alpha-adaptin in presynaptic vesicle recycling. *Cell.* 88:767–776.

Granseth, B., B. Odermatt, S.J. Royle, and L. Lagnado. 2006. Clathrin-mediated endocytosis is the dominant mechanism of vesicle retrieval at hippocampal synapses. *Neuron.* 51:773–786.

Grant, B., and D. Hirsh. 1999. Receptor-mediated endocytosis in the *Caenorhabditis elegans* oocyte. *Mol. Biol. Cell.* 10:4311–4326.

Hammarlund, M., M.T. Palfreyman, S. Watanabe, S. Olsen, and E.M. Jorgensen. 2007. Open syntaxin docks synaptic vesicles. *PLoS Biol.* 5:e198.

Harris, T.W., E. Hartwieg, H.R. Horvitz, and E.M. Jorgensen. 2000. Mutations in synaptojanin disrupt synaptic vesicle recycling. *J. Cell Biol.* 150:589–600.

Published December 1, 2008

Haucke, V., M.R. Wenk, E.R. Chapman, K. Farsad, and P. De Camilli. 2000. Dual interaction of synaptotagmin with mu2- and alpha-adaptin facilitates clathrin-coated pit nucleation. *EMBO J.* 19:6011–6019.

Heuser, J.E., and T.S. Reese. 1973. Evidence for recycling of synaptic vesicle membrane during transmitter release at the frog neuromuscular junction. *J. Cell Biol.* 57:315–344.

Honing, S., D. Ricotta, M. Krauss, K. Spate, B. Spolaore, A. Motley, M. Robinson, C. Robinson, V. Haucke, and D.J. Owen. 2005. Phosphatidylinositol-(4,5)-bisphosphate regulates sorting signal recognition by the clathrin-associated adaptor complex AP2. *Mol. Cell.* 18:519–531.

Jorgensen, E.M., E. Hartwieg, K. Schuske, M.L. Nonet, Y. Jin, and H.R. Horvitz. 1995. Defective recycling of synaptic vesicles in synaptotagmin mutants of *Caenorhabditis elegans*. *Nature.* 378:196–199.

Keen, J.H. 1987. Clathrin assembly proteins: affinity purification and a model for coat assembly. *J. Cell Biol.* 105:1989–1998.

Lee, J., G.D. Jongeward, and P.W. Sternberg. 1994. unc-101, a gene required for many aspects of *Caenorhabditis elegans* development and behavior, encodes a clathrin-associatd protein. *Genes Dev.* 8:60–73.

Lewin, D.A., and I. Mellman. 1998. Sorting out adaptors. *Biochim. Biophys. Acta.* 1401:129–145.

Liu, Q., B. Chen, Q. Ge, and Z.W. Wang. 2007. Presynaptic Ca2+/calmodulin-dependent protein kinase II modulates neurotransmitter release by activating BK channels at *Caenorhabditis elegans* neuromuscular junction. *J. Neurosci.* 27:10404–10413.

Mahaffey, D.T., J.S. Peeler, F.M. Brodsky, and R.G. Anderson. 1990. Clathrin-coated pits contain an integral membrane protein that binds the AP-2 subunit with high affinity. *J. Biol. Chem.* 265:16514–16520.

Martina, J.A., C.J. Bonangelino, R.C. Aguilar, and J.S. Bonifacino. 2001. Stonin 2: an adaptor-like protein that interacts with components of the endocytic machinery. *J. Cell Biol.* 153:1111–1120.

Matsui, W., and T. Kirchhausen. 1990. Stabilization of clathrin coats by the core of the clathrin-associated protein complex AP-2. *Biochemistry.* 29:10791–10798.

Maycox, P.R., E. Link, A. Reetz, S.A. Morris, and R. Jahn. 1992. Clathrin-coated vesicles in nervous tissue are involved primarily in synaptic vesicle recycling. *J. Cell Biol.* 118:1379–1388.

Motley, A., N.A. Bright, M.N. Seaman, and M.S. Robinson. 2003. Clathrin-mediated endocytosis in AP-2–depleted cells. *J. Cell Biol.* 162:909–918.

Newton, A.J., T. Kirchhausen, and V.N. Murthy. 2006. Inhibition of dynamin completely blocks compensatory synaptic vesicle endocytosis. *Proc. Natl. Acad. Sci. USA.* 103:17955–17960.

Nguyen, M., A. Alfonso, C.D. Johnson, and J.B. Rand. 1995. *Caenorhabditis elegans* mutants resistant to inhibitors of acetylcholinesterase. *Genetics.* 140:527–535.

Nonet, M.L., A.M. Holgado, F. Brewer, C.J. Serpe, B.A. Norbeck, J. Holleran, L. Wei, E. Hartwieg, E.M. Jorgensen, and A. Alfonso. 1999. UNC-11, a *Caenorhabditis elegans* AP180 homologue, regulates the size and protein composition of synaptic vesicles. *Mol. Biol. Cell.* 10:2343–2360.

Ohno, H., J. Stewart, M.C. Fournier, H. Bosshart, I. Rhee, S. Miyatake, T. Saito, A. Gallusser, T. Kirchhausen, and J.S. Bonifacino. 1995. Interaction of tyrosine-based sorting signals with clathrin-associated proteins. *Science.* 269:1872–1875.

Owen, D.J., and P.R. Evans. 1998. A structural explanation for the recognition of tyrosine-based endocytotic signals. *Science.* 282:1327–1332.

Pan, C.L., P.D. Baum, M. Gu, E.M. Jorgensen, S.G. Clark, and G. Garriga. 2008. *C. elegans* AP-2 and retromer control Wnt signaling by regulating mig-14/Wntless. *Dev. Cell.* 14:132–139.

Phan, H.L., J.A. Finlay, D.S. Chu, P.K. Tan, T. Kirchhausen, and G.S. Payne. 1994. The *Saccharomyces cerevisiae* APS1 gene encodes a homolog of the small subunit of the mammalian clathrin AP-1 complex: evidence for functional interaction with clathrin at the Golgi complex. *EMBO J.* 13:1706–1717.

Richmond, J.E., and E.M. Jorgensen. 1999. One GABA and two acetylcholine receptors function at the *C. elegans* neuromuscular junction. *Nat. Neurosci.* 2:791–797.

Robinson, M.S. 2004. Adaptable adaptors for coated vesicles. *Trends Cell Biol.* 14:167–174.

Robinson, M.S., and J.S. Bonifacino. 2001. Adaptor-related proteins. *Curr. Opin. Cell Biol.* 13:444–453.

Rohde, G., D. Wenzel, and V. Haucke. 2002. A phosphatidylinositol (4,5)-bisphosphate binding site within μ2-adaptin regulates clathrin-mediated endocytosis. *J. Cell Biol.* 158:209–214.

Schuske, K.R., J.E. Richmond, D.S. Matthies, W.S. Davis, S. Runz, D.A. Rube, A.M. van der Bliek, and E.M. Jorgensen. 2003. Endophilin is required for synaptic vesicle endocytosis by localizing synaptojanin. *Neuron.* 40:749–762.

Schuske, K., M.T. Palfreyman, S. Watanabe, and E.M. Jorgensen. 2007. UNC-46 is required for trafficking of the vesicular GABA transporter. *Nat. Neurosci.* 10:846–853.

Shim, J., and J. Lee. 2000. Molecular genetic analysis of apm-2 and aps-2, genes encoding the medium and small chains of the AP-2 clathrin-associated protein complex in the nematode *Caenorhabditis elegans*. *Mol. Cells.* 10:309–316.

Simpson, F., A.A. Peden, L. Christopoulou, and M.S. Robinson. 1997. Characterization of the adaptor-related protein complex, AP-3. *J. Cell Biol.* 137:835–845.

Traub, L.M. 2003. Sorting it out: AP-2 and alternate clathrin adaptors in endocytic cargo selection. *J. Cell Biol.* 163:203–208.

Verstreken, P., O. Kjaerulff, T.E. Lloyd, R. Atkinson, Y. Zhou, I.A. Meinertzhagen, and H.J. Bellen. 2002. Endophilin mutations block clathrin-mediated endocytosis but not neurotransmitter release. *Cell.* 109:101–112.

Verstreken, P., T.W. Koh, K.L. Schulze, R.G. Zhai, P.R. Hiesinger, Y. Zhou, S.Q. Mehta, Y. Cao, J. Roos, and H.J. Bellen. 2003. Synaptojanin is recruited by endophilin to promote synaptic vesicle uncoating. *Neuron.* 40:733–748.

Walther, K., M.K. Diril, N. Jung, and V. Haucke. 2004. Functional dissection of the interactions of stonin 2 with the adaptor complex AP-2 and synaptotagmin. *Proc. Natl. Acad. Sci. USA.* 101:964–969.

Zhang, B., Y.H. Koh, R.B. Beckstead, V. Budnik, B. Ganetzky, and H.J. Bellen. 1998. Synaptic vesicle size and number are regulated by a clathrin adaptor protein required for endocytosis. *Neuron.* 21:1465–1475.

Zhang, J.Z., B.A. Davletov, T.C. Sudhof, and R.G. Anderson. 1994. Synaptotagmin I is a high affinity receptor for clathrin AP-2: implications for membrane recycling. *Cell.* 78:751–760.

Published December 1, 2008

Supplemental Material

JCB

Gu et al., http://www.jcb.org/cgi/content/full/jcb.200806088/DC1

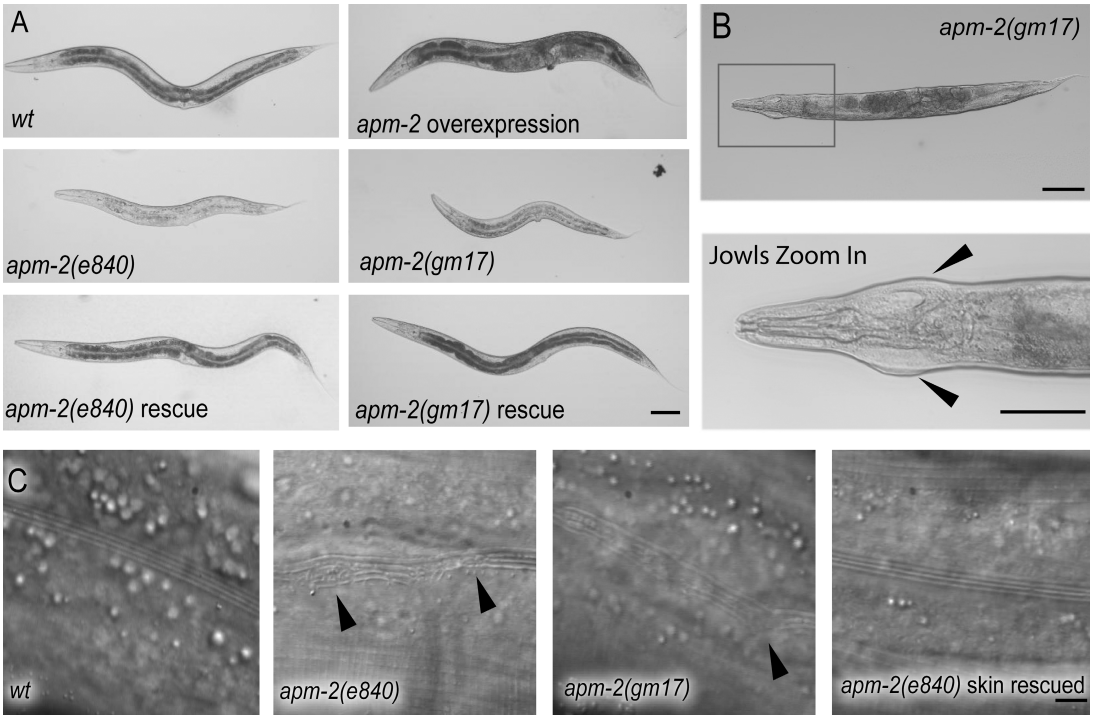

Figure S1. **Rescue of the *apm-2* mutant phenotype.** (A) Bright field images of various *apm-2* genotypes are shown. For the wild type with overexpressed APM-2, the *apm-2* DNA was injected at 10 ng/µl; for *apm-2(e840)* and *apm-2(gm17)* rescued worms, the *apm-2* DNA was injected at 0.25 ng/µl. Bar, 100 µm. (B) Jowls phenotype of *apm-2* mutants. An *apm-2(gm17)* adult hermaphrodite (top) and enlargement of head of the same animal (bottom). Arrowheads indicate jowls. Bars, 100 µm. (C) Alae are cuticular ridges along the sides of animals. Both *apm-2* alleles exhibit breaks or buckles in the alae (arrowheads). The mosaic *apm-2(e840)* strain expressing APM-2::GFP in just the skin is rescued for breaks in the alae. Strain and genotype of skin-rescued strain: EG4029 *apm-2(e840)X; oxEx753[Ppdi-2::APM-2(cDNA)::GFP (pMG8) Punc-122::GFP]*. Bar, 5 µm.

Published December 1, 2008

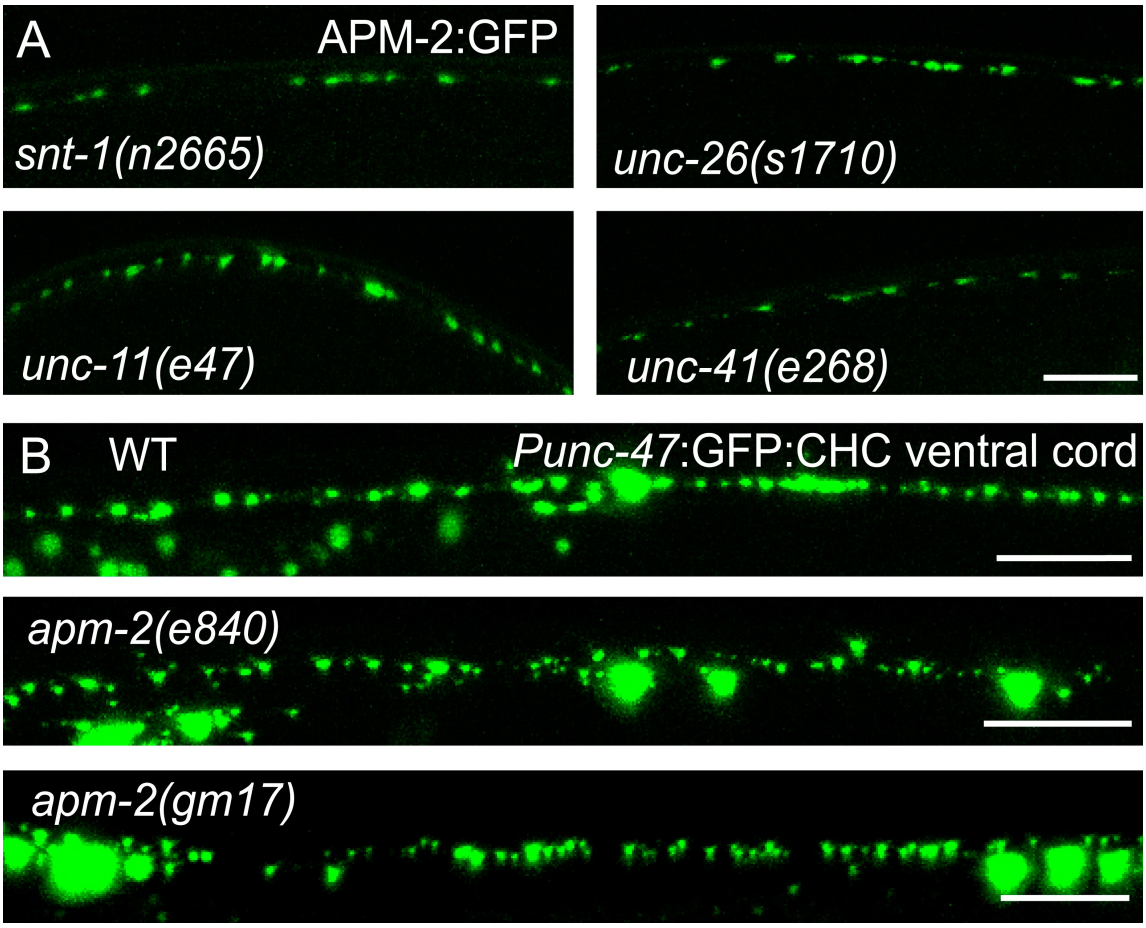

Figure S2. **APM-2 is not mislocalized in endocytic mutants.** (A) APM-2::GFP in the dorsal nerve cord of GABA neurons in *snt-1(n2665)*, *unc-11(e47)*, *unc-26(s1710)*, and *unc-41(e268)* animals. All of these mutants exhibit defects in endocytosis in *C. elegans* (Jorgensen, E.M., E. Hartwieg, K. Schuske, M.L. Nonet, Y. Jin, and H.R. Horvitz. 1995. *Nature*. 378:196–199; Zhang, B., Y.H. Koh, R.B. Beckstead, V. Budnik, B. Ganetzky, and H.J. Bellen. 1998. *Neuron*. 21:1465–1475; Nonet, M.L., A.M. Holgado, F. Brewer, C.J. Serpe, B.A. Norbeck, J. Holleran, L. Wei, E. Hartwieg, E.M. Jorgensen, and A. Alfonso. 1999. *Mol. Biol. Cell.* 10:2343–2360; Harris, T.W., E. Hartwieg, H.R. Horvitz, and E.M. Jorgensen. 2000. *J. Cell Biol.* 150:589–600; Martina, J.A., C.J. Bonangelino, R.C. Aguilar, and J.S. Bonifacino. 2001. *J. Cell Biol.* 153:1111–1120). The fluorescent punctas correspond to synaptic varicosities along the dorsal muscles. (B) Clathrin heavy chain exhibits a punctate distribution in the ventral nerve cords of GABA neurons in both wild-type (EG3381 *oxIs164[Punc-47::GFP::CHC-1 lin-15(+)]IV; lin-15(n765)X*) and *apm-2* animals (EG3735 *oxIs164[Punc-47:GFP::CHC-1 lin-15(+)]IV; apm-2(e840)X* and EG3564 *oxIs164[Punc-47::GFP::CHC-1 lin-15(+)]IV; apm-2(gm17)X*). The large fluorescent spots are the cell bodies of neurons. Bars, 10 μm.

Published December 1, 2008

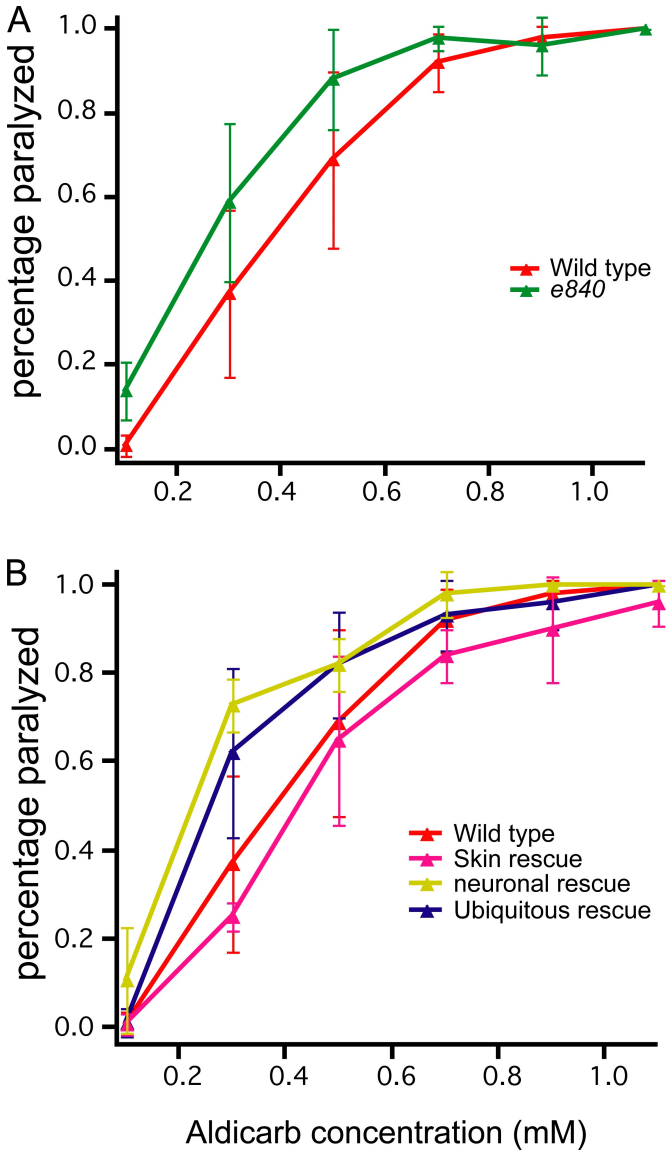

Figure S3. **Aldicarb sensitivity.** Percentage of adult animals paralyzed at given concentration after 4 h. (A) *apm-2(e840)* is aldicarb hypersensitive at 0.1 mM ($P < 0.01$), but it is not significantly different from wild type at other concentrations. (B) Aldicarb sensitivity of *apm-2(e840)* tissue-specific rescued animals. Ubiquitous and skin rescued animals are not significantly different from the wild type. Neuronal rescued animals are aldicarb hypersensitive at 0.3 mM ($P < 0.05$), but are not significantly different from wild type at other concentrations. For each genotype, 100 animals were tested at each concentration, except for neuronal rescue for which only 40 animals were tested at each concentration because of the paucity of transgenic animals. Values are expressed as mean ± SEM.

Published December 1, 2008

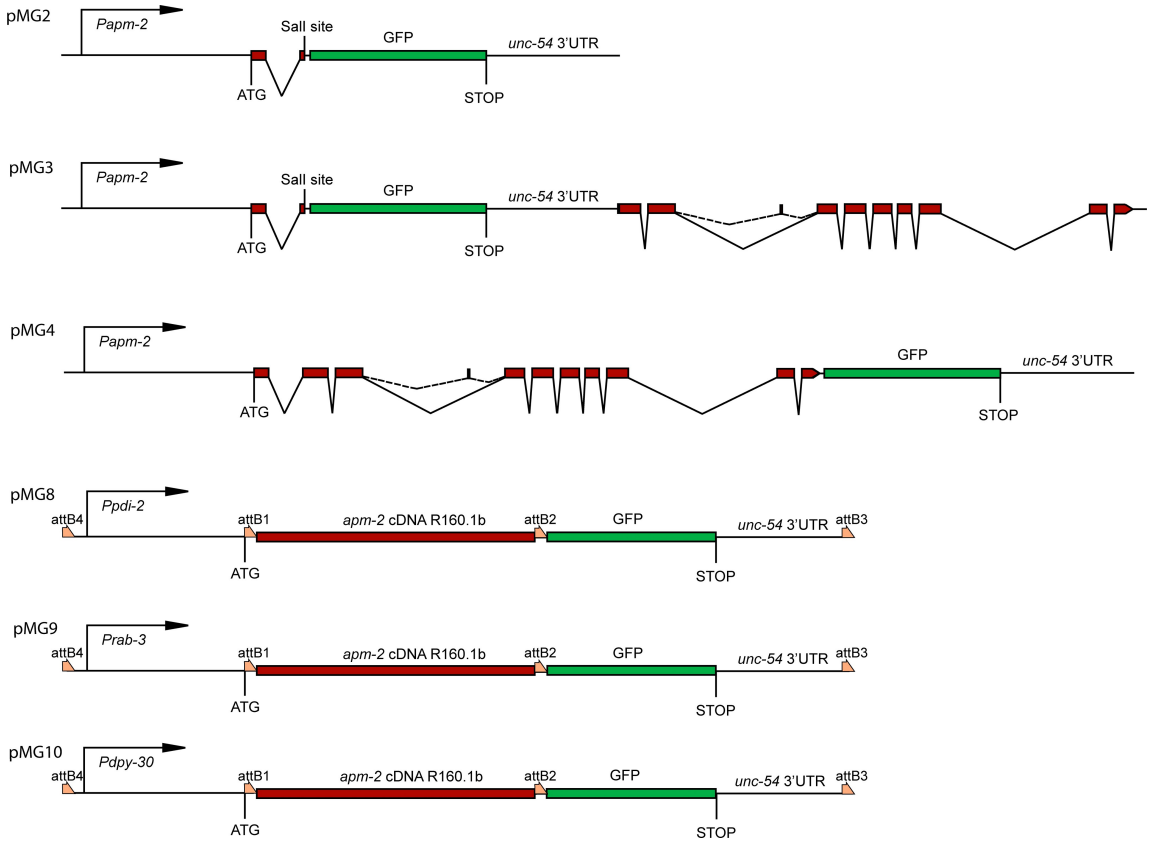

Figure S4. **Cartoon structure of *apm-2::GFP* DNA constructs.**

Published December 1, 2008

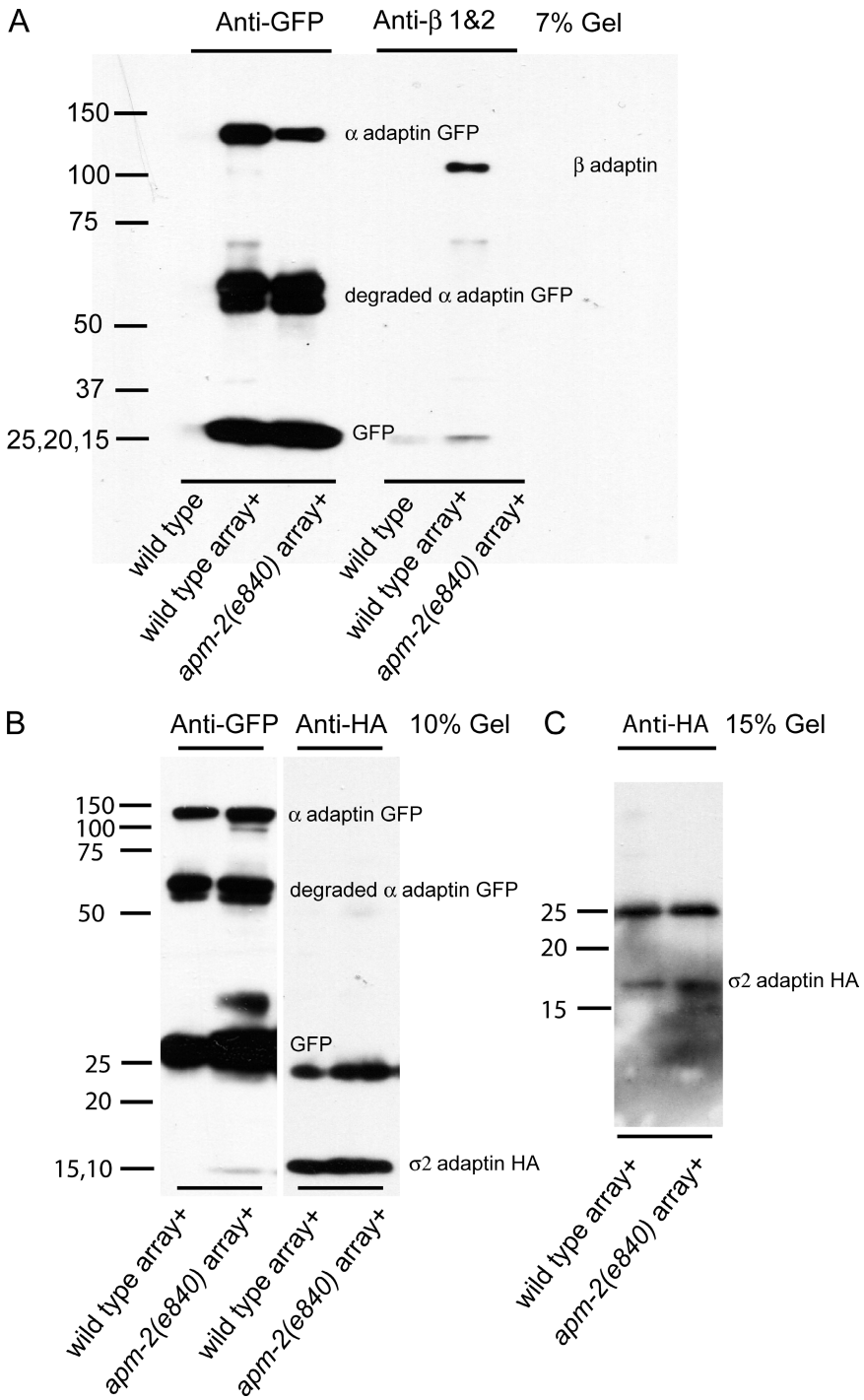

Figure S5. **Assembly of AP2 with or without μ2.** (A) Agarose beads conjugated with rat anti-GFP IgG2a were used to pull down APA-2::GFP from the worm lysate (strain carries array *oxEx1275[Papa-2::APA-2::GFP; Punc-122::GFP]*.). The presence of APA-2::GFP and APB-1 from the pull-down samples were tested by Western blot. The failure to pull down β adaptin in the *apm-2* mutants was confirmed in four blots, from injections of the APA-2::GFP transgene at 1 and 10 ng/μl. (B) Agarose beads conjugated with rat anti-GFP IgG2a were used to pull down APA-2::GFP from the worm lysate (strain carries array *oxEx1276[Papa-2::APA-2::GFP; Paps-2::APS-2::HA; Punc-122::GFP]*.). The presence of APA-2::GFP and APS-2::HA from the pull-down samples was tested by Western blot. (C) The molecular mass of APS-2::HA could not be resolved from 10% SDS-PAGE in B. The same samples were run again in 15% SDS-PAGE and blotted with anti-HA mouse IgG2b.

CHAPTER 3

AP2 SUBUNITS CONTRIBUTE INDEPENDENTLY TO SYNAPTIC VESICLE ENDOCYTOSIS IN *CAENORHABDITIS ELEGANS*.

My contribution to this work includes the following:

1. Isolating the null allele of *apa-2*, which encodes the orthologue of α adaptin in *C. elegans.*
2. Investigating the pre-synaptic localization of APA-2.
3. Examining the distribution of vesicle proteins in the dorsal nerve cord in *apa-2* and *apm-2 apa-2* double mutants
4. Tissue-specific rescue of *apa-2* and *apm-2 apa-2* mutants
5. Electron microscopy imaging of motor neurons in the ventral nerve cord from *apa-2*, *apm-2 apa-2* mutants and tissue-specific rescued animals
6. Thrashing assay on *apa-2* and *apm-2 apa-2* mutants

Shigeki Watanabe (University of Utah, Salt lake City) contributed to the following:
Electron microscopy analysis of *apa-2, apm-2 apa-2* mutants and tissue-specific rescued animals.

Qiang Liu (University of Utah, Salt lake City) contributed to the following:
Electrophysiological analysis of *apa-2, apm-2 apa-2* mutants and tissue-specific rescued animals.

Abstract

Multiple mechanisms for synaptic vesicle endocytosis might co-exist at presynaptic terminals. To determine the importance of clathrin-mediated endocytosis for synaptic vesicle recycling, we conducted a genetic screen and isolated a null allele of α adaptin from the AP2 complex in *C. elegans*. We found, in the absence of α adaptin, the other half of the AP2 complex is still localized and functioning. By building the double mutant with the existing μ2 adaptin knockout, we eliminated the entire AP2 complex from the worms. The double adaptin mutants exhibit a low survival rate; however, they can be rescued to a maintainable strain by introducing α and μ2 adaptins specifically back to the hypodermis. Ultrastructural analysis suggests that in α adaptin mutants, the total number of synaptic vesicles is reduced by 50% in motor neurons, which is similar to what has been observed from μ2 adaptin mutants. The double adaptin mutants have a more severe phenotype with a 70% vesicle reduction. When assayed by electrophysiology, skin-rescued α adaptin mutants exhibit 50% spontaneous release and 75% evoked release. The skin-rescued double mutants show more severe phenotypes with 30% spontaneous release and 50% evoked response. However, all of these mutants have mild swimming defects when assayed by worm thrashing. Taken together, our data suggest that most synaptic vesicles are recycled through an AP2-dependent process in *C. elegans* motor neurons. However, we have found that there is an AP2-independent endocytosis mechanism, either clathrin-dependent or clathrin-independent, that supports the observed residual synaptic vesicle recycling.

Introduction

Synaptic vesicles need to be recycled and refilled with neurotransmitters locally to support the high rate of neurotransmission at nerve terminals. Clathrin mediated-endocytosis has been confirmed as one mechanism for synaptic vesicle recycling (Augustine et al., 2006; Granseth et al., 2006; Logiudice et al., 2009). However different mechanisms of endocytosis have also been observed. One of them is bulk endocytosis, which tends to happen when synapses are under sustained or high-frequency stimulation (Gaffield et al., 2009; Meunier et al., 2010). Another mechanism is clathrin-independent kiss-and-run, which has fast kinetics with a τ of 1 s or less (Aravanis et al., 2003; Gandhi and Stevens, 2003). It is still controversial whether neurons employ all of these mechanisms or if only clathrin-mediated endocytosis is required.

To provide a better understanding of synaptic vesicle endocytosis, we disrupted clathrin-mediated endocytosis by eliminating the major adaptor AP2. The AP2 complex has four subunits– two big subunits, α and β2 adaptin, a medium subunit, μ2 adaptin, and a small subunit, σ2 adaptin. It functions at the plasma membrane as an interaction hub for clathrin, transmembrane cargoes and other endocytic accessory proteins (Robinson, 2004; Traub, 2003). Because of this, genetically disrupting AP2 components induces embryonic lethality in mice and *Drosophila* (Gonzalez-Gaitan and Jackle, 1997; Mitsunari et al., 2005). However, worms missing μ2 adaptin are egg-laying defective but can grow to adulthood (Pan et al., 2008). Our previous studies suggest that the relatively mild phenotype from worm μ2 adaptin mutants is likely due to the residual function of AP2. In *C. elegans,* α and σ2 adaptins are still capable of forming half of the AP2 complex and α is localized to the plasma membrane in the absence of μ2 (Gu et al., 2008). This agrees

with the crystallography data suggesting α is more closely associated with σ2 and μ2 is more closely associated with β2 (Collins et al., 2002a).

α adaptin contains an N-terminal trunk domain and a C-terminal appendage domain. The trunk domain is part of the AP2 core complex and has a $PI(4,5)P_2$ binding site that is responsible for AP2 localization at the plasma membrane (Collins et al., 2002a). The appendage domain can physically associate with endocytic accessory proteins through two interaction sites. One of them recognizes WxxF motifs found in synaptojanin, AAK1, and stonin2 (Mishra et al., 2004; Praefcke et al., 2004). The other binds DPW/F or FxDXF motifs found in binding partners including amphiphysin, Eps15 and Epsin (Owen et al., 1999). This mechanism of one common interaction site with multiple targets allows temporal and spatial regulation of clathrin-mediated endocytosis.

In *Drosophila,* a hypomorphic allele of α adaptin leads to slow moving larvae with inefficient FM-dye uptake upon stimulation at boutons (Gonzalez-Gaitan and Jackle, 1997). In cultured hippocampal neurons endocytosis is significantly slowed down but not abolished when AP2 is knocked down by 96% (Kim and Ryan, 2009). These findings suggest a requirement for AP2 in synaptic vesicle endocytosis. Here we characterize mutants lacking α adaptin, which is encoded by the gene *apa-2* in *C. elegans*. We demonstrat that in the absence of α adaptin, μ2 adaptin is capable of localizing to the cell surface and regulating the endocytosis of AP2-dependent cargo. In contrast, σ2 adaptin is essentially gone in the absence of α subunit. To completely block AP2 functions, we find that α and μ2 subunits must be removed simultaneously. For synaptic vesicle recycling, α adaptin is partially responsible for the synaptic localization of a subset of synaptic-vesicle proteins and the *apa-2* mutants show 50% reduction in the number of synaptic

vesicles. Only 30% of synaptic vesicles remain in skin rescued α and μ2 adaptin double mutant neurons, and these neurons exhibit 50% of the normal amount of evoked release after electrical stimulation. Behaviorally, both α adaptin mutants and α and μ2 adaptin skin-rescued double mutants are essentially not defective in a swimming assay. Taken together, our data demonstrate that AP2 complex is capable of working as two loosely-connected half complexes because blocking AP2 functions in *C. elegans* requires elimination of both α and μ2 adaptins. Surprisingly, some synaptic vesicles still appear to recycle at AP2-deficient synapses. This is possibly due to compensation by a functionally redundant clathrin adaptor or may represent a residual clathrin-independent endocytosis mechanism.

Results

Isolation of α adaptin null alleles

Based on phylogenetic analysis, the α adaptin ortholog in worms is encoded by the gene *apa-2* (Figure 3.1A, D). We have identified two alleles of *apa-2* (Figure 3.1B). The first allele, *b1044*, contains a 925 bp deletion, which starts within the second intron and ends in the middle of the fourth exon. We isolated a second allele, *ox422,* from a non-complementation screen for *b1044*. This allele has an A to T transition that changes K215 to an early stop. We failed to detect any wild-type APA-2 proteins in western blots from both of these alleles (Figure 3.1C), suggesting they are likely null alleles.

To determine where *apa-2* is expressed, we generated an APA-2::GFP fusion expressed under the control of the *apa-2* promoter. This construct can fully rescue *apa-2* mutants (data not shown), which is inconsistent with a previous study claiming that a C-terminal tagged α adaptin is completely nonfunctional (Motley et al., 2006). The GFP

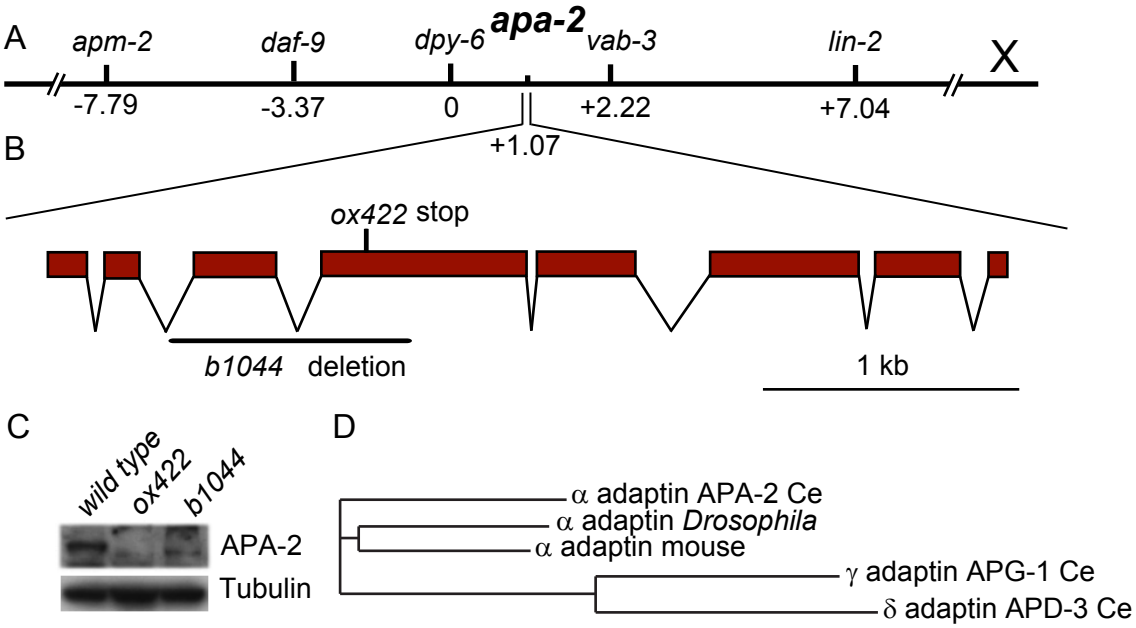

Figure 3.1. *apa-2* cloning. (A) Genetic map position of *apa-2* on chromosome X. (B) Genomic structure of the *apa-2* gene. The *b1044* allele deletes 925 bp from the second intron to the fourth exon. *ox422* is a A to T transition at Lys215, which is changed to a stop. (C) Western blot for detecting α adaptin expression in *apa-2* mutants. Both alleles of *apa-2* failed to show any α adaptin expression, suggesting they are null alleles. Antibodies are rabbit polyconal anti- α adaptin and mouse monoclonal anti-tubulin. (D) Phylogenetic tree of α adaptins from mouse, *Drosophila* and *C. elegan*s and the corresponding adaptins from other worm AP complexes. Accession numbers are listed as follows: α adaptin APA-2 Ce: NP_509572.1; α adaptin *Drosophila:* NP_476819.2; α adaptin mouse: NP_031485.3; γ adaptin APG-1 Ce: NP_740937.1 and δ adaptin APD-3 Ce: NP_494570.1.

signals are observed ubiquitously in transgenic worms (Figure 3.2A). Specifically, the fusion protein is expressed in three major tissues: nervous system, intestine and hypodermis (Figure 3.2B). In addition, GFP expression is also found around the vulva region and on the cell surface of coelomocytes (*C. elegans* scavenger cells) (Figure 3.2A). Thus APA-2 is broadly expressed in *C. elegans* in a pattern similar to that of μ2 adaptin (Gu et al., 2008).

α adaptin and μ2 adaptin play different roles in the *C. elegans* hypodermis

α adaptin *(apa-2)* mutants are grossly similar to μ2 adaptin *(apm-2)* mutants. Both adaptin mutants are egg-laying defective, and low percentages of both have cuticle protrusions on either side of the head. However the variable dumpy phenotype of *apa-2* is less severe than that of *apm-2* (Figure 3.3A). In μ2 adaptin mutants, expression of APM-2 under a skin-specific promoter can fully restore the worm body-length back to wild-type levels, whereas neuron-specific rescue has no effect on the dumpiness (Gu et al., 2008). We followed the same rescuing strategy for *apa-2* mutants (Figure 3.3B). In most aspects, the results for α and μ2 adaptin are similar: APA-2::GFP driven by a ubiquitous promoter can fully rescue the mutant animals (Figure 3.3C). Both skin- and neuron-rescued *apa-2* animals are egg-laying defective. The cuticle protrusions are rescued by hypodermal expression but not neuronal expression of APA-2 (Figure 3.3C). However, unlike in μ2 adaptin, the dumpy phenotype of *apa-2* is restored by neuron-specific rescue but not skin-specific rescue, and the neuron-rescued worms are even longer than the wild type (Figure 3.3A, C). This result suggests that α adaptin has different functions in the worm hypodermis compared to μ2 adaptin and different subunits of AP2 are not required

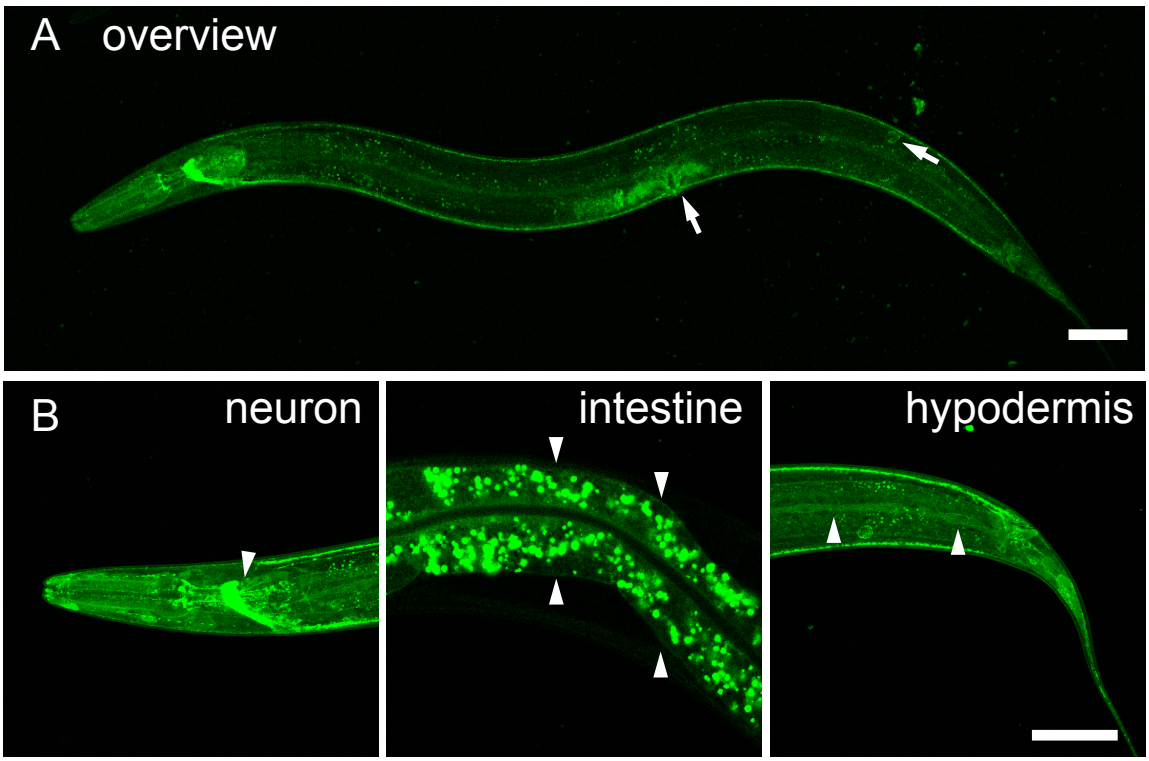

Figure 3.2. APA-2 is expressed ubiquitously as μ2 adaptin. (A) The expression pattern of translational fusion protein APA-2::GFP in young adult hermaphrodite. The worm is oriented dorsal up and anterior left. The white arrows indicate the GFP expression around the vulva region and in the scavenger cell, coelomocyte. (B) APA-2::GFP is expressed in three major tissues: neurons, intestine and hypodermis. The white arrow heads indicate the GFP expression in head nerve ring, intestine cells and seam cells from hypodermis. The scale bar represents 50 μm.

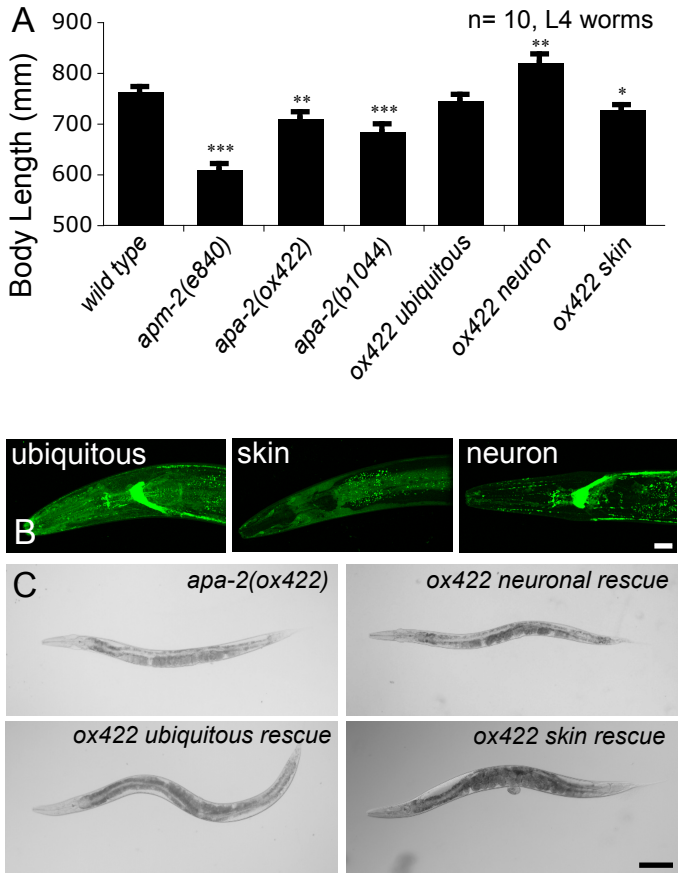

Figure 3.3. *apa-2(ox422)* tissue-specific rescu**e.** (A) Body length quantification of *apm-2(e840)* (null allele of µ2 adaptin)*, apa-2* mutants and *apa-2* tissue-specifc rescued animals. Average body length in µm ± SEM: wild type 762.79 ± 9.70; *apm-2(e840)* 609.35 ± 12.08; *apa-2(ox422)* 710.83 ± 12.23; *apa-2(b1044)* 684.26 ± 15.14; ubiquitous rescued *apa-2(ox422)* 773 ± 11.90; neuronal rescued *apa-2(ox422)* 820.32 ± 16.91; skin rescued *apa-2(ox422)* 727.45 ± 10.04. n = 10 L4 worms. (B) APA-2::GFP expression pattern under different promoters. Ubiquitous expression is driven by the *dpy-30* promoter. Hypodermal expression (skin) is driven by the *dpy-7* promoter. Neuronal expression is driven by the *rab-3* promoter. Worms are oriented anterior left and dorsal up. Images are confocal Z-stack projections through the whole worm or the tissue of interest. All worms were imaged under identical conditions. The scale bar represents 20 µm. (C) Bright field images of tissue-specific rescued *apa-2* mutants. Worms are rescued by strains carrying single-copy inserted transgenes. Ubiquitously rescued *apa-2* mutants are wild-type. Hypodermal rescued *apa*-2 mutants don't have jowls but are still Dpy and Egl. Neuronal rescued *apa-2* mutants are Egl with jowls but are not Dpy. The scale bar represents 100 µm. * P<0.05, ** P<0.01, *** P<0.001.

equally in every cell.

μ2 adaptin functions in the absence of α adaptin

In our previous study, we demonstrated that α adaptin is capable of localizing to the plasma membrane and forming a half AP2 complex with σ2 in μ2 adaptin mutants (Gu et al., 2008). Since both α and μ2 adaptins have a PI(4, 5)P_2 binding site (Collins et al., 2002a), we wondered if μ2 adaptin is also localized to the cell surface in the absence of the α subunit. Ubiquitously expressing APM-2::GFP can rescue *apm-2* mutants (data not shown). In these worms, the cell surface localization of APM-2::GFP molecules is most easily visualized on maturing oocytes in worm gonads (Figure 3.4A). Without α adaptin, APM-2::GFP is still present at plasma membrane (Figure 3.4A) although its total protein level is reduced (Figure 3.4B). This result suggests α adaptin contributes to the stability of AP2 complex; however, μ2 adaptin is properly recruited to the cell surface in the absence of α adaptin.

Although μ2 adaptin exhibits correct subcellular localization in *apa-2* mutants, it might be unable to mediate the endocytosis of AP2-dependent cargo. To test this, we examined the endocytosis of wntless (MIG-14) in both *apm-2* and *apa-2* mutants. Without the μ2 subunit, MIG-14::GFP shows strong accumulation on the cell surface in intestine cells, whereas in the absence of α adaptin, only mild accumulation of MIG-14::GFP is observed (Figure 3.4C-D). We also examined the endocytosis of a clathrin-independent cargo, human IL-2 receptor alpha subunit Tac (hTAC). This protein lacks internalization signal but still gets internalized through arf-6 dependent recycling (Radhakrishna and Donaldson, 1997). In *C. elegans,* hTAC goes to the basolateral

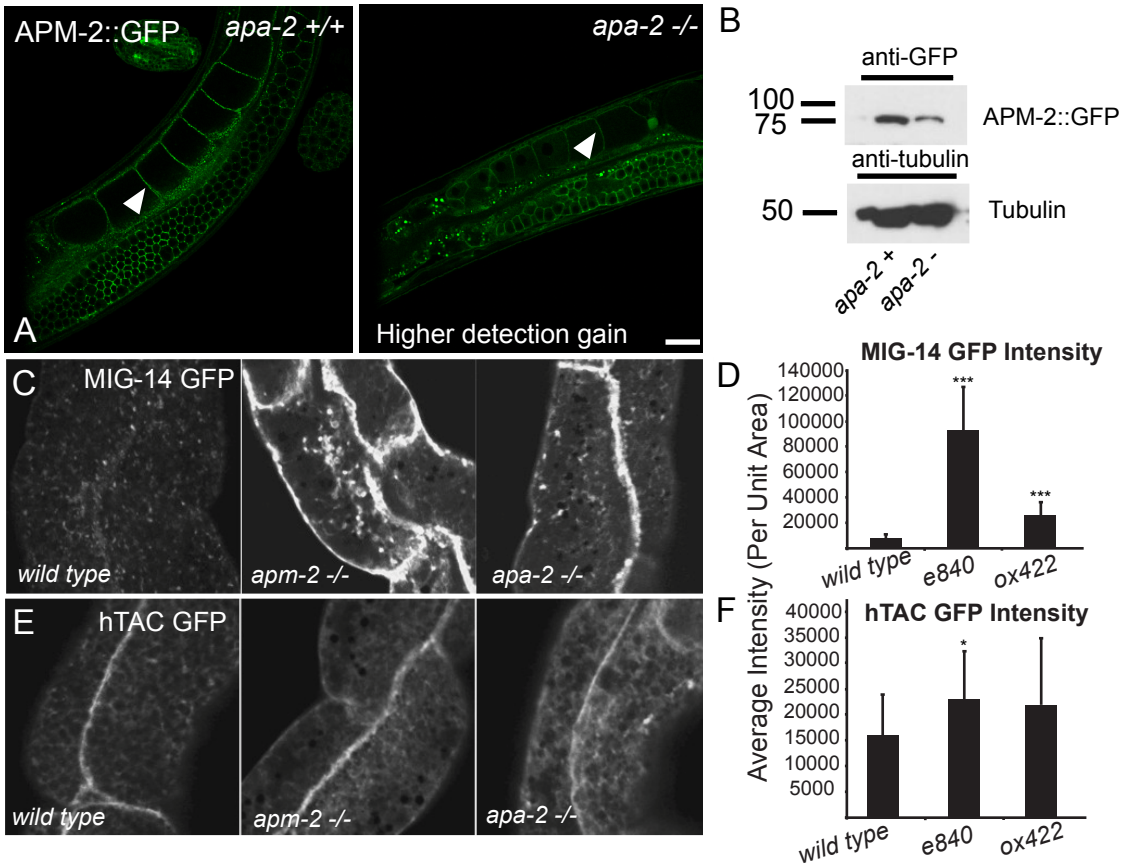

Figure 3.4. APM-2 is destabilized but functional in *apa-2* mutants. (A) APM-2::GFP expression in adult worm gonads. GFP signals are enriched at the plasma membrane, indicated by white arrow heads. The allele *apa-2(ox422)* is used. *apm-2::GFP* is driven by ubiquitous promoter *Pdpy-30* and the fusion protein can fully rescue *apm-2* mutants back to wild type (data not shown). The scale bar represents 20 μm. (B) Western blot for detecting the expression level of μ2 adaptin GFP in *apa-2(ox422).* The APM-2::GFP is reduced by 58% in the absence of *apa-2.* Antibodies are mouse monoclonal anti-GFP and anti-tubulin. (C) Endocytosis of an AP2-dependent cargo MIG-14 in worm intestine. MIG-14 is accumulated at the cell surface after disrupting the adaptor complex AP2. The defect is severe in *apm-2(e840)* but is mild in *apa-2(ox422).* (D) Quantification of total fluorescent intensity of MIG-14 in wild type and AP2 mutants. Fluorescent intensity mean±STD: *wild type* 7363±3498 n=18; *apm-2(e840)* 92648±34237 n=18; *apa-2(ox422)* 25110±11570 n=18. (E) Endocytosis of an AP2-independent cargo hTAC in worm intestine. hTAC endocytosis is essentially unaffected in AP2 mutants. (F) Quantification of total fluorescent intensity of hTAC in wild type and AP2 mutants. Fluorescent intensity mean±STD: *wild type* 16080±7875 n=18; *apm-2(e840)* 22948±9488 n=18; *apa-2(ox422)* 21950±12953 n=18. * P<0.05, ** P<0.01, *** P<0.001.

membrane of the intestine and its endocytosis is unaffected in either adaptin mutant (Figure 3.4E-F). These data suggest μ2 adaptin is the key subunit of AP2 mediating MIG-14 endocytosis. In the absence of α adaptin, μ2 adaptin is still localized to the cell surface and promotes the endocytosis of AP2-dependent cargo.

AP2 function is blocked in α and μ2 double mutants

If AP2 functions are essentially eliminated by mutating one of its subunits, the phenotypes of α and μ2 adaptin double mutants should resemble those of either adaptin single mutant. We used two independent allele combinations (*apm-2(e840) apa-2(ox422)* and *apm-2(gm17) apa-2(b1044)*) to build *apm-2 apa-2* double mutants. When *apa-2* and *apm-2* mutants are crossed together, the double mutants are actually much worse than either of the single mutants (Figure 3.5A). They grow extremely slowly and show a high-death rate with small brood size, which is reminiscent of the lethality phenotype of AP2 mutants from other organisms (Gonzalez-Gaitan and Jackle, 1997; Mitsunari et al., 2005). However, occasionally there are double mutants that grow to adulthood, suggesting that there are endocytosis mechanisms in the worm that do not depend on AP2 for viability.

To further test if AP2 is completely eliminated in *apa-2 apm-2* double mutants, we investigated the subcellular localization and the protein expression level of σ2 adaptin in these AP2 mutants. σ2 is the small subunit of AP2 and is encoded by the gene *aps-2* in *C. elegans*. In wild type, the expression pattern of APS-2::GFP is similar to that of APA-2::GFP. The plasma membrane localization of APS-2::GFP can be easily observed in maturing oocytes. In the absence of α adaptin, APS-2::GFP is essentially gone and its cell surface localization is totally disrupted; however, in *apm-2* mutants, APS-2::GFP is still present and could maintain its cell surface and synaptic localization (Figure 3.5B). A

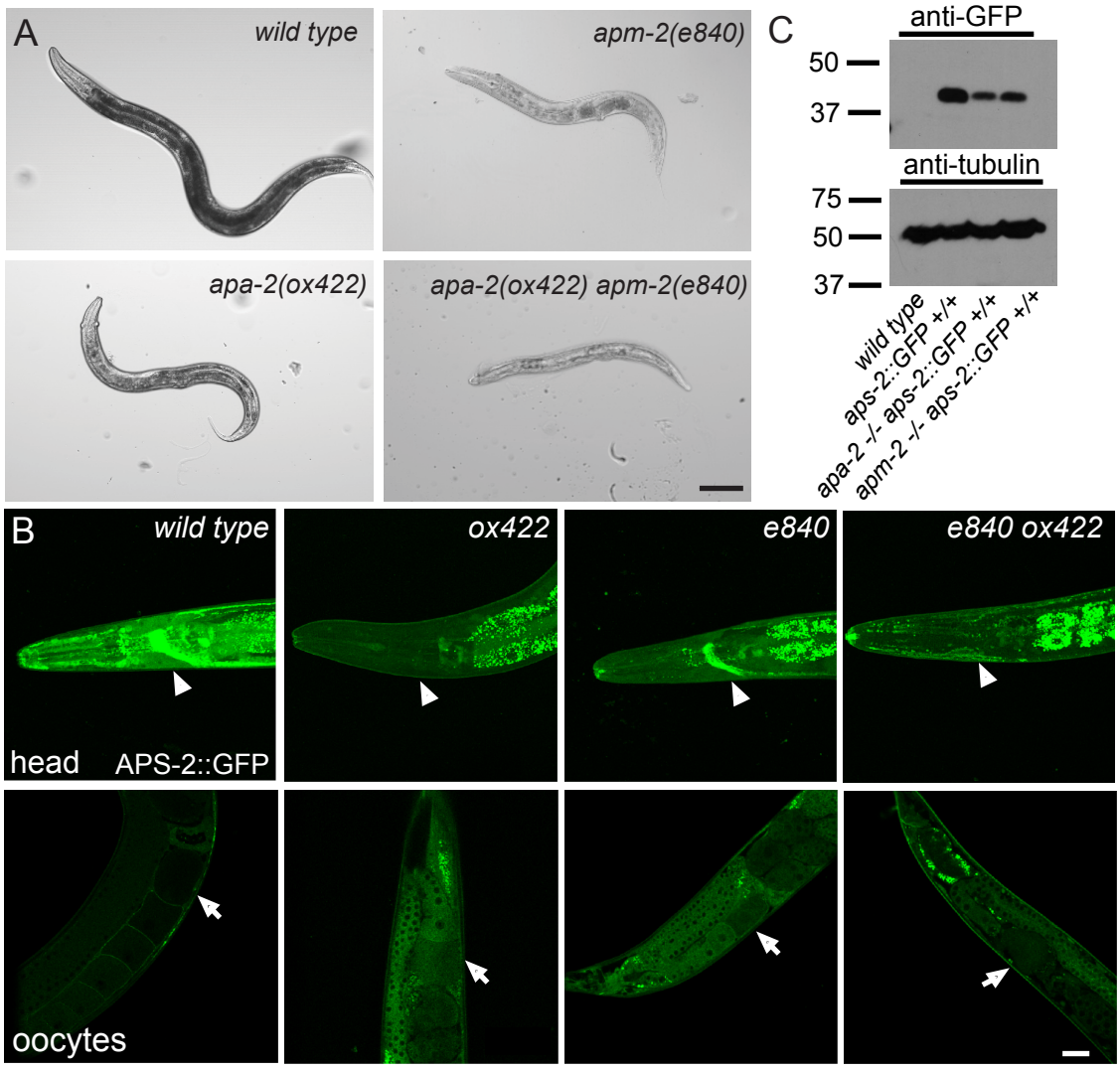

Figure 3.5. AP2 complex is essentially eliminated in *apm-2 apa-2* double mutants. (A) Bright field images of *wild type, apm-2(e840), apa-2(ox422)* and *apm-2(e840) apa-2(ox422)*. The *apm-2(e840) apa-2(ox422)* double mutant is sicker than either of the single mutants. The scar bar represents 100 μm. (B) APS-2::GFP localization in different AP2 mutants. APS-2::GFP can still maintain its synaptic localization in neurons and its cell surface localization in oocytes without *apm-2*. These localizations are totally disrupted in the absence of *apa-2.* The synaptic localization is indicated by white arrow heads and the cell surface localization is indicated by white arrows. The scale bar represents 20 μm. (C) Western blot for detecting the expression level of σ2 adaptin GFP in *apa-2(ox422)* and *apm-2(e840).* The protein level is reduced by 60% in *apa-2(ox422)* and is reduced by 46% in *apm-2(e840).* Antibodies are mouse monoclonal anti-GFP and anti-tubulin.

western blot for GFP also shows a more severe reduction of APS-2::GFP in *apa-2* mutants compared to *apm-2* mutants (Figure 3.5C). These results are consistent with the crystallography data that σ2 more closely associates with α adaptin to form half of the AP2 complex (Collins et al., 2002a). APS-2::GFP also shows a similar loss of cell surface localization in *apm-2 apa-2* double mutants to that of *apa-2* single mutants (Figure 3.5B). Because β adaptin is shared between AP1 and AP2 in *C. elegans*, all adaptins specific to AP2 complex are eliminated in *apm-2 apa-2* double mutants. Due to the low viability of this double mutant, it is almost impossible to maintain it as a regular lab strain. However, when α and μ2 adaptins are simultaneously introduced back into the hypodermis, 100% of the double mutants grow into adults. These rescued animals are still egg-laying defective and slow-growing.

Taken together, our data suggest residual function of AP2 remains in both *apa-2* and *apm-2* single mutants but that the entire AP2 complex is eliminated when α and μ2 adaptin are mutated simultaneously. Skin-rescued α and μ2 adaptin double mutants can grow into viable adults, thus allowing the opportunity to study AP2-knockout synapses in a living organism.

Vesicle protein localization in α mutants

Proteins involved in synaptic vesicle endocytosis should localize to synapses. We assayed the synaptic localization of APA-2 by expressing an *apa-2::GFP* fusion construct specifically in GABAergic neurons. In this subset of neurons, APA-2 colocalizes with a synaptic vesicle protein, synaptobrevin, in both the dorsal and ventral nerve cords (Figure 3.6A). This result suggests α adaptin, similar to μ2 adaptin (Gu et al., 2008), associates with synaptic varicosities.

Figure 3.6. APA-2 colocalizes with synaptobrevin at synapses and is partially required for synaptic localization of a subset of synaptic vesicle proteins. (A) Young adult hermaphrodites were used for imaging. Left: APA-2 and synaptobrevin localize at the dorsal nerve cord from GABAergic neurons. Top, GFP–tagged APA-2 in the GABA neuron processes in the dorsal nerve cord. Middle, tagRFP-tagged synaptobrevin in the GABA neuron processes in the dorsal nerve cord. Synaptobrevin is localized to synaptic regions. The fluorescent puncta correspond to synaptic varicosities along the dorsal muscles (white arrow head). Bottom, merged image demonstrates that APA-2-GFP colocalizes with synaptobrevin at synapses. Right: APA-2 and synaptobrevin localization at the ventral nerve cord from GABAergic neurons. A GABA neuron cell body is indicated by the white arrow. Images are confocal Z-stack projections through the worm nerve cord. The scale bar represents 10 μm. (B) Synaptic localization of synaptic vesicle proteins in *apa-2* and *apm-2 apa-2* double mutants. For UNC-47 and synaptogyrin (SNG), GFP-tagged proteins were expressed in GABAergic neurons and imaged in the dorsal nerve cord. Presynaptic varicosities of neuromuscular junctions along the dorsal nerve cord of an adult hermaphrodite are visible as fluorescent puncta. For synaptotagmin (SNT), GFP-tagged protein is expressed in all neurons under its own promoter and imaged in ventral sublateral cords. The axon regions with increased fluorescence are indicated by white arrow heads. Images are confocal Z-stack projection through the worm nerve cord. The scale bar represents 10 μm. (C) Quantification of the average fluorescent intensity ratio between axon region and synaptic region. Ratio of SNT-1::GFP mean± SEM: *wild type* 0.041±0.007 n=10; *apa-2(ox422)* 0.204±0.029 n=10; *apa-2(b1044)* 0.196±0.017 n=10; *apm-2(e840) apa-2(ox422)* 0.219±0.032 n=6. Ratio of UNC-47::GFP mean± SEM: *wild type* 0.108±0.004 n=8; *apa-2(ox422)* 0.239±0.009 n=8; *apa-2(b1044)* 0.22±0.024 n=7; *apm-2(e840) apa-2(ox422)* 0.247±0.032 n=6. Ratio of SNG-1::GFP mean± SEM: *wild type* 0.077±0.008 n=8; *apa-2(ox422)* 0.116±0.019 n=10; *apa-2(b1044)* 0.095±0.011 n=10; *apm-2(e840) apa-2(ox422)* 0.143±0.032 n=5. * $P<0.05$, ** $P<0.01$, *** $P<0.001$.

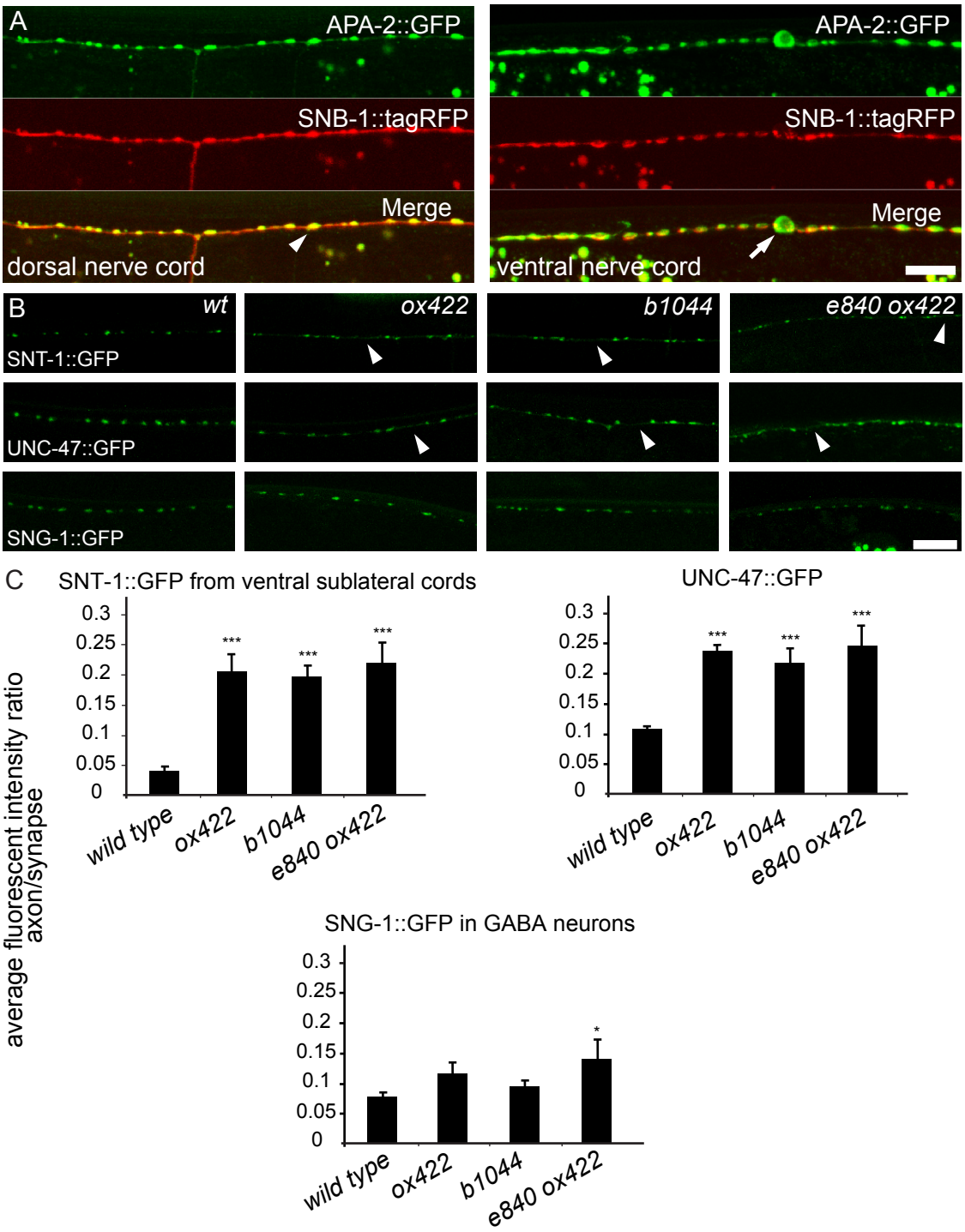
A
APA-2::GFP
SNB-1::tagRFP
Merge
dorsal nerve cord
APA-2::GFP
SNB-1::tagRFP
Merge
ventral nerve cord
B
wt
ox422
b1044
e840 ox422
SNT-1::GFP
UNC-47::GFP
SNG-1::GFP
C
SNT-1::GFP from ventral sublateral cords
UNC-47::GFP
SNG-1::GFP in GABA neurons
average fluorescent intensity ratio
axon/synapse
0.3
0.25
0.2
0.15
0.1
0.05
0
***
*
wild type
ox422
b1044
e840 ox422

One basic function of adaptors is to nucleate transmembrane cargoes into clathrin-coated pits. However the mechanism for resorting synaptic-vesicle proteins into pits is still poorly understood. We examined the requirement of AP2 in recycling several synaptic-vesicle proteins. Synaptotagmin I is well known as a binding partner of AP2 (Haucke et al., 2000; Zhang et al., 1994). In α adaptin and α μ2 adaptin double mutants, the fluorescence of synaptotagmin::GFP is slightly increased in the axonal region; however, most of the GFP signals are still enriched at synaptic varicosities (Figure 3.6B, C). This result suggests AP2 is not essential for synaptotagmin I endocytosis, which supports the idea that the AP2 binding site of synaptotagmin I is a regulator of endocytosis but not an internalization signal (Jarousse and Kelly, 2001). The next vesicle protein we tested was the vesicular GABA transporter, UNC-47. Because AP2 has been found to be involved in the trafficking of the vesicular acetylcholine transporter (Barbosa et al., 2002; Kim and Hersh, 2004), we wondered if AP2 is also required for the trafficking of UNC-47. The GFP distribution of UNC-47 is similar to that of synaptotagmin I (Figure 3.6B, C), which is consistent with a previous finding that the LAMP-related protein UNC-46 recruits UNC-47 to synapses (Schuske et al., 2007). We also tested the vesicle protein synaptogyrin. The synaptic localization of this protein has been found to be independent of the μ2 adaptin of AP2 (Zhao and Nonet, 2001). Here we again confirmed that its synaptic localization is almost unaffected by the absence of either α adaptin or the whole AP2 complex (Figure 3.6B, C). Thus our data suggest that AP2 contributes to the recycling of a subset of synaptic-vesicle proteins but it is not the specific adaptor for any of the proteins tested above.

Vesicle number is reduced in *apa-2* and *apm-2 apa-2* double mutants

The mild mislocalization of synaptotagmin I and UNC-47 in *apa*-2 mutants implies that endocytosis at synapses is compromised. To elucidate the role of AP2 in synaptic vesicle recycling, we used electron microscopy to directly visualize synaptic vesicles at motor neurons synapses (Figure 3.7).

The size of synaptic vesicles is roughly normal in *apa*-2 and skin-rescued *apm-2 apa-2* double mutants (Figure 3.8A), suggesting that the AP2 complex is not absolutely required for regulating vesicle size. However the number of vesicles is reduced in *apa-2(ox422)* mutants. Compared to wild type, *apa-2* mutants only have 56% the number of vesicles in cholinergic neurons and 29% in GABAergic neurons (Figure 3.8B). A similar amount of vesicle loss was also observed in *apa-2(b1044)* (data not shown). Neuron-rescue of *apa-2* fully restores the number of synaptic vesicles to the wild-type level, which suggests the defect is due to the loss of APA-2 within neurons. Unexpectedly, the skin-rescued *apa-2* animals are partially rescued for synaptic vesicle number in both cholinergic (71%) and GABAergic (59%) neurons (Figure 3.8B), suggesting hypodermis can regulate synaptic activity to some extent. Compared to the skin-rescued *apa-2(ox422)* mutants, the skin-rescued *apm-2(e840) apa-2(ox422)* double mutants have only 28% of the number of vesicles in cholinergic neurons and 31% in GABAergic neurons (Figure 3.8B). Since skin-rescued *apm-2* mutants still have 69% of synaptic vesicles (Gu et al., 2008), this result actually proves the idea that eliminating the function of AP2 requires knocking out both the α and μ2 adaptins. Taken together, our data suggest that AP2 plays an important role at motor neuron synapses and contributes to 70% of synaptic vesicle recycling.

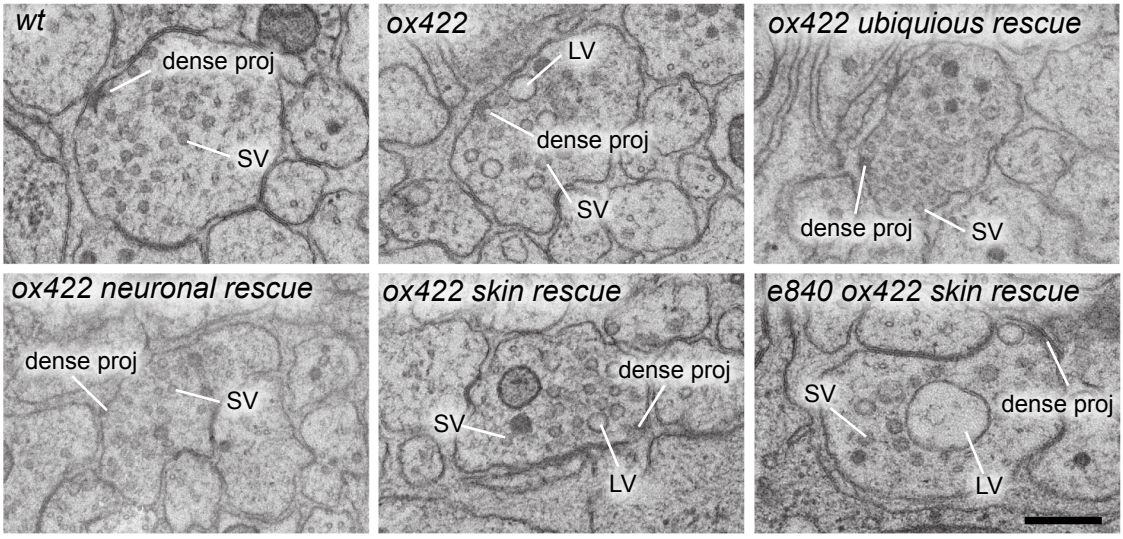

Figure 3.7. Neuromuscular junction ultrastructure of adaptin mutants. Representative images of neuromuscular junctions in the ventral nerve cord. The scale bar represents 200 nm. Abbreviations: SV, synaptic vesicle; LV, large vesicle; dense proj, dense projection.

Figure 3.8. Ultrastructure analysis of adaptin mutants. (A) Vesicle diameters are identical in wild type, *apa-2(ox422), apa-2(ox422)* tissue specific rescued and *apm-2(e840) apa-2(ox422)* skin-rescued animals. Average size of synaptic vesicles per profile containing a dense projection nm ± SEM: wild type ACh 28.38 ± 0.63, n= 17 vesicles; *apa-2(ox422)* ACh 28.67 ± 0.8, n= 8 vesicles; ubiquitous rescued *apa-2(ox422)* ACh 27.74 ± 0.54, n= 19 vesicles; neuronal rescued *apa-2(ox422)* ACh 27.79 ± 0.55, n= 22 vesicles; skin rescued *apa-2(ox422)* ACh 31.23 ± 0.75, n= 15 vesicles; skin rescued *apm-2(e840) apa-2(ox422)* ACh 32.51 ± 1.05, n= 5 vesicles wild type GABA 28.29 ± 0.45, n= 33 vesicles; *apa-2(ox422)* GABA 30.98 ± 0.99, n= 8 vesicles; ubiquitous rescued *apa-2(ox422)* GABA 27.51 ± 0.45, n= 30 vesicles; neuronal rescued *apa-2(ox422)* GABA 28.86 ± 0.52, n= 24 vesicles; skin rescued *apa-2(ox422)* GABA 31.52 ± 0.64, n= 18 vesicles; skin rescued *apm-2(e840) apa-2(ox422)* GABA 31.83 ± 0.96, n= 9 vesicles. (B) The number of synaptic vesicles is reduced in neurons lacking APM-2 or APM-2 and APA-2. Average number of synaptic vesicles per profile containing a dense projection ± SEM: wild type ACh 22 ± 1.41, n=35 synapses; *apa-2(ox422)* ACh 12.32 ± 1.06, n=66 synapses; ubiquitous rescued *apa-2(ox422)* ACh 19.11 ± 1.09, n=54 synapses; neuronal rescued *apa-2(ox422)* ACh 25.1 ± 1.47, n=49 synapses; skin rescued *apa-2(ox422)* ACh 15.59 ± 0.79, n=97 synapses; skin rescued *apm-2(e840) apa-2(ox422)* ACh 6.16 ± 0.76, n=47 synapses; wild type GABA 36.87 ± 1.46, n=36 synapses; *apa-2(ox422)* GABA 10.73 ± 0.74, n=46 synapse; ubiquitous rescued *apa-2(ox422)* GABA 33.88 ± 1.43, n=33 synapses; neuronal rescued *apa-2(ox422)* GABA 32.5 ± 2.65, n=40 synapses; skin rescued *apa-2(ox422)* GABA 21.73 ± 1.33, n=45 synapses; skin rescued *apm-2(e840) apa-2(ox422)* GABA 11.48 ± 0.94, n=52 synapses. (C) The number of large vesicles is greatly increased in neurons lacking APA-2. Average number of large vesicles per profile containing a dense projection ± SEM: wild type ACh 0.33 ± 0.11, n= 30 synapses; *apa-2(ox422)* ACh 3.06 ± 0.34, n= 72 synapses; ubiquitous rescued *apa-2(ox422)* ACh 0.68 ± 0.13, n= 43 synapses; neuronal rescued *apa-2(ox422)* ACh 0.56 ± 0.08, n= 62 synapses; skin rescued *apa-2(ox422)* ACh 1.8 ± 0.2, n= 97 synapses; skin rescued *apm-2(e840) apa-2(ox422)* ACh 2.24 ± 0.29, n= 53 synapses; wild type GABA 0.86 ± 0.13, n= 41 synapses; *apa-2(ox422)* GABA 4.87 ± 0.52, n= 43 synapses; ubiquitous rescued *apa-2(e840)* GABA 0.94 ± 0.22, n= 32 synapses; neuronal rescued *apa-2(ox422)* GABA 1.03 ± 0.18, n= 37 synapses; skin rescued *apa-2(ox422)* GABA 3.64 ± 0.54, n= 45 synapses; skin rescued *apm-2(e840) apa-2(ox422)* GABA 4.8 ± 0.42, n= 50 synapses. (D) Cumulative vesicle diameter curves in cholinergic neurons. * $P<0.05$, ** $P<0.01$, *** $P<0.001$.

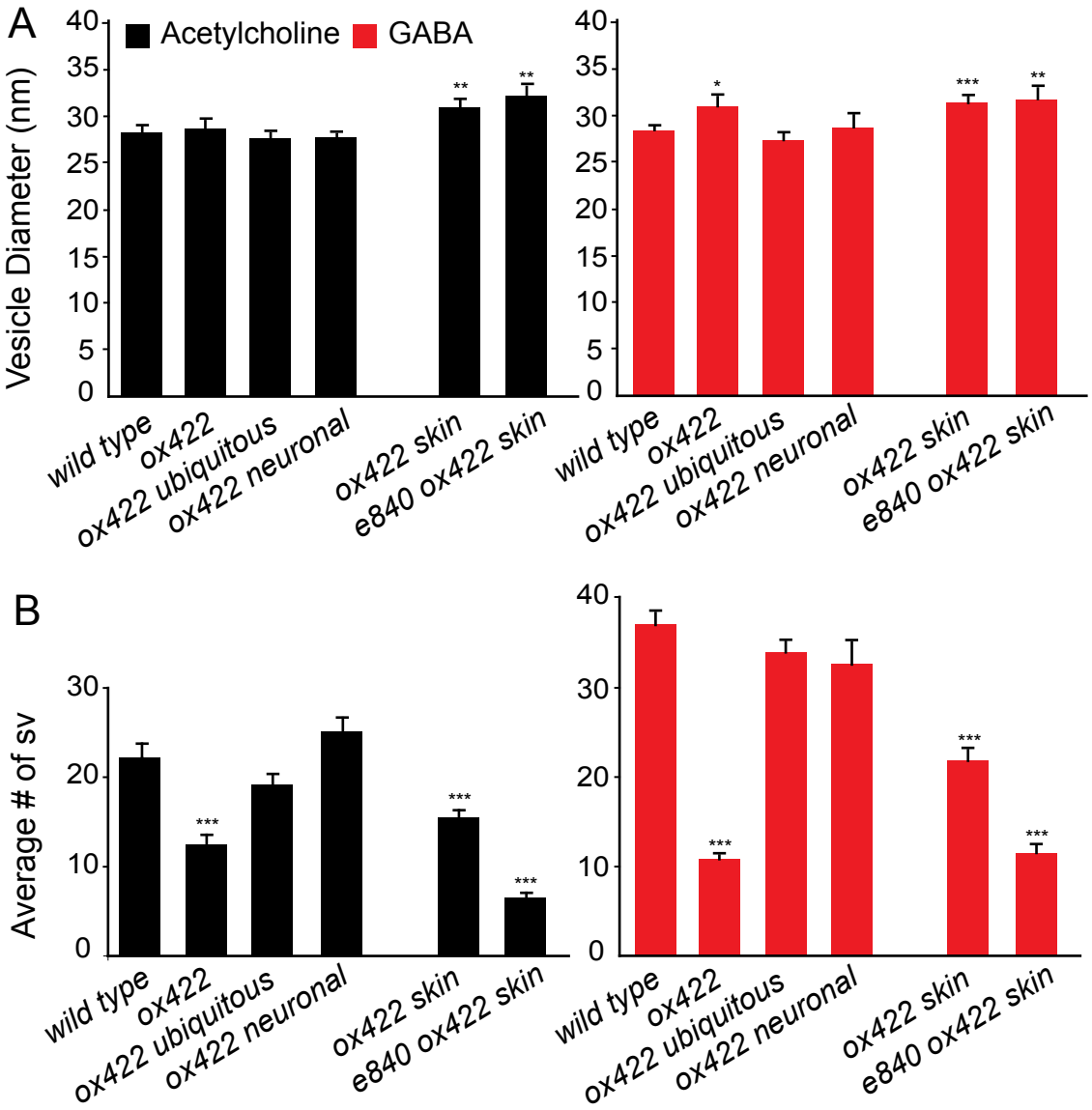
A
Acetylcholine
GABA
Vesicle Diameter (nm)
40
35
30
25
20
15
10
5
0
**
**
*
***
**
wild type
ox422
ox422 ubiquitous
ox422 neuronal
ox422 skin
e840 ox422 skin
B
Average # of sv
30
20
10
0
***
***
***
***
***
***
wild type
ox422
ox422 ubiquitous
ox422 neuronal
ox422 skin
e840 ox422 skin

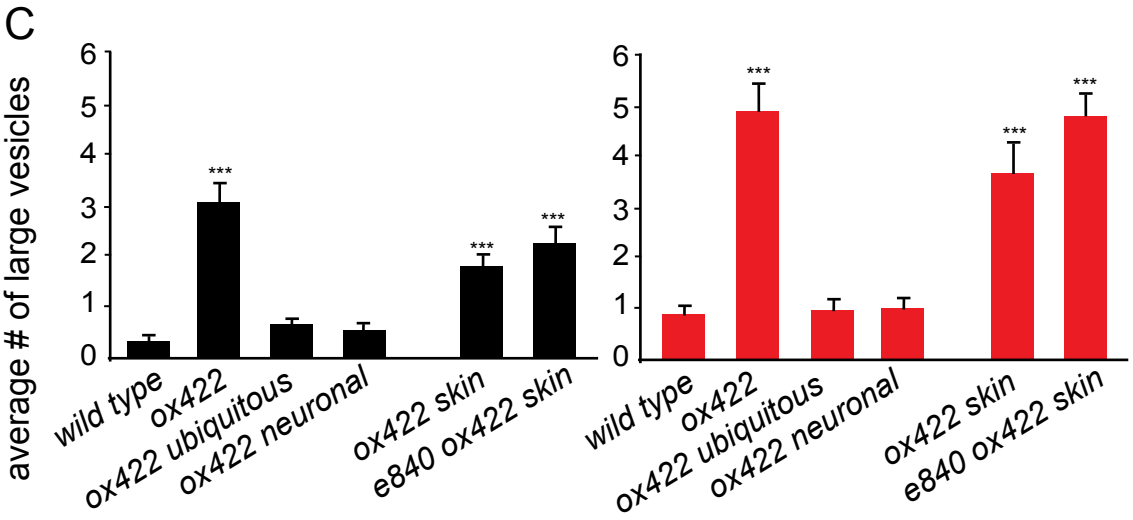
C
average # of large vesicles
0
1
2
3
4
5
6
***
wild type
ox422
ox422 ubiquitous
ox422 neuronal
ox422 skin
e840 ox422 skin

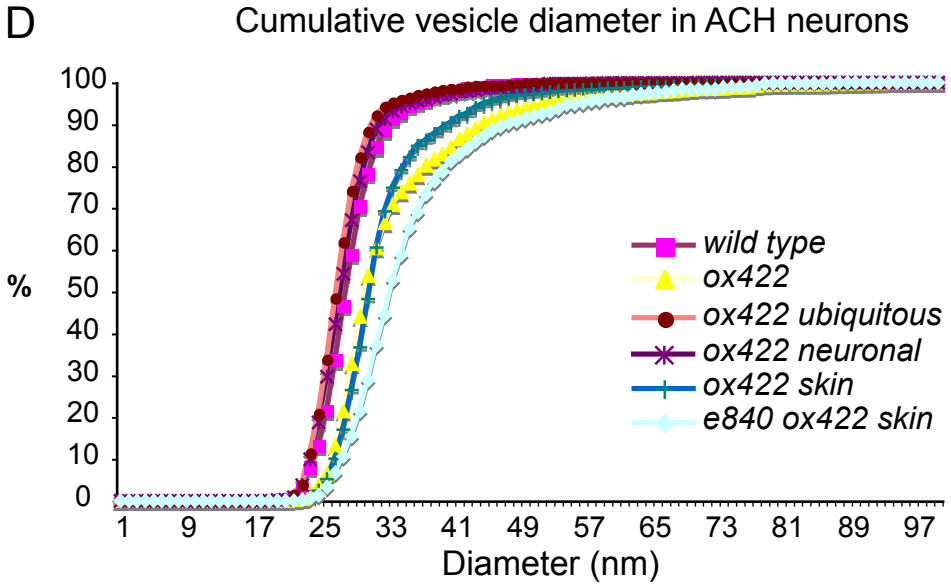
D
Cumulative vesicle diameter in ACH neurons
%
0
10
20
30
40
50
60
70
80
90
100
1
9
17
25
33
41
49
57
65
73
81
89
97
Diameter (nm)
wild type
ox422
ox422 ubiquitous
ox422 neuronal
ox422 skin
e840 ox422 skin

Another noticeable phenotype by electron microscopy is that *apa-2(ox422)* synapses have an accumulation of large vesicles (diameter > 40nm) (Figure 3.8C, D). A similar phenotype is observed in skin-rescued *apm-2 apa-2* double mutants (Figure 3.8C, D). We speculate that these large vesicles are endosome intermediates generated by bulk endocytosis. This observation suggests that there may be a shift from clathrin-mediated endocytosis to bulk endocytosis in *apa-2* mutant synapses.

apa-2 and *apm-2 apa-2* double mutants have impaired neurotransmission

In the absence of AP2, the number of synaptic vesicles is largely reduced, which is likely to affect neurotransmission at synapses. Here we assayed the direct release of neurotransmitters by electrophysiology (Figure 3.9A, B). In *apa-2(ox422)* mutants, the amplitude from spontaneously released vesicles is increased by 40% (Figure 3.9C). Since AP2 is known to regulate the recycling of AMPA (Kastning et al., 2007) and GABA(A) receptors (Kittler et al., 2005; Vithlani and Moss, 2009), the enhanced mini amplitude could be due to an increase in postsynaptic receptor number. We found this not to be the case, as the neuronal rescued *apa-2* mutants exhibit a normal mini amplitude (Figure 3.9C), suggesting the mini defect is caused by a loss of APA-2 specifically in neurons. The increased mini amplitude might be from direct release of large vesicles accumulated in *apa-2* mutants.

In our previous study, we demonstrated that skin-rescued *apm-2* mutants have 60% of the normal rate of minis, which is roughly proportional to the number of residual synaptic vesicles (Gu et al., 2008). Surprisingly, *apa-2* mutants have a noticeable 80% reduction in mini frequency. The skin-rescued *apa-2* animals that only lose 30% of synaptic vesicles partially restore the mini frequency to 50% (Figure 3.9D). Therefore,

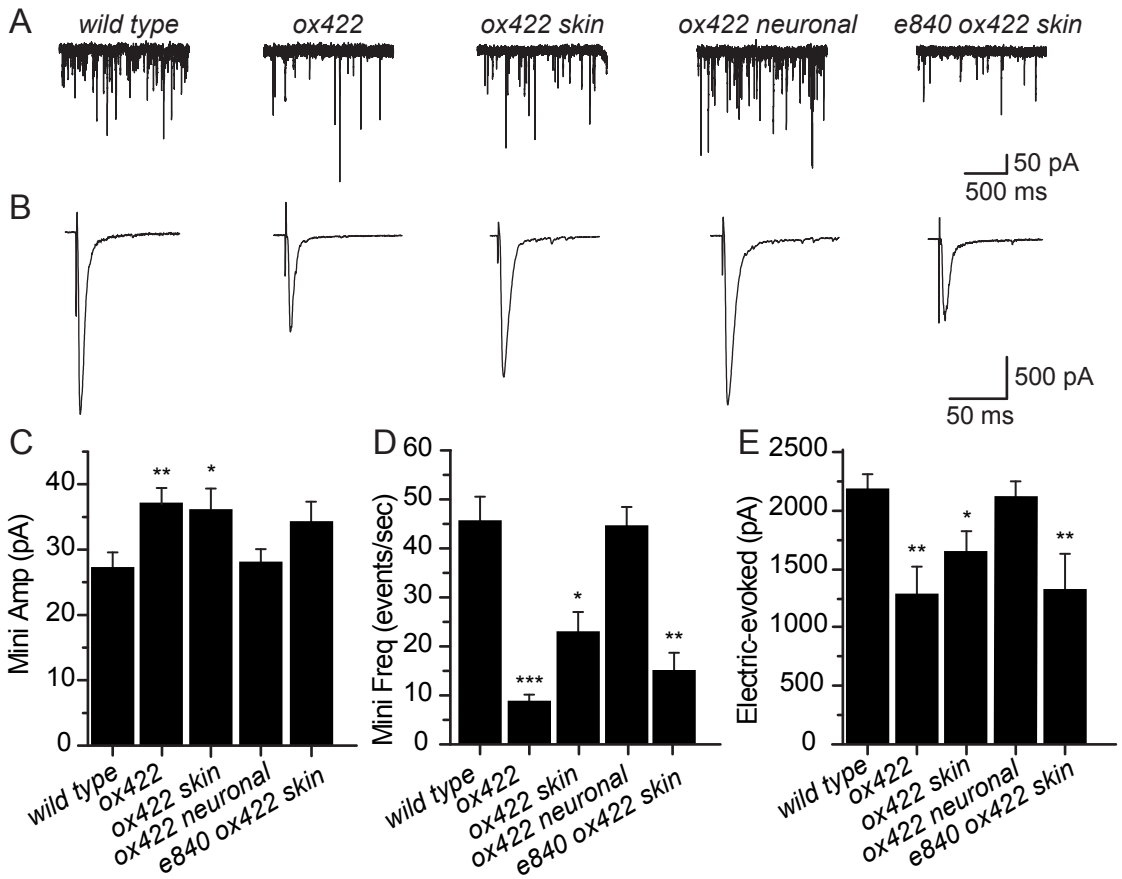

Figure 3.9. Electrophysiological analysis at neuromuscular junctions of various *apa-2(ox422)* tissue specific rescued worms and skin-rescued *apm-2(e840) apa-2(ox422)* double mutants. (A) sample traces of miniature postsynaptic current (mPSC) recorded from *wild type*, *apa-2(ox422)*, *apa-2(ox422)* neuronal rescued, *apa-2(ox422)* skin rescued, *apm-2(e840) apa-2(ox422)* skin rescued worms. (B) sample traces of evoked postsynaptic current (ePSC) recorded from above animals. (C Summary of mPSC amplitude (pA±SEM): *wild type* 26.39±2.48 n=16; *apa-2(ox422)* 36.9±2.48 n=19; *ox422 skin-res* 35.22±3.6 n=9; *ox422 neu-res* 28.06±2.43 n=21; *ox422; e840 skin-res* 33.28±3.77 n=9. (D)Summary of mPSC frequency (Hz± SEM): *wild type* 43.93±5.92 n=16; *apa-2(ox422)* 7.75±1.52 n=19; *ox422 skin-res* 22.48±4.54 n=9; *ox422 neu-res* 44.85±4.79 n=21; *ox422; e840 skin-res* 14.15±3.99 n=9. (E) Summary of ePSC amplitude (nA±SEM): *wild type* 2159.55±131.12 n=11; *apa-2(ox422)* 1259.06±274.86 n=5; *ox422 skin-res* 1627.33±181.97 n=6; *ox422 neu-res* 2090.67±149.03 n=6; *ox422; e840 skin-res* 1264.32±323.68 n=6. * P<0.05, ** P<0.01, *** P<0.001.

APA-2 might have a specific role to facilitate the recycling of spontaneously released vesicles. However this phenotype is gone when *apm-2 apa-2* double mutant is built. The skin-rescued *apm-2 apa-2* double mutants with 30% vesicles exhibit also 30% mini frequency.

We also evaluated the evoked release from *apa-2* and *apm-2 apa-2* skin-rescued double mutants by electrical stimulation. There is a 30% reduction of evoked release in skin-rescued *apa-2* mutants, which can be rescued by expressing *apa-2* in neurons. The skin-rescued doubles exhibit 50% evoked response (Figure 3.9E). Since skin-rescued *apm-2 apa-2* double mutants have only 30% of vesicles left, the defect of evoked response is in general milder than that of vesicle reduction, which suggests limited amount of releasing sites are available during an acute stimulation.

Adaptin mutants exhibit mild behavioral defects

Mutants of *apa-2* have wild-type forward and slightly jerky backward movements on agar plates. The skin-rescued *apm-2 apa-2* double mutants are sicker in general; however, the best-rescued animals move similarly to *apa-2* mutants. To quantify their movement defects, worms were placed in drops of liquid and the number of body bends per minute was counted. *apa-2* mutants have a 15% reduction in their thrashing rate. Introducing *apa-2* back into either the skin or neurons can rescue this defect. The skin-rescued *apm-2 apa-2* double mutants with the best locomotion on agar plates were picked for this assay. These animals have a similar thrashing rate as that of *apa-2* mutants (Figure 3.10), indicating that neurons without AP2 can still release enough neurotransmitter to support worm swimming. Thus, in the absence of AP2, synaptic-vesicle recycling continues at worm synapses.

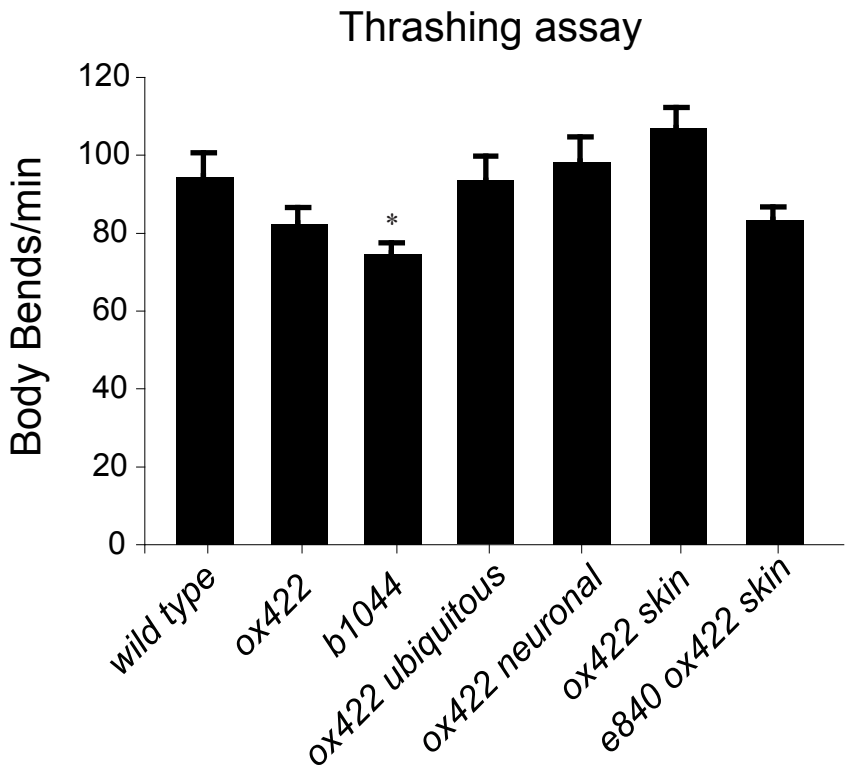

Figure 3.10. Adaptin mutants are moderately impaired for movement. Worms were placed in buffer and body bends were counted for 60 seconds. The thrashing rate for a*pa*-2 (EG6147) and skin-rescued *apm-2 apa*-2 (EG6151) double mutants is reduced by about 15%. Expression of APA-2 under a ubiquitous promoter (EG6149), a skin promoter (EG6150), or a neuronal promoter (EG6148) rescues thrashing. Average body bends per minute ± SEM: wild type 94.4 ± 6.0; *apa-2(ox422)* 82.4 ± 3.97; *apa-2(b1044)* 74.6 ± 2.69; ubiquitous rescued *apa-2(ox422)* 93.4 ± 6.15; neuronal rescued *apa-2(ox422)* 98.2 ± 6.26; skin rescued *apa-2(ox422)* 106.8 ± 5.19; skin rescued *apm-2(e840) apa-2(ox422)* 83.2 ± 3.2. n = 5 adult hermaphrodites. * $P<0.05$.

Discussion

In this study, we characterized the *C. elegans* α adaptin mutant *apa-2.* We found that in the absence of *apa-2*, the small subunit of AP2, σ2 is essentially eliminated whereas the medium subunit of AP2, μ2, can still maintain its plasma membrane localization and promote the endocytosis of AP2-dependent cargo. When we crossed the *apa-2* mutants into our previously characterized *apm-2* mutants, we found the double mutant combination to be worse than either of the single mutants. Thus, in *C. elegans,* completely blocking AP2 functions requires removing α and μ2 adaptins simultaneously. Therefore, we propose that AP2 functions as two loosely connected half complexes. Disrupting half of the complex will destabilize but not eliminate the other half.

We demonstrated that we can eliminate essentially the entire AP2 adaptor complex from worms. After introducing these two adaptins back into the hypodermis, the lethal double mutants are rescued successfully to viable adults. *apa-2* and skin-rescued *apm-2 apa-2* double mutants have relatively normal locomotion which is contradictory to the phenotype observed in *Drosophila* α adaptin mutants (Gonzalez-Gaitan and Jackle, 1997). AP2 deficient synapses have a 70% reduction in synaptic vesicles and a 50% decrease in their evoked response. This suggests that although the majority of synaptic vesicle endocytosis depends on AP2 in *C. elegans,* the residual vesicles can still be recycled to support locomotion. Since there are so many other adaptor proteins, clathrin-mediated endocytosis may still be working without AP2, but at a lower efficiency. However, almost all of the adaptors interact with AP2, for instance the LDLR adaptor Dab2 (Morris and Cooper, 2001) and the GPCR adaptor β arrestin (Edeling et al., 2006). Furthermore α and β adaptins can interact with many different endocytic accessory

proteins for spatial and temporal regulation of clathrin-coated pits, but it is difficult for another adaptor to fulfill the role of AP2 as an interaction hub. Thus the best candidates to substitute AP2 are other AP adaptor complexes. There is evidence suggesting β1 and β2 adaptins are partially redundant. Silencing the β1 and β2 subunits simultaneously is required to recapitulate the phenotype of α adaptin RNAi (Keyel et al., 2008). Considering the fact that there is only one β adaptin shared by AP1 and AP2 in *C. elegans,* it is likely that AP1 partially takes over the job of AP2 in *apm-2 apa-2* double mutants. This has been observed in cultured hippocampal neurons (Kim and Ryan, 2009). In addition, neurons from σ1 adaptin knockout mice have an accumulation of endosomal intermediates at synapses (Glyvuk et al., 2010). We observed the same phenotype in *apa-2* mutants. It is possible that synaptic-vesicle biogenesis can happen either at endosomal intermediates through AP1 or at plasma membrane through AP2. Large vesicle accumulation in the σ1 adaptin knockout is likely due to the blocking of synaptic vesicle biogenesis. In the case of *apa-2* mutants, the endocytic balance shifts towards bulk endocytosis, illustrated by the increase in endosomal intermediates in synapses lacking APA-2. Thus AP1 and AP2 possibly contribute to synaptic vesicle endocytosis at different subcellular compartments. Since clathrin-mediated endocytosis is unlikely to be completely blocked in AP2 knockout worms, it is still not clear whether clathrin-independent endocytosis contributes to the residual vesicle recycling.

Taken together, our data suggest an important role for AP2 in synaptic vesicle endocytosis at worm synapses. However, in the absence of AP2, synaptic vesicle recycling continues through AP2-independent mechanisms.

Materials and methods

Strains

The wild strain is Bristol N2. The reference strain EG6147 for *apa-2(ox422) X* was outcrossed seven times before phenotypic analysis. The reference strain EG4739 for *apa-2(b1044) X* was outcrossed twice before phenotypic analysis. All *oxSi* strains were generated by mosSCI (Frokjaer-Jensen et al., 2008), so the exogenous genes were inserted as a single copy.

The strain used in APA-2 translational GFP experiment was: EG4521 *lin-15(n765ts)X oxEx947[apa-2::GFP lin-15(+)]*.

The strains used in APM-2::GFP localization experiment were: EG6291 *oxSi54[Pdpy-30::apm-2::GFP unc-119(+)]II apm-2(e840)X* and EG6292 *oxSi54[Pdpy-30::apm-2::GFP unc-119(+)]II apm-2(e840) apa-2(ox422)X*.

The strains used in APS-2::GFP localization experiment were: EG6293 *oxSi108[aps-2::GFP unc-119(+)]II unc-119(ed3)III;* EG6294 *oxSi108[aps-2::GFP unc-119(+)]II apm-2(e840)X;* EG6295 *oxSi108[aps-2::GFP unc-119(+)]II apa-2(ox422)X* and EG6296 *+/szT1[lon-2(e678)]I oxSi108[aps-2::GFP unc-119(+)]II szT1/apm-2(e840) apa-2(ox422)X*.

The strain used in the APA-2 and SNB-1 colocalization experiment was: EG6155 *dkIs160[Punc-25::GFP::apt-4 unc-119(+)] oxEx1411[Punc-47::snb-1::tagRFP Punc-122::GFP]*.

The strains used in the vesicle protein localization experiment were: EG5932 *snt-1(md290)II; unc-119(ed3)III; oxSi180[snt-1::GFP unc-119(+)]IV*; EG6156 *oxSi180[snt-1::GFP unc-119(+)]IV; apa-2(ox422)X*; EG6157 *oxSi180[snt-1::GFP*

unc-119(+)]IV; apa-2(b1044)X; EG6159 *+/szT1[lon-2(e678)]I; oxSi180[snt-1::GFP unc-119(+)]IV; szT1/apm-2(e840) apa-2(ox422)X*; EG5717 *unc-119(ed3)III; oxSi36[unc-47::GFP unc-119(+)]IV*; EG6160 *oxSi36[unc-47::GFP unc-119(+)]IV; apa-2(ox422)X*; EG6161 *oxSi36[unc-47::GFP unc-119(+)]IV; apa-2(b1044)X*; EG6162 *+/szT1[lon-2(e678)]I; oxSi36[unc-47::GFP unc-119(+)]IV; szT1/apm-2(e840) apa-2(ox422)X*; EG6163 *unc-119(ed3)III; oxSi184[Punc-47::sng-1::GFP unc-119(+)]IV*; EG6164 *oxSi184[Punc-47::sng-1::GFP unc-119(+)]IV; apa-2(ox422)X;* EG6165 *oxSi184[Punc-47::sng-1::GFP unc-119(+)]IV; apa-2(b1044)X* and EG6166 *+/szT1[lon-2(e678)]I; oxSi184[Punc-47::sng-1::GFP unc-119(+)]IV; szT1/apm-2(e840) apa-2(ox422).*

The strains used for electron microscopy and electrophysiology were: EG6147 *apa-2(ox422)X;* EG 6149 *oxSi254[Pdpy-30::apa-2::GFP, unc-119(+)]II, apa-2(ox422)X;* EG6148 *oxSi253[Prab-3::apa-2::GFP, unc-119(+)]II, apa-2(ox422)X;* EG6150 *oxSi53[Pdpy-7::apa-2::GFP unc-119(+)]II, apa-2(ox422)X* and EG6151 *apm-2(e840) apa-2(ox422)X, oxEx1452[Pdpy-7::apa-2::mCherry Pdpy-7::apm-2::GFP Punc-122::GFP].*

GFP and mosSCI constructs

Multisite Gateway three fragment construction vectors were used (Invitrogen catalog no.12537-023) for generating all constructs. pENTRY4-1 was used as the promoter entry. Promoters include *Pdpy-30, Pdpy-7, Prab-3* and *Punc-47* and do not include the initiating methionine codon (ATG). PENTRY1-2 was used as the ORF entry, including *apa-2(cDNA), apm-2(cDNA)* and *sng-1*, all of which have an ATG at the beginning but no stop at the end. PENTRY2-3 was used for the C-terminal tag and 3'UTR entry, including *GFP-unc-54 3'UTR* and *mCherry-unc-54 3'UTR.* The destination vectors

are Gateway pDEST R4-R3, pCFJ150 for mosSCI on chromosome II and pCFJ201 for mosSCI on chromosme IV (Frokjaer-Jensen et al., 2008).

1.2 kb *aps-2* promoter region and 1kb *aps-2* genomic coding sequence were directly cloned by PCR from *wild-type* genomic DNA. GFP with *unc-54* 3'UTR was fused to the C-terminus of *aps-2* and the entire fusion fragment was dropped between the restriction sites BssHII and SpeI on pCFJ151 for mosSCI on chromosome II.

Microinjection

The final DNA concentration of each injection mix is 100 ng/ul. This target concentration was obtained with the addition of Fermentas 1kb DNA ladder (#SM0311).

APA-2 translational GFP experiment: pMG16 *apa-2::GFP* was injected into *lin-15(n765ts)X* animals at 1 ng/ul. The coinjection marker *lin-15(+)* was used at 50 ng/ul.

APA-2 and synaptobrevin colocalization experiment: pRH324 *Punc-47::snb-1::tagRFP* was injected into wild type (N2) at 0.25ng/ul. The coinjection marker *Punc-122::GFP* was used at 50 ng/ul. In the next generation, transgenic worms were picked. One of the transgenic lines *oxEx1411* was crossed into *dkIs160 [Punc-25::GFP::apt-4 unc-119(+)]*.

apm-2 apa-2 double mutant skin rescue: pMG50 *Pdpy-7::apm-2::GFP* and pMG40 *Pdpy-7::apa-2::mCherry* were coinjected into the adaptin double-mutant balanced strain EG6158 *+/szT1[lon-2(e678)] I; szT1/apm-2(e840) apa-2(ox422) X* at 1ng/ul each. The coinjection marker was *Punc-122::GFP* at 50ng/ul. In the next generation, rescued Egl worms were picked and maintained. One of the lines, EG6151, was used in the electron microscopy and electrophysiology assays.

Western blot analysis

Worm samples were prepared by boiling 1 volume of worm pellet in 1 volume of 2X loading buffer for 5 mins. Samples were run on a 10% SDS-PAGE gel then transferred to PVDF transfer membrane (Immobilon). The primary antibody for adaptin was a rabbit polyclonal anti APA-2 at a dilution of 1:500 (generously provided by Barth Grant). Primary antibody incubation was done in 5% BSA at 4 degrees overnight. The primary antibody for the standard control was 12G10 mouse monoclonal anti-tubulin (Developmental Studies Hybridoma Bank) at a dilution of 1:10,000. Primary antibody incubation was done in 5% BSA at room temperature for 1 hour. Secondary antibodies were anti-rabbit and mouse IgG fragments conjugated with HRP (GE Healthcare). Secondary incubations were done in 5% BSA at room temperature for 45 mins. Detection reagent used was SuperSignal West Dura (Thermo scientific).

For anti-GFP western blot, the primary antibody for GFP was mouse monoclonal anti-GFP at a dilution of 1:5000 (Clontech Cat. No. 632375). Primary antibody incubation was done in 5% sea block blocking buffer (Pierce prod#37527) at 4 degrees overnight.

Confocal microscopy

Worms are immobilized by using 2% phenoxy propanol and imaged on a Pascal LSM5 confocal microscope using a Zeiss plan-Neofluar 10x 0.3 NA, 20x 0.5 NA, 40x 1.3 NA oil or Zeiss plan-apochromat 63x 1.4NA oil objectives.

Electron microscopy

Wild-type (N2); EG6147 apa-2(ox422)X; EG 6149 oxSi254[Pdpy-30::apa-2::GFP, unc-119(+)]II, apa-2(ox422)X; EG6148 oxSi253[Prab-3::apa-2::GFP, unc-119(+)]II, apa-2(ox422)X; EG6150 oxSi[Pdpy-7::apa-2::GFP unc-119(+)]II, apa-2(ox422)X; EG6151 apm-2(e840) apa-2(ox422)X, oxEx[Pdpy-7::apa-2::mCherry Pdpy-7::apm-2::GFP Punc-122::GFP] adult nematodes were prepared in parallel for transmission electron microscopy as previously described (Hammarlund et al., 2007). Briefly, 10 young adult hermaphrodites were placed onto a freeze chamber (100µm well of type A specimen carrier) containing space-filling bacteria, covered with a type B specimen carrier flat side down, and frozen instantaneously in the BAL-TEC HPM 010 (BAL-TEC, Liechtenstein). This step was repeated for animals of all genotypes. Then, the frozen animals were fixed in Leica EM AFS system with 1% osmium tetroxide and 0.1% uranyl acetate in anhydrous acetone for 2 days at –90ºC and for 38.9 more hours with gradual temperature increase (6ºC/hr to –20ºC over 11.7 hours, constant temperature at -20ºC for 16 hours, and 10ºC/hr to 20ºC over 4 hours). The fixed animals were embedded in araldite resin following the infiltration series (30% araldite/acetone for 4 hours, 70% araldite/acetone for 5 hours, 90% araldite/acetone for over night, and pure araldite for 8 hours). Mutant and control blocks were blinded. Ribbons of ultra-thin (33 nm) serial sections were collected using an Ultracut 6 microtome at the level of the anterior reflex of the gonad. Images were obtained on a Hitachi H-7100 electron microscope using a Gatan digital camera. Two hundred and fifty ultra-thin contiguous sections were cut, and the ventral nerve cord was reconstructed from two animals representing each genotype. Image analysis was performed using Image J software. The numbers of synaptic vesicles

(~30nm), dense-core vesicles (~40nm) and large vesicles (>40nm) in each synapse were counted. Their distance from the presynaptic specialization and the plasma membrane, as well as their diameter, was measured in acetylcholine neurons VA and VB and the GABA neuron VD. A synapse was defined as the serial sections containing a dense projection as well as sections on either side of that density, which contain synaptic vesicles numbers above the average number of synaptic vesicles per profile.

Electrophysiology

C. elegans were grown at room temperature (22–24°C) on agar plates with a layer of OP50 Escherichia coli. Adult hermaphrodite animals were used for electrophysiological analysis. Postsynaptic currents (mPSCs and ePSCs) at the NMJ were recorded as previously described (Liu et al., 2007) using a technique originally developed by Richmond (Richmond et al., 1999). Briefly, an animal was immobilized on a sylgard coated glass coverslip by applying a cyanoacrylate adhesive along the dorsal side. A longitudinal incision was made in the dorsolateral region. After clearing the viscera, the cuticle flap was folded back and glued to the coverslip, exposing the ventral nerve cord and two adjacent muscle quadrants. A ZEISS AXIOSKOP microscope equipped with a 40X water immersion lens and 15X eyepieces were used for viewing the preparation. Borosilicate glass pipettes with a tip resistance of 3~5 MΩ were used as electrodes for voltage clamping. The classical whole-cell configuration was obtained by rupturing the patch membrane of a gigaohm seal formed between the recording electrode and a body wall muscle cell. The cell was voltage-clamped at –60 mV to record mPSCs and ePSCs. ePSCs were evoked by applying a 0.5 ms square wave current pulse at a supramaximal voltage (25V) through a stimulation electrode placed in close apposition to the ventral

nerve cord. Postsynaptic currents were amplified with a HEKA EP10 amplifier (InstruTECH), and acquired with Patchmaster software (HEKA). Data were sampled at a rate of 10 kHz after filtering at 2 kHz. The recording pipette solution contained the following (in mM): 120 KCl, 20 KOH, 5 TES, 0.25 CaCl2, 4 MgCl2, 36 sucrose, 5 EGTA, and 4 Na2ATP, pH adjusted to 7.2 with KOH, osmolarity 310~320 mOsm. The standard external solution included the following (in mM): 150 NaCl, 5 KCl, 5 CaCl2, 1 MgCl2, 5 sucrose, 10 glucose and 15 HEPES, pH adjusted to 7.35 with NaOH, osmolarity 330~340 mOsm.

Amplitude and frequency of mPSCs were analyzed using MiniAnalysis (Synaptosoft, Decatur, GA). A detection threshold of 10 pA was used in initial automatic analysis, followed by visual inspections to include missed events (≥5 pA) and to exclude false events resulting from baseline fluctuations. Amplitudes of ePSCs were measured with Fitmaster (HEKA). The amplitude of the largest peak of ePSCs from each experiment was used for statistical analysis. Data were imported into Origin, version 7.5 (OriginLab, Northampton, MA), for graphing and statistical analysis. A unpaired t test was used for statistical comparisons. A value of $p < 0.05$ is considered statistically significant. All values are expressed as mean ± s.e.m. n is the number of worms that were recorded from.

Thrashing assay

A single worm was placed into a 50ul drop of M9 solution. The worm was allowed to adapt to the liquid environment for 2 min. The number of body bends was counted for 60s for each genotype (n=5).

Image quantification

All worm nerve cord images were exported as 8-bit RGB files. ImageJ 1.43u was used for quantification. The region of interest was selected by hand-drawing. The total pixel intensity and the total number of pixels were recorded to calculate the average fluorescent intensity at both synaptic regions and axonal regions. Each image gives a ratio of fluorescent intensity between synapses and axons. n means the number of images used in quantification.

References

Alvarez de Toledo, G., R. Fernandez-Chacon, and J.M. Fernandez. 1993. Release of secretory products during transient vesicle fusion. *Nature*. 363:554-8.

Andersson, F., P. Low, and L. Brodin. 2010. Selective perturbation of the BAR domain of endophilin impairs synaptic vesicle endocytosis. *Synapse*. 64:556-60.

Aravanis, A.M., J.L. Pyle, and R.W. Tsien. 2003. Single synaptic vesicles fusing transiently and successively without loss of identity. *Nature*. 423:643-7.

Augustine, G.J., J.R. Morgan, C.A. Villalba-Galea, S. Jin, K. Prasad, and E.M. Lafer. 2006. Clathrin and synaptic vesicle endocytosis: studies at the squid giant synapse. *Biochem Soc Trans*. 34:68-72.

Bao, H., N.E. Reist, and B. Zhang. 2008. The Drosophila epsin 1 is required for ubiquitin-dependent synaptic growth and function but not for synaptic vesicle recycling. *Traffic*. 9:2190-205.

Barbosa, J., Jr., L.T. Ferreira, C. Martins-Silva, M.S. Santos, G.E. Torres, M.G. Caron, M.V. Gomez, S.S. Ferguson, M.A. Prado, and V.F. Prado. 2002. Trafficking of the vesicular acetylcholine transporter in SN56 cells: a dynamin-sensitive step and interaction with the AP-2 adaptor complex. *J Neurochem*. 82:1221-8.

Chen, H., S. Fre, V.I. Slepnev, M.R. Capua, K. Takei, M.H. Butler, P.P. Di Fiore, and P. De Camilli. 1998. Epsin is an EH-domain-binding protein implicated in clathrin-mediated endocytosis. *Nature*. 394:793-7.

Collins, B.M., A.J. McCoy, H.M. Kent, P.R. Evans, and D.J. Owen. 2002a. Molecular architecture and functional model of the endocytic AP2 complex. *Cell*. 109:523-35.

Collins, B.M., A.J. McCoy, H.M. Kent, P.R. Evans, and D.J. Owen. 2002b. Molecular architecture and functional model of the endocytic AP2 complex. *Cell*. 109:523-535.

Danglot, L., and T. Galli. 2007. What is the function of neuronal AP-3? *Biol Cell*. 99:349-61.

David, C., P.S. McPherson, O. Mundigl, and P. de Camilli. 1996. A role of amphiphysin in synaptic vesicle endocytosis suggested by its binding to dynamin in nerve terminals. *Proc Natl Acad Sci U S A*. 93:331-5.

Dawson, J.C., J.A. Legg, and L.M. Machesky. 2006. Bar domain proteins: a role in tubulation, scission and actin assembly in clathrin-mediated endocytosis. *Trends Cell Biol*. 16:493-8.

De Camilli, P., H. Chen, J. Hyman, E. Panepucci, A. Bateman, and A.T. Brunger. 2002. The ENTH domain. *FEBS Lett*. 513:11-8.

De Camilli, P., K. Takei, and P.S. McPherson. 1995. The function of dynamin in endocytosis. *Curr Opin Neurobiol*. 5:559-65.

Diril, M.K., M. Wienisch, N. Jung, J. Klingauf, and V. Haucke. 2006. Stonin 2 is an AP-2-dependent endocytic sorting adaptor for synaptotagmin internalization and recycling. *Dev Cell*. 10:233-44.

Dittman, J., and T.A. Ryan. 2009. Molecular circuitry of endocytosis at nerve terminals. *Annu Rev Cell Dev Biol*. 25:133-60.

Edeling, M.A., S.K. Mishra, P.A. Keyel, A.L. Steinhauser, B.M. Collins, R. Roth, J.E. Heuser, D.J. Owen, and L.M. Traub. 2006. Molecular switches involving the AP-2 beta2 appendage regulate endocytic cargo selection and clathrin coat assembly. *Dev Cell*. 10:329-42.

Fergestad, T., and K. Broadie. 2001. Interaction of stoned and synaptotagmin in synaptic vesicle endocytosis. *J Neurosci*. 21:1218-27.

Fergestad, T., W.S. Davis, and K. Broadie. 1999. The stoned proteins regulate synaptic vesicle recycling in the presynaptic terminal. *J Neurosci*. 19:5847-60.

Ford, M.G., I.G. Mills, B.J. Peter, Y. Vallis, G.J. Praefcke, P.R. Evans, and H.T. McMahon. 2002. Curvature of clathrin-coated pits driven by epsin. *Nature*. 419:361-6.

Frokjaer-Jensen, C., M.W. Davis, C.E. Hopkins, B.J. Newman, J.M. Thummel, S.P. Olesen, M. Grunnet, and E.M. Jorgensen. 2008. Single-copy insertion of transgenes in Caenorhabditis elegans. *Nat Genet*. 40:1375-83.

Gaffield, M.A., L. Tabares, and W.J. Betz. 2009. Preferred sites of exocytosis and endocytosis colocalize during high- but not lower-frequency stimulation in mouse motor nerve terminals. *J Neurosci*. 29:15308-16.

Gaidarov, I., and J.H. Keen. 1999. Phosphoinositide-AP-2 interactions required for targeting to plasma membrane clathrin-coated pits. *J Cell Biol*. 146:755-64.

Gandhi, S.P., and C.F. Stevens. 2003. Three modes of synaptic vesicular recycling revealed by single-vesicle imaging. *Nature*. 423:607-13.

Glyvuk, N., Y. Tsytsyura, C. Geumann, R. D'Hooge, J. Huve, M. Kratzke, J. Baltes, D. Boening, J. Klingauf, and P. Schu. 2010. AP-1/sigma1B-adaptin mediates endosomal synaptic vesicle recycling, learning and memory. *EMBO J*. 29:1318-30.

Gonzalez-Gaitan, M., and H. Jackle. 1997. Role of Drosophila alpha-adaptin in presynaptic vesicle recycling. *Cell*. 88:767-76.

Granseth, B., B. Odermatt, S.J. Royle, and L. Lagnado. 2006. Clathrin-mediated endocytosis is the dominant mechanism of vesicle retrieval at hippocampal synapses. *Neuron*. 51:773-86.

Grigliatti, T.A., L. Hall, R. Rosenbluth, and D.T. Suzuki. 1973. Temperature-sensitive mutations in Drosophila melanogaster. XIV. A selection of immobile adults. *Mol Gen Genet*. 120:107-14.

Gu, M., K. Schuske, S. Watanabe, Q. Liu, P. Baum, G. Garriga, and E.M. Jorgensen. 2008. Mu2 adaptin facilitates but is not essential for synaptic vesicle recycling in Caenorhabditis elegans. *J Cell Biol*. 183:881-92.

Hammarlund, M., M.T. Palfreyman, S. Watanabe, S. Olsen, and E.M. Jorgensen. 2007. Open syntaxin docks synaptic vesicles. *PLoS Biol*. 5:e198.

Harada, S., I. Hori, H. Yamamoto, and R. Hosono. 1994. Mutations in the unc-41 gene cause elevation of acetylcholine levels. *J Neurochem*. 63:439-46.

Harris, T.W., E. Hartwieg, H.R. Horvitz, and E.M. Jorgensen. 2000. Mutations in synaptojanin disrupt synaptic vesicle recycling. *J Cell Biol*. 150:589-600.

Haucke, V., M.R. Wenk, E.R. Chapman, K. Farsad, and P. De Camilli. 2000. Dual interaction of synaptotagmin with mu2- and alpha-adaptin facilitates clathrin-coated pit nucleation. *EMBO J*. 19:6011-9.

Heuser, J.E., and T.S. Reese. 1973. Evidence for recycling of synaptic vesicle membrane during transmitter release at the frog neuromuscular junction. *J Cell Biol*. 57:315-

44.

Horvath, C.A., D. Vanden Broeck, G.A. Boulet, J. Bogers, and M.J. De Wolf. 2007. Epsin: inducing membrane curvature. *Int J Biochem Cell Biol*. 39:1765-70.

Itoh, T., and P. De Camilli. 2006. BAR, F-BAR (EFC) and ENTH/ANTH domains in the regulation of membrane-cytosol interfaces and membrane curvature. *Biochim Biophys Acta*. 1761:897-912.

Jakobsson, J., H. Gad, F. Andersson, P. Low, O. Shupliakov, and L. Brodin. 2008. Role of epsin 1 in synaptic vesicle endocytosis. *Proc Natl Acad Sci U S A*. 105:6445-50.

Jarousse, N., and R.B. Kelly. 2001. The AP2 binding site of synaptotagmin 1 is not an internalization signal but a regulator of endocytosis. *J Cell Biol*. 154:857-66.

Jorgensen, E.M., E. Hartwieg, K. Schuske, M.L. Nonet, Y. Jin, and H.R. Horvitz. 1995. Defective recycling of synaptic vesicles in synaptotagmin mutants of Caenorhabditis elegans. *Nature*. 378:196-9.

Jung, N., M. Wienisch, M. Gu, J.B. Rand, S.L. Muller, G. Krause, E.M. Jorgensen, J. Klingauf, and V. Haucke. 2007. Molecular basis of synaptic vesicle cargo recognition by the endocytic sorting adaptor stonin 2. *J Cell Biol*. 179:1497-510.

Kalthoff, C., J. Alves, C. Urbanke, R. Knorr, and E.J. Ungewickell. 2002. Unusual structural organization of the endocytic proteins AP180 and epsin 1. *J Biol Chem*. 277:8209-16.

Kastning, K., V. Kukhtina, J.T. Kittler, G. Chen, A. Pechstein, S. Enders, S.H. Lee, M. Sheng, Z. Yan, and V. Haucke. 2007. Molecular determinants for the interaction between AMPA receptors and the clathrin adaptor complex AP-2. *Proc Natl Acad Sci U S A*. 104:2991-6.

Kazazic, M., V. Bertelsen, K.W. Pedersen, T.T. Vuong, M.V. Grandal, M.S. Rodland, L.M. Traub, E. Stang, and I.H. Madshus. 2009. Epsin 1 is involved in recruitment of ubiquitinated EGF receptors into clathrin-coated pits. *Traffic*. 10:235-45.

Keyel, P.A., J.R. Thieman, R. Roth, E. Erkan, E.T. Everett, S.C. Watkins, J.E. Heuser, and L.M. Traub. 2008. The AP-2 adaptor beta2 appendage scaffolds alternate cargo endocytosis. *Mol Biol Cell*. 19:5309-26.

Kim, M.H., and L.B. Hersh. 2004. The vesicular acetylcholine transporter interacts with clathrin-associated adaptor complexes AP-1 and AP-2. *J Biol Chem*. 279:12580-7.

Kim, S.H., and T.A. Ryan. 2009. Synaptic vesicle recycling at CNS snapses without AP-2. *J Neurosci*. 29:3865-74.

Kittler, J.T., G. Chen, S. Honing, Y. Bogdanov, K. McAinsh, I.L. Arancibia-Carcamo, J.N. Jovanovic, M.N. Pangalos, V. Haucke, Z. Yan, and S.J. Moss. 2005. Phospho-dependent binding of the clathrin AP2 adaptor complex to GABAA receptors regulates the efficacy of inhibitory synaptic transmission. *Proc Natl Acad Sci U S A*. 102:14871-6.

Koshiba, S., T. Kigawa, A. Kikuchi, and S. Yokoyama. 2002. Solution structure of the epsin N-terminal homology (ENTH) domain of human epsin. *J Struct Funct Genomics*. 2:1-8.

Legendre-Guillemin, V., S. Wasiak, N.K. Hussain, A. Angers, and P.S. McPherson. 2004. ENTH/ANTH proteins and clathrin-mediated membrane budding. *J Cell Sci*. 117:9-18.

Liu, Q., B. Chen, Q. Ge, and Z.W. Wang. 2007. Presynaptic Ca2+/calmodulin-dependent protein kinase II modulates neurotransmitter release by activating BK channels at Caenorhabditis elegans neuromuscular junction. *J Neurosci*. 27:10404-13.

Logiudice, L., P. Sterling, and G. Matthews. 2009. Vesicle recycling at ribbon synapses in the finely branched axon terminals of mouse retinal bipolar neurons. *Neuroscience*. 164:1546-56.

Maritzen, T., J. Podufall, and V. Haucke. 2010. Stonins--specialized adaptors for synaptic vesicle recycling and beyond? *Traffic*. 11:8-15.

Martina, J.A., C.J. Bonangelino, R.C. Aguilar, and J.S. Bonifacino. 2001. Stonin 2: an adaptor-like protein that interacts with components of the endocytic machinery. *J Cell Biol*. 153:1111-20.

Maycox, P.R., E. Link, A. Reetz, S.A. Morris, and R. Jahn. 1992. Clathrin-coated vesicles in nervous tissue are involved primarily in synaptic vesicle recycling. *J Cell Biol*. 118:1379-88.

McIntire, S.L., E. Jorgensen, and H.R. Horvitz. 1993. Genes required for GABA function in Caenorhabditis elegans. *Nature*. 364:334-7.

McPherson, P.S., E.P. Garcia, V.I. Slepnev, C. David, X. Zhang, D. Grabs, W.S. Sossin, R. Bauerfeind, Y. Nemoto, and P. De Camilli. 1996. A presynaptic inositol-5-phosphatase. *Nature*. 379:353-7.

Mello, C.C., J.M. Kramer, D. Stinchcomb, and V. Ambros. 1991. Efficient gene transfer in C.elegans: extrachromosomal maintenance and integration of transforming sequences. *EMBO J*. 10:3959-70.

Meunier, F.A., T.H. Nguyen, C. Colasante, F. Luo, R.K. Sullivan, N.A. Lavidis, J. Molgo, S.D. Meriney, and G. Schiavo. 2010. Sustained synaptic-vesicle recycling by bulk

endocytosis contributes to the maintenance of high-rate neurotransmitter release stimulated by glycerotoxin. *J Cell Sci*. 123:1131-40.

Miller, K.G., A. Alfonso, M. Nguyen, J.A. Crowell, C.D. Johnson, and J.B. Rand. 1996. A genetic selection for Caenorhabditis elegans synaptic transmission mutants. *Proc Natl Acad Sci U S A*. 93:12593-8.

Mishra, S.K., M.J. Hawryluk, T.J. Brett, P.A. Keyel, A.L. Dupin, A. Jha, J.E. Heuser, D.H. Fremont, and L.M. Traub. 2004. Dual engagement regulation of protein interactions with the AP-2 adaptor alpha appendage. *J Biol Chem*. 279:46191-203.

Mitsunari, T., F. Nakatsu, N. Shioda, P.E. Love, A. Grinberg, J.S. Bonifacino, and H. Ohno. 2005. Clathrin adaptor AP-2 is essential for early embryonal development. *Mol Cell Biol*. 25:9318-23.

Moerman, D.G., G.M. Benian, and R.H. Waterston. 1986. Molecular cloning of the muscle gene unc-22 in Caenorhabditis elegans by Tc1 transposon tagging. *Proc Natl Acad Sci U S A*. 83:2579-83.

Morgan, J.R., K. Prasad, W. Hao, G.J. Augustine, and E.M. Lafer. 2000. A conserved clathrin assembly motif essential for synaptic vesicle endocytosis. *J Neurosci*. 20:8667-76.

Morris, S.M., and J.A. Cooper. 2001. Disabled-2 colocalizes with the LDLR in clathrin-coated pits and interacts with AP-2. *Traffic*. 2:111-23.

Motley, A.M., N. Berg, M.J. Taylor, D.A. Sahlender, J. Hirst, D.J. Owen, and M.S. Robinson. 2006. Functional analysis of AP-2 alpha and mu2 subunits. *Mol Biol Cell*. 17:5298-308.

Nguyen, M., A. Alfonso, C.D. Johnson, and J.B. Rand. 1995. Caenorhabditis elegans mutants resistant to inhibitors of acetylcholinesterase. *Genetics*. 140:527-35.

Nonet, M.L., A.M. Holgado, F. Brewer, C.J. Serpe, B.A. Norbeck, J. Holleran, L. Wei, E. Hartwieg, E.M. Jorgensen, and A. Alfonso. 1999. UNC-11, a Caenorhabditis elegans AP180 homologue, regulates the size and protein composition of synaptic vesicles. *Mol Biol Cell*. 10:2343-60.

Owen, D.J., and P.R. Evans. 1998. A structural explanation for the recognition of tyrosine-based endocytotic signals. *Science*. 282:1327-32.

Owen, D.J., Y. Vallis, M.E. Noble, J.B. Hunter, T.R. Dafforn, P.R. Evans, and H.T. McMahon. 1999. A structural explanation for the binding of multiple ligands by the alpha-adaptin appendage domain. *Cell*. 97:805-15.

Owen, D.J., Y. Vallis, B.M. Pearse, H.T. McMahon, and P.R. Evans. 2000. The structure

and function of the beta 2-adaptin appendage domain. *EMBO J*. 19:4216-27.

Pan, C.L., P.D. Baum, M. Gu, E.M. Jorgensen, S.G. Clark, and G. Garriga. 2008. C. elegans AP-2 and retromer control Wnt signaling by regulating mig-14/Wntless. *Dev Cell*. 14:132-9.

Phillips, A.M., M. Ramaswami, and L.E. Kelly. 2010. Stoned. *Traffic*. 11:16-24.

Phillips, A.M., M. Smith, M. Ramaswami, and L.E. Kelly. 2000. The products of the Drosophila stoned locus interact with synaptic vesicles via synaptotagmin. *J Neurosci*. 20:8254-61.

Polo, S., S. Sigismund, M. Faretta, M. Guidi, M.R. Capua, G. Bossi, H. Chen, P. De Camilli, and P.P. Di Fiore. 2002. A single motif responsible for ubiquitin recognition and monoubiquitination in endocytic proteins. *Nature*. 416:451-5.

Praefcke, G.J., M.G. Ford, E.M. Schmid, L.E. Olesen, J.L. Gallop, S.Y. Peak-Chew, Y. Vallis, M.M. Babu, I.G. Mills, and H.T. McMahon. 2004. Evolving nature of the AP2 alpha-appendage hub during clathrin-coated vesicle endocytosis. *EMBO J*. 23:4371-83.

Radhakrishna, H., and J.G. Donaldson. 1997. ADP-ribosylation factor 6 regulates a novel plasma membrane recycling pathway. *J Cell Biol*. 139:49-61.

Rand, J.B., and R.L. Russell. 1985. Molecular basis of drug-resistance mutations in C. elegans. *Psychopharmacol Bull*. 21:623-30.

Richmond, J.E., W.S. Davis, and E.M. Jorgensen. 1999. UNC-13 is required for synaptic vesicle fusion in C. elegans. *Nat Neurosci*. 2:959-64.

Robinson, M.S. 2004. Adaptable adaptors for coated vesicles. *Trends Cell Biol*. 14:167-74.

Robinson, M.S., and J.S. Bonifacino. 2001. Adaptor-related proteins. *Curr Opin Cell Biol*. 13:444-53.

Rosenthal, J.A., H. Chen, V.I. Slepnev, L. Pellegrini, A.E. Salcini, P.P. Di Fiore, and P. De Camilli. 1999. The epsins define a family of proteins that interact with components of the clathrin coat and contain a new protein module. *J Biol Chem*. 274:33959-65.

Schuske, K., M.T. Palfreyman, S. Watanabe, and E.M. Jorgensen. 2007. UNC-46 is required for trafficking of the vesicular GABA transporter. *Nat Neurosci*. 10:846-53.

Schuske, K.R., J.E. Richmond, D.S. Matthies, W.S. Davis, S. Runz, D.A. Rube, A.M. van

der Bliek, and E.M. Jorgensen. 2003. Endophilin is required for synaptic vesicle endocytosis by localizing synaptojanin. *Neuron*. 40:749-62.

Slepnev, V.I., G.C. Ochoa, M.H. Butler, and P. De Camilli. 2000. Tandem arrangement of the clathrin and AP-2 binding domains in amphiphysin 1 and disruption of clathrin coat function by amphiphysin fragments comprising these sites. *J Biol Chem*. 275:17583-9.

Smith, S.M., R. Renden, and H. von Gersdorff. 2008. Synaptic vesicle endocytosis: fast and slow modes of membrane retrieval. *Trends Neurosci*. 31:559-68.

Spruce, A.E., L.J. Breckenridge, A.K. Lee, and W. Almers. 1990. Properties of the fusion pore that forms during exocytosis of a mast cell secretory vesicle. *Neuron*. 4:643-54.

Takei, K., O. Mundigl, L. Daniell, and P. De Camilli. 1996. The synaptic vesicle cycle: a single vesicle budding step involving clathrin and dynamin. *J Cell Biol*. 133:1237-50.

Traub, L.M. 2003. Sorting it out: AP-2 and alternate clathrin adaptors in endocytic cargo selection. *J Cell Biol*. 163:203-8.

Traub, L.M., M.A. Downs, J.L. Westrich, and D.H. Fremont. 1999. Crystal structure of the alpha appendage of AP-2 reveals a recruitment platform for clathrin-coat assembly. *Proc Natl Acad Sci U S A*. 96:8907-12.

Verstreken, P., O. Kjaerulff, T.E. Lloyd, R. Atkinson, Y. Zhou, I.A. Meinertzhagen, and H.J. Bellen. 2002. Endophilin mutations block clathrin-mediated endocytosis but not neurotransmitter release. *Cell*. 109:101-12.

Verstreken, P., T.W. Koh, K.L. Schulze, R.G. Zhai, P.R. Hiesinger, Y. Zhou, S.Q. Mehta, Y. Cao, J. Roos, and H.J. Bellen. 2003. Synaptojanin is recruited by endophilin to promote synaptic vesicle uncoating. *Neuron*. 40:733-48.

Vithlani, M., and S.J. Moss. 2009. The role of GABAAR phosphorylation in the construction of inhibitory synapses and the efficacy of neuronal inhibition. *Biochem Soc Trans*. 37:1355-8.

Walther, K., M.K. Diril, N. Jung, and V. Haucke. 2004. Functional dissection of the interactions of stonin 2 with the adaptor complex AP-2 and synaptotagmin. *Proc Natl Acad Sci U S A*. 101:964-9.

Zhang, B., Y.H. Koh, R.B. Beckstead, V. Budnik, B. Ganetzky, and H.J. Bellen. 1998. Synaptic vesicle size and number are regulated by a clathrin adaptor protein required for endocytosis. *Neuron*. 21:1465-75.

Zhang, J.Z., B.A. Davletov, T.C. Sudhof, and R.G. Anderson. 1994. Synaptotagmin I is a high affinity receptor for clathrin AP-2: implications for membrane recycling. *Cell*. 78:751-60.

Zhao, H., and M.L. Nonet. 2001. A conserved mechanism of synaptogyrin localization. *Mol Biol Cell*. 12:2275-89.

CHAPTER 4

CLATHRIN ADAPTOR PROTEIN UNC-41, STONEDB/STONIN HOMOLOG IS REQUIRED FOR SYNAPTIC FUNCTION IN *CAENORHABDITIS ELEGANS*

My contribution to this work including the following:

1. Generating *GFP::unc-41* construct
2. Confocal imaging of GFP::UNC-41 in *snt-1* mutants.
3. Building *unc-41; apm-2* double mutant.
4. Confocal imaging of the synaptic localization of vesicle proteins in *unc-41*.
5. Overexpressing SNT-1::GFP under different conditions in *unc-41*

Gregory P. Mullen (Oklahoma Medical Research Foundation, Oklahoma City) contributed to the following:

1. Sequencing analysis and cloning of *unc-41*.
2. Analysis of *unc-41* expression pattern.

Shigeki Watanabe (University of Utah, Salt lake City) contributed to the following:

Electron microscopy analysis of *unc-41* and *unc-41; apm-2* mutants

Abstract

Recycling of synaptic vesicle proteins requires the participation of clathrin-associated adaptors such as AP2 and AP180. Each type of adaptors is likely to recognize different transmembrane cargo proteins. One class of adaptors, the Stonins, are thought to link the synaptic vesicle protein Synaptotagmin 1 to the clathrin coated pit, facilitating the recovery and sorting of this vesicular protein. The *unc-41* gene in the nematode *Caenorhabditis elegans* encodes two protein isoforms with strong similarity to the *Drosophila* STNB and mammalian stonin 2 proteins. The UNC-41 isoforms are differentially expressed in the *C. elegans* nervous system; UNC-41A is expressed in all neurons, while UNC-41B is expressed in a subset of neurons, including the GABA motor neurons in the ventral nerve cord. The synaptotagmin I binding motif (KYE) in the μ-homologous domain of UNC-41 is critical for its synaptic localization, however UNC-41 still localizes to synapses in various synaptotagmin mutants. Ultrastructural analysis indicates that *unc-41*mutants have 50% reduction of synaptic vesicles. Consistent with it, in *unc-41* mutants, synaptic vesicle proteins are partially mislocalized and synaptotagmin I is completely mislocalized from synapses in sublateral nerve cords. In addition, over-expression of Synaptotagmin I can't bypass the requirement of UNC-41, suggesting that UNC-41 is essential to recruit Synaptotagmin 1 to sites of synaptic vesicle endocytosis in *C. elegans*.

Introduction

The release of neurotransmitters at synapses occurs through the regulated fusion of synaptic vesicles with the plasma membrane. The recovery of synaptic vesicle proteins and the reconstitution of functional synaptic vesicles, in turn, are dependent on a large

complex of proteins associated with clathrin (Dittman and Ryan, 2009). However the mechanism to re-sort synaptic vesicle proteins into endocytic pits is still not clear. Adaptors, such as the AP2 complex, recruit transmembrane cargo proteins to endocytic sites and link clathrin to the membrane (Robinson and Bonifacino, 2001). During synaptic vesicle endocytosis, the adaptor AP180 has been identified as the specific adaptor for recruiting V-SNARE synaptobrevin (Nonet et al., 1999; Zhang et al., 1998). However the adaptors for various other vesicle proteins remain undecided. One adaptor called stonin that is similar to the medium subunit of AP complex has been proposed to be the specific adaptor to recycle vesicle protein synaptotagmin I.

StonedB (STNB), the founding member of the STNB/stonin family, was identified in *Drosophila* in a screen for temperature-sensitive paralytic mutants (Grigliatti et al., 1973). Stoned mutants exhibit a variety of behavioral, electrophysiological, and ultrastructural defects that suggest that synaptic vesicle recycling is severely compromised (Fergestad et al., 1999). Two STNB homologs, designated stonin 1 and stonin 2, have been identified in mice and humans (Martina et al., 2001). Of the two mammalian homologs, Stonin 2 is more closely related to STNB, and like the *Drosophila* protein, has been implicated in synaptic vesicle recycling (Diril et al., 2006; Walther et al., 2004).

Experiments in *Drosophila* suggest STNB interacts with the C2B domain of the synaptic vesicle protein synaptotagmin I (Phillips et al., 2010; Phillips et al., 2000). More recently, mammalian cell culture indicates that stonin-2 proteins bind to the C2 domains, preferentially to C2A domain of synaptotagmin 1 and are required for the efficient recovery of synaptotagmin after synaptic vesicle fusion (Jung et al., 2007). The μ-

homology domain of stonin mediates interactions with the C2 domains of synaptotagmin I (Jung et al., 2007; Phillips et al., 2000). The endocytosis of synaptotagmin I by stonin is likely to be AP2 dependent (Diril et al., 2006) and it is possibly through the interactions between Stonins and the ear domain of alpha subunits from AP2 to incorporate stonin-synaptotagmin complex into clathrin-coated pits (Maritzen et al., 2010). Replacing μ-homology domain with μ2 subunit from AP2 failed to rescue the lethality of Stoned mutants, suggesting distinct roles of stonin and μ2 adaptin at synapses (Phillips et al., 2010). Intriguingly, overexpression of Synaptotagmin 1 in Drosophila rescues the lethality and synaptic vesicle recycling defects observed in Stoned mutants (Fergestad and Broadie, 2001). Thus, the current view is that synaptotagmin recruitment to sites of endocytosis is the major function of STNB/stonin 2 proteins.

To characterize the role of Stonins in synaptic vesicle endocytosis we characterized *unc-41*, the stonin ortholog in the nematode *Caenorhabditis elegans*. *unc41* mutants exhibit uncoordinated movement, resistance to inhibitors of cholinesterase, elevated levels of acetylcholine, slow growth, and small adult size (Harada et al., 1994; Nguyen et al., 1995; Rand and Russell, 1985). This set of phenotypes is usually associated with defects in acetylcholine release or synaptic vesicle function (Miller et al., 1996; Nguyen et al., 1995). In addition, *unc-41* animals display a defecation-expulsion defect associated with defective GABA function (McIntire et al., 1993). These phenotypes suggest that *unc-41* encodes a protein important for the release of most or all neurotransmitters. Here we characterize the *unc-41* gene. The *unc-41* gene is transcribed from two promoters that produce isoforms that differ at the amino terminus by the presence or absence of a nonconserved extension. The UNC-41 isoforms are

differentially expressed in the *C. elegans* nervous system and are localized to synapses. Synaptic vesicle numbers are 50% depleted in *unc-41* mutants. No further reduction of synaptic vesicles is observed in *unc-41; apm-2* (the medium subunit of AP2) double mutants suggesting UNC-41 functions in the same endocytic pathway with AP2. Moreover, synaptic vesicle proteins are partially mislocalized from synaptic region in *unc-41* mutants. Especially, synaptotagmin I exhibits complete mislocalization from synapses in sublateral nerve cords. This finding is reminiscent of the localization defect of synaptobrevin observed in AP180 mutants (Nonet et al., 1999). However, when synaptotagmin I is overexpressed in *unc-41* mutants, the mutant phenotypes are not improved. This suggests providing more synaptotagmin I can't bypass the requirement of UNC-41 in synaptic vesicle endocytosis. Thus the major function of UNC-41 is to recruit synaptotagmin I.

Results

Cloning and genomic organization of the *unc-41* gene

We cloned *unc-41* by transposon tagging (see methods and materials), and found that it corresponds to the gene C27H6.1. The *unc-41* gene consists of 12 exons and extends over approximately 9-kb of genomic DNA (Figure 4.1A). A genomic clone containing the entire *unc-41* coding region plus 3529-bp of upstream sequence fully rescued the *unc-41* locomotion and defecation phenotypes. The longest composite cDNA, designated *unc-41A*, consists of all 12 exons, with a 5' trans-spliced SL1 leader (Figure 4.1A). In addition, a number of cDNA clones were identified with the SL1 leader trans-spliced to the 5'-end of exon 3, suggesting that exon 3 is an alternative starting exon. The cDNAs beginning at exon 3 were designated *unc-41B*. If both of the transcripts have the

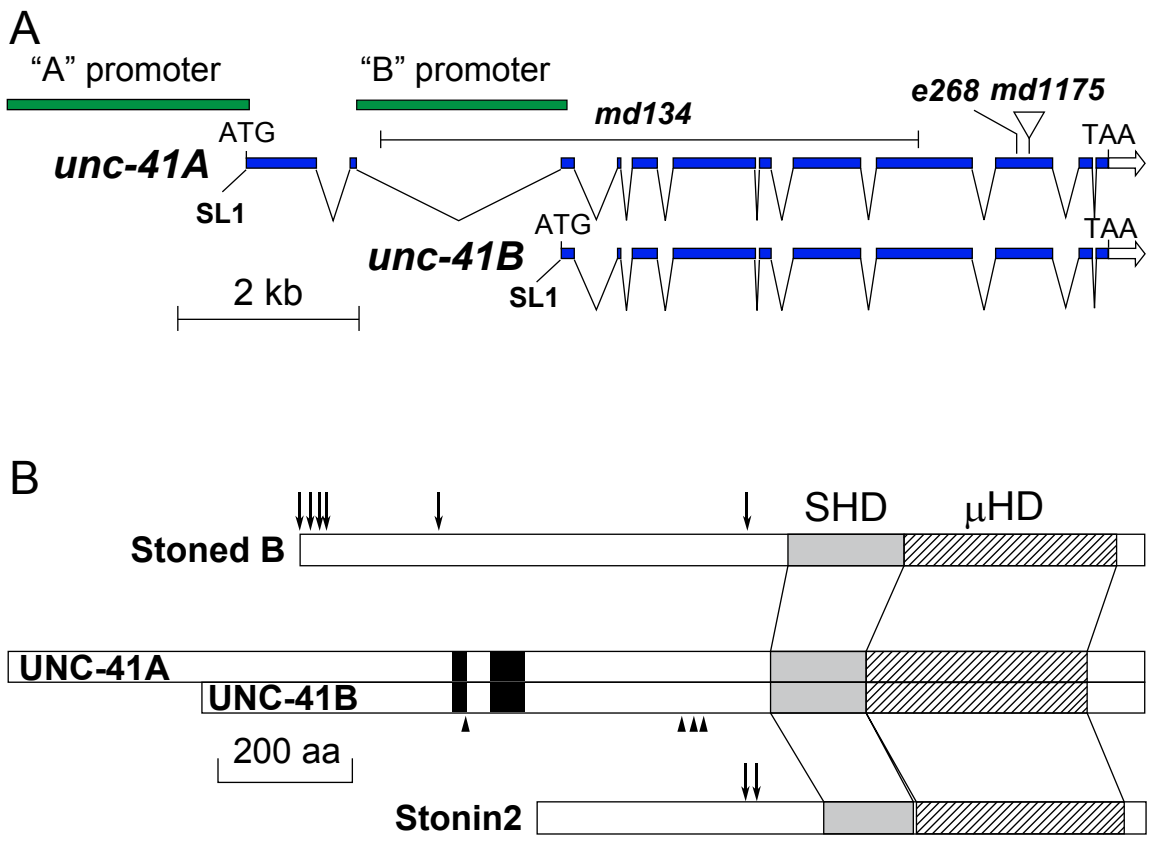

Figure 4.1. *unc-41* cloning. (A) Diagram of the *unc-41* gene, showing intron–exon structure, and location of relevant mutations. The *unc-41* gene consists of twelve exons spanning ~9 kb of genomic DNA, and encodes two protein isoforms of ~188 and 160 kDa. The location of the two promoter regions is shown in green, and the locations of several *unc-41* mutations are indicated. (B) The *unc-41* gene products are homologous to the *Drosophila* Stoned B and mammalian Stonin 2 proteins. Each of these proteins possesses a central stonin-homology domain (SHD) and a C-terminal μ-homology domain (μHD). Significant sequence similarity between the proteins is limited to the stonin- and μ-homology domains. Arrows indicate NPF motifs for interacting EH domain proteins such as Eps15, and arrowheads indicate DPF motifs for interacting with AP2.

same 3'-end, the predicted sizes would be 5.3 kb (*unc-41A*) and 4.5 kb (*unc-41B*). Except for the alternative 5'-ends, we found no evidence for additional structural heterogeneity in the *unc-41* gene products.

Northern blot analysis revealed two low abundance *unc-41* transcripts: a 5.3 kb gene product that hybridizes to probes derived from both the 5' and 3' regions of the gene, and a 4.5 kb gene product that is recognized by probes from the entire gene except for exons 1 and 2 (data not shown). The sizes and hybridization patterns of these two bands are consistent with the structures of the two cDNAs shown in Figure 4.1A.

Sequence comparisons demonstrate that the *unc-41* gene encodes the *C. elegans* homolog of STNB and Stonin 2. A carboxy terminal domain of approximately 500 amino acids is strongly conserved in homologs from all three species (Figure 4.1B). UNC-41 and STNB are approximately 45% identical, and UNC-41 and mouse stonin-2 are approximately 31% identical in this region. The domain organization of the two UNC-41 isoforms is similar to that of the other members of stonins. The N-terminal region does not share significant sequence similarity with other members of this family, but contains two proline-rich regions (Figure 4.1B black box), and has been termed the proline-rich domain (PRD). Following this is a domain found only in members of the stonin family called the stonin homology domain (SHD). The C-terminal domain is similar to the signal-binding domain of the μ subunits of AP complexes, and is called the μ-homology domain (μHD). There is no apparent similarity between any part of the UNC-41 proteins and the *stonedA* gene product.

unc-41 expression pattern

As described above, the two *unc-41* transcripts have alternate 5' exons; *unc-41A* begins with exon 1 and *unc-41B* begins with exon 3. To determine if these gene products were transcribed from different promoters, we generated reporter constructs with the putative *unc-41A* regulatory region (2672-bp upstream of exon 1) or the *unc-41B* regulatory region (2343-bp upstream of exon 3) driving CFP or YFP expression. We found that both reporter constructs were expressed almost exclusively in the nervous system (Figure 4.2). The *unc-41A* reporter was expressed in most or all neurons in *C. elegans*, while the *unc-41B* reporter was expressed in a subset of neurons, including the GABA motor neurons (DD and VD cells) in the ventral nerve cord (Figure 4.2). A significant number of neurons did not express *unc-41B*; these included the ventral cord cholinergic motorneurons (VA, VB, DA, DB, VC, and AS cells). We conclude that the *unc-41A* and *B* gene products are chiefly expressed in the nervous system, and that the *unc-41B* protein is restricted to a subset of *unc-41A*-expressing cells.

Sequence analysis of *unc-41* mutants

We identified the sequence alterations associated with 33 *unc-41* alleles. Sixteen of the mutations were associated with DNA rearrangements leading to altered fragment lengths. These included 13 alleles with Tc1 transposon insertions, a 176-bp tandem duplication, and two significant (≥100-bp) deletions. The remaining seventeen alleles included six point mutations (base-substitutions) and eleven small insertions or deletions, and all led to termination codons or frameshifts. The canonical allele, *e268*, is associated with a base substitution in exon 10, which converts Trp1468 to a stop codon (Figure 4.1A); it is likely to be a null allele. It was noteworthy that we did not identify any

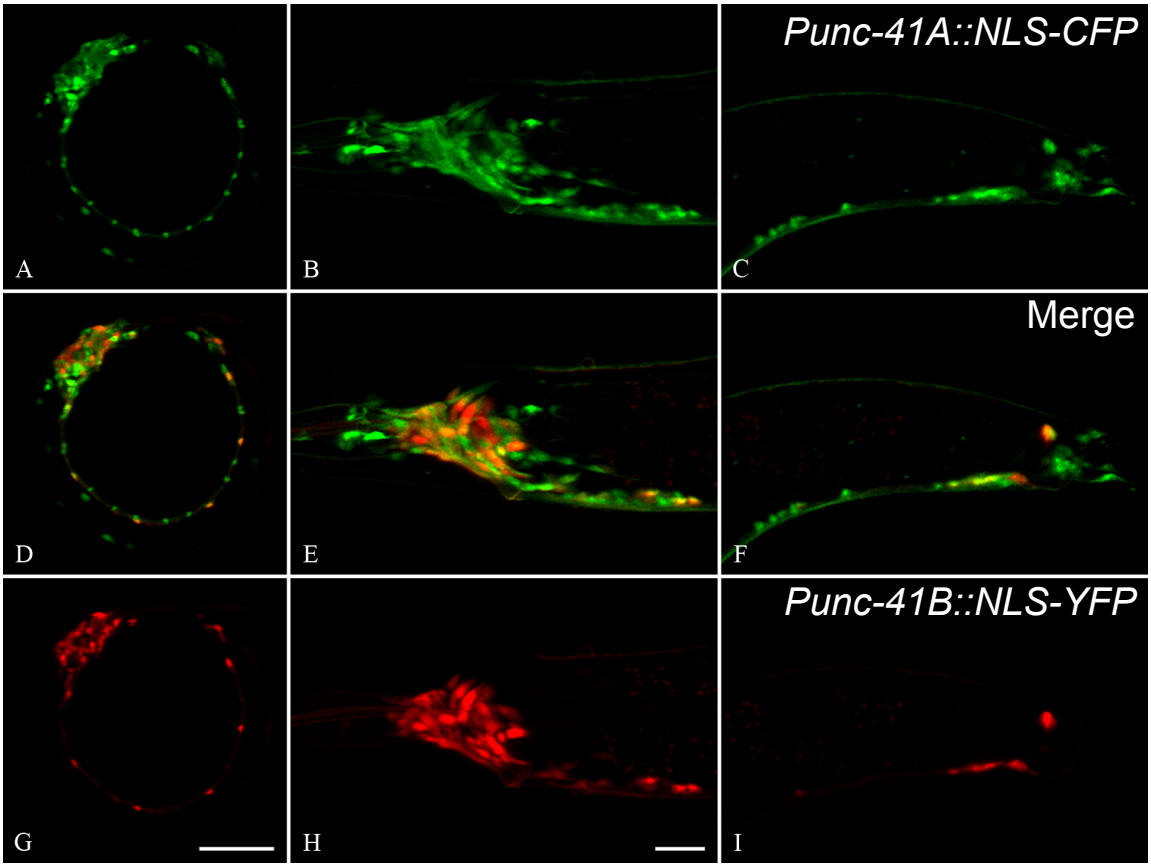

Figure 4.2. *unc-41* expression pattern. The *unc-41* gene products are differentially expressed in the *C. elegans* nervous system. Transgenic animals carrying the *Punc-41A::*NLS-CFP (green, A-F) and *Punc-41B::*NLS-YFP (red, D-I) transgenes were imaged on a confocal microscope. An L1 larva is shown in the left column. The head region of an adult hermaphrodite is shown in B, E, H, and K, and the tail section is shown in C, F, I, and L. Anterior is to the left, ventral is down, and the bar is 10 µm.

missense mutations, even among the EMS-induced alleles.

The synaptic localization of UNC-41 does not require synaptotagmin I

The UNC-41 binding motif to synaptotagmin I C2A domain is the three residues KYE in μ-homologous domain. Mutating KYE to AAA strongly impairs the interaction between UNC-41 and synaptotagmin I, which causes transfected synaptotagmin I to get accumulated on the plasma membrane in HEK293 cells (Jung et al., 2007). In *C. elegans*, UNC-41 with KYE to AAA mutation can be expressed normally in the nervous system; however it loses its synaptic localization and diffuses throughout axons (Jung et al., 2007). Therefore we predicted that UNC-41 is recruited to synapses by synaptotagmin I. To test this, GFP::UNC-41 is expressed in wild type and *snt-1(md290)* mutant. In both cases, the fusion protein is highly enriched in the nervous system and is localized properly to synapses (Figure 4.3), suggesting synaptotagmin I is not necessary for UNC-41 synaptic localization. Previous study from mammalian stonin2 demonstrates that stonin2 co-localizes with several synaptotagmin paralogues: Syt1, Syt2 and Syt9 at the cell surface (Diril et al., 2006), which suggests functional redundancy might exist within synaptotagmin family for stonin2 recruitment. In *C. elegans*, there are 6 synaptotagmin paralogues from *snt-1* to *snt-6*. We further tested synaptic localization of GFP::UNC-41 in two different synaptotagmin triple mutants *snt-4, snt-1, snt-2* and *snt-6, snt-1, snt-3.* As a result, UNC-41::GFP still maintains its synaptic localization even in these mutants (Figure 4.3). Thus, either the remaining synaptotagmins in the triple mutants recruit UNC-41 or UNC-41 is localized to synapses by proteins other than synaptotagmins.

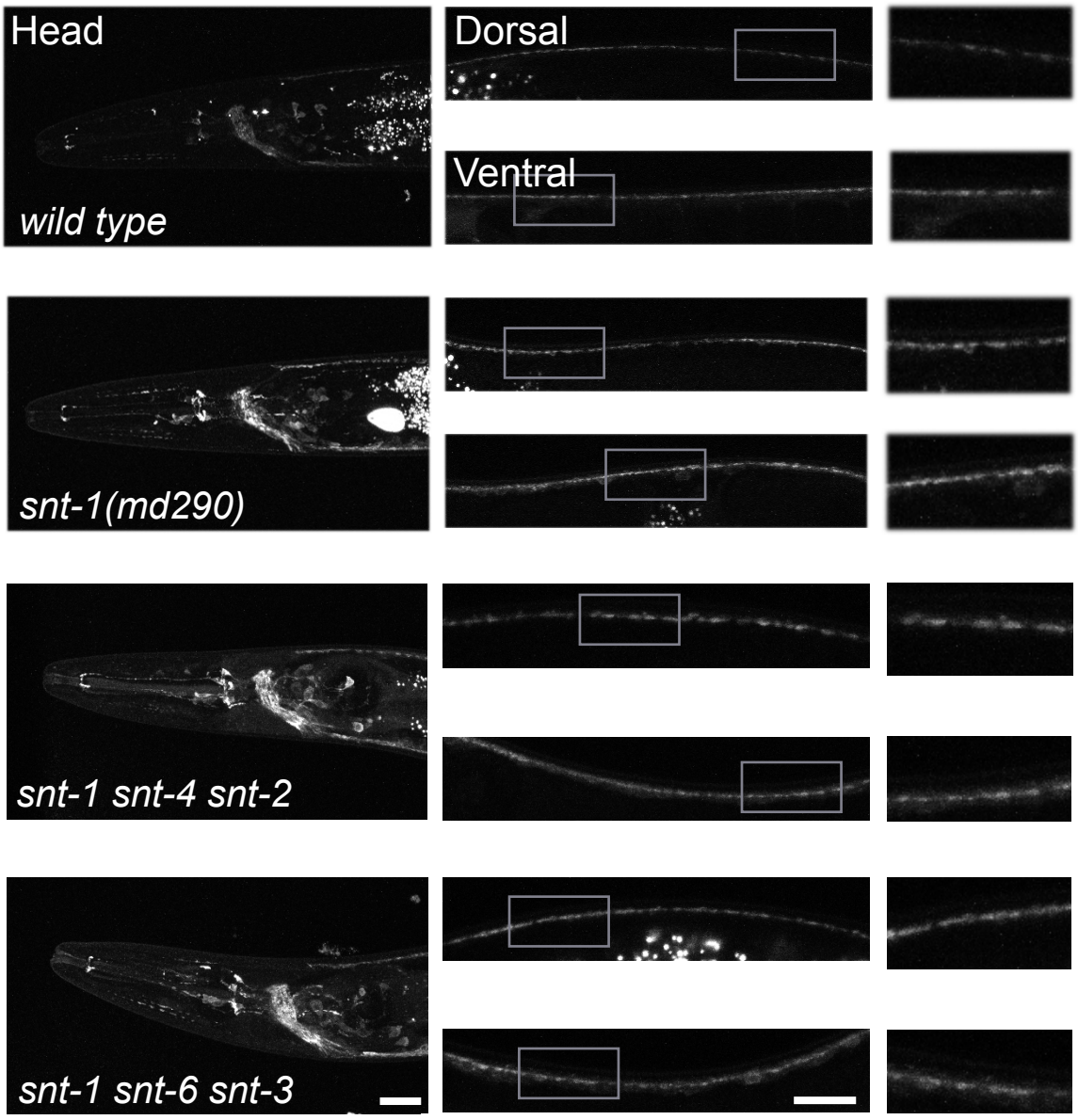

Figure 4.3. GFP::UNC-41 can properly localize to the synapses in various *snt* mutants Punc-41A::gfp::unc-41B exprssion pattern in wild-type, *snt-1(md290), snt-4(ok503) snt-1(md290)snt-2(tm1711)* and *snt-6(tm3686)snt-1(md290)snt-3(tm2426).* The scale bar represents 20 μm.

Ultrastructural analysis of *unc-41* mutants

Because of the potential role of Stonins in synaptic vesicle endocytosis, we quantified synaptic vesicles numbers using electron microscopy in *unc-41* mutants (Figure 4.4A). We observed a 50% reduction of vesicles in both acetylcholine and GABA motor neurons (Figure 4.4B). The number of docked vesicles is proportionally reduced suggesting that the phenotype is not caused by a specific loss in docking (Figure 4.4C). In addition, there is a slight increase in the diameter of synaptic vesicles from 28.5 nm in the wild type to around 32 nm in the *unc-41(e268)* mutant (Figure 4.4D).

Both μ2 adaptin and stonin contain a μ-homology domain. The reduction in synaptic vesicles in *unc-41* is roughly similar to that of *apm-2* (Gu et al., 2008). In both cases, the phenotype is less severe than that of severe endocytosis defects such as those observed in synaptojanin mutants (Harris et al., 2000). It is possible that μ2 adaptin and stonin provide somewhat redundant functions. To test this, we performed ultrastructural analysis on the *unc-41(e268) apm-2(e840)* double mutant (Figure 4.4A). The double mutant shows almost identical phenotypes to the *unc-41* single mutant (Figure 4.4B-D). These data suggest that μ2 adaptin and stonin/UNC-41 do not have significant functional redundancy but rather function in the same pathway during synaptic vesicle endocytosis.

Synaptic localization of vesicle proteins is disrupted in *unc-41* mutants

Because synaptic vesicles are partially depleted in *unc-41* mutants, the recycling of synaptic vesicle proteins from the cell surface is possibly compromised. This would cause vesicle proteins to accumulate at the plasma membrane and then diffuse away from synapses. We investigated the synaptic localization of the following vesicle proteins in *unc-41* mutants: synaptobrevin, GABA transporter UNC-47 and synaptotagmin I. All of

Figure 4.4. Ultrastructural analysis of synaptic structure in *unc-41* mutants. (A) Representative images of neuromuscular junctions in the ventral nerve cord of wild type, *unc-41(e268)* and *unc-41(e268) apm-2(e840)*. Bar, 200nm. sv, synaptic vesicle; dense proj, dense projection. (B) The number of synaptic vesicles is reduced in *unc-41(e268)* and *unc-41(e268) apm-2(e840)* mutants. Average number of synaptic vesicles per profile containing a dense projection in nanometers ± SEM is as follows: wild-type acetylcholine, 19.63 ± 1.28, *n* = 38 synapses; *unc-41(e268)* acetylcholine, 9.53 ± 0.52, *n* = 40 synapses; *unc-41(e268), apm-2(e840)* acetylcholine, 8.93 ± 0.72, *n* = 30 synapses; wild-type GABA, 25.11 ± 1.17, *n* = 36 synapses; *unc-41(e268)* GABA, 14.51 ± 0.81, *n* = 45 synapses; *unc-41(e268), apm-2(e840)* GABA, 11.64 ± 0.84, *n* = 39 synapses. (C) The number of docked synaptic vesicles is reduced in *unc-41(e268)* and *unc-41(e268) apm-2(e840)* mutants. Average number of docked synaptic vesicles per profile containing a dense projection in nanometers ± SEM is as follows: wild-type acetylcholine, 1.82 ± 0.16, *n* = 38 synapses; *unc-41(e268)* acetylcholine, 1.05 ± 0.13, *n* = 40 synapses; *unc-41(e268), apm-2(e840)* acetylcholine 0.9 ± 0.1, *n* = 30 synapses; wild-type GABA, 2.36 ± 0.17, *n* = 36 synapses; *unc-41(e268)* GABA, 1.13 ± 0.12, *n* = 45 synapses; *unc-41(e268), apm-2(e840)* GABA, 1.46 ± 0.13, *n* = 39 synapses. (D) Vesicle diameters are slightly increased in *unc-41(e268)* and *unc-41(e268), apm-2(e840)* mutants. Average size of synaptic vesicles per profile containing a dense projection in nanometers ± SEM is as follows: wild-type acetylcholine, 28.52 ± 0.12, *n* = 733 vesicles; *unc-41(e268)* acetylcholine, 31.51 ± 0.29, *n* = 380 vesicles; *unc-41(e268), apm-2(e840)* acetylcholine, 31.55 ± 0.22, *n* = 265 vesicles; wild-type GABA, 28.7 ± 0.11, *n* = 904 vesicles; *unc-41(e268)* GABA, 34.5 ± 0.27, *n* = 652 vesicles; *unc-41(e268), apm-2(e840)* GABA, 32.18 ± 0.24, *n* = 453 vesicles. *** $P<0.001$.

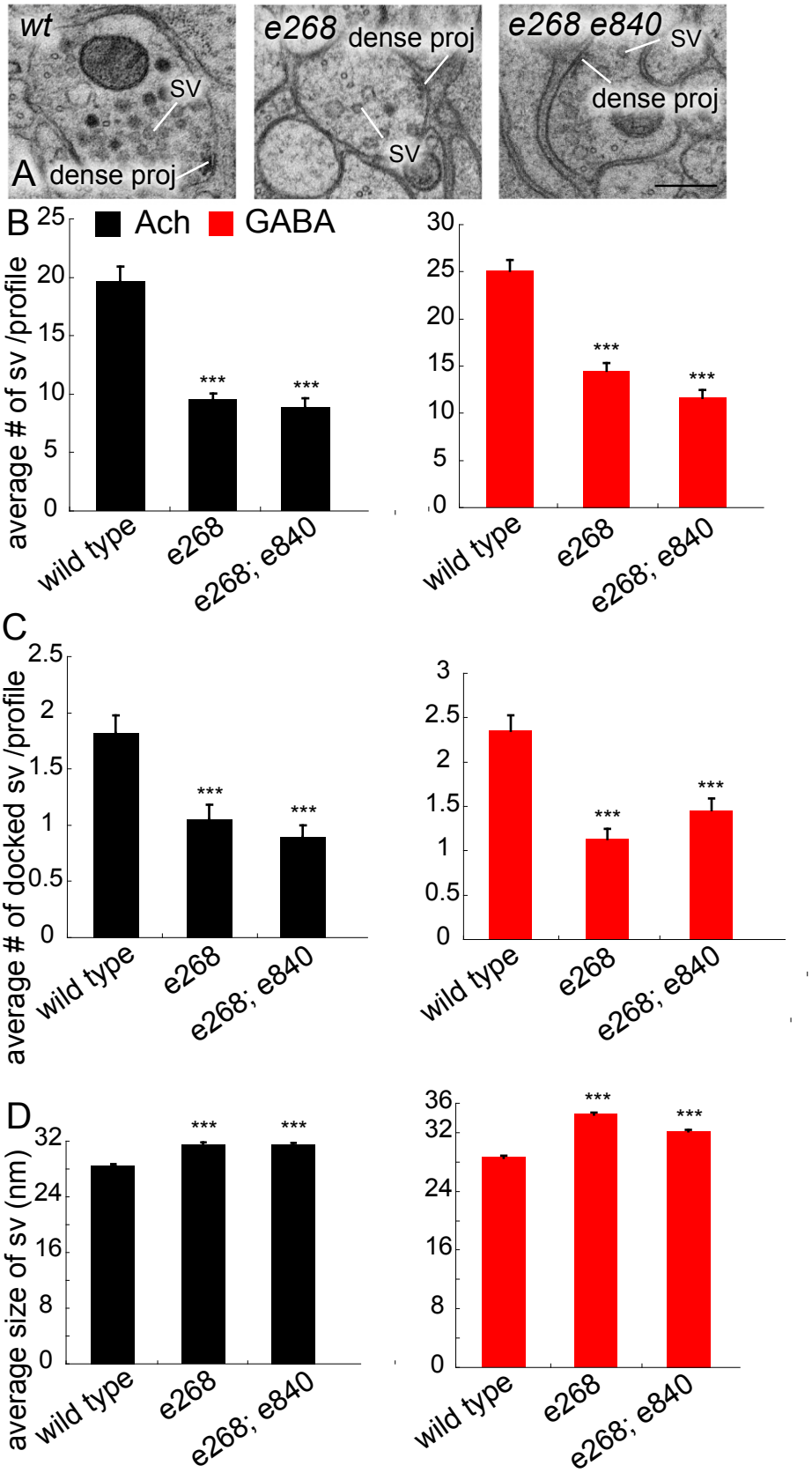
wt
SV
A dense proj
e268
dense proj
SV
e268 e840
SV
dense proj
B
Ach
GABA
average # of sv /profile
25
20
15
10
5
0
30
25
20
15
10
5
0
***
wild type
e268
e268; e840
C
average # of docked sv /profile
2.5
2
1.5
1
0.5
0
3
2.5
2
1.5
1
0.5
0
D
average size of sv (nm)
32
24
16
8
0
36
32
24
16
8
0

these GFP tagged vesicle proteins are normally clustered at synapses in wild type; however they exhibit increased axonal fluorescence in *unc-41* mutants suggesting these proteins are mislocalized from synapses (Figure 4.5). Consistent with the studies from *Drosophila* (Fergestad et al., 1999), the localization of synaptotagmin I is affected the most (Figure 4.5). This result suggests that in *C. elegans*, UNC-41 is required to recycle synaptotagmin I after exocytosis. The localization defect of other vesicle proteins in *unc-41* mutant is caused either directly by missing UNC-41 or indirectly by mislocalized synaptotagmin I because syanptotagmin I is required for synaptic vesicle endocytosis (Jorgensen et al., 1995).

Recruiting synaptotagmin I is the major function of UNC-41

If UNC-41 is the adaptor for resorting synaptotagmin I back into recycled vesicles, providing more synaptotagmin I should be able to bypass the requirement of UNC-41. A particularly compelling observation that supports this view is that overexpression of Synaptotagmin 1 in *Drosophila* rescues the lethality and synaptic vesicle recycling deficits associated with StonedB mutations (Fergestad and Broadie, 2001). We attempted to duplicate these experiments in *C. elegans* by overexpressing functional SNT-1::GFP fusions. When the *snt-1::GFP* construct is expressed at its endogenous level, the fusion proteins localize exclusively to synapses (Figure 4.6A) and fully rescue the *snt-1* null phenotype (data not shown). The same construct was injected directly into *unc-41* mutants at 25 ng/μl to overexpress SNT-1:GFP. From the trasgenic animals of the next generation, the fluorescent intensity of GFP is greatly increased and SNT-1::GFP starts to accumulate on the cell surface of neuronal cell bodies (Figure 4.6A); however these animals still have an uncoordinated body posture (Figure 4.6B) and retain locomotory

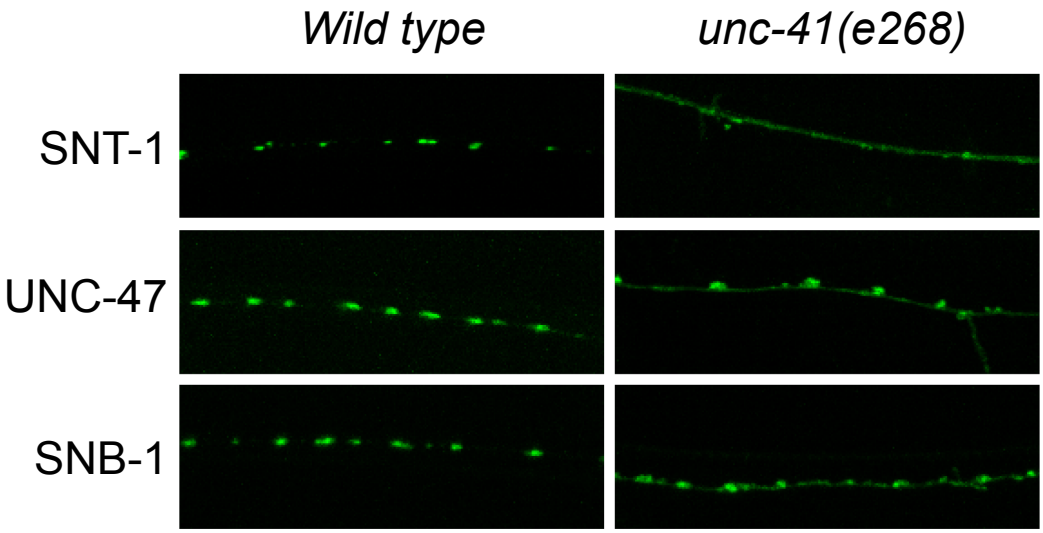

Figure 4.5. The synaptic localization of vesicle proteins is disrupted in *unc-41* null mutants. *snt-1::GFP* and *unc-47::GFP* are integrated into worm genome as single copy insertion by mosSCI. *Punc-25::snb1::GFP* is integrated into worm genome as multiple copies by X-ray. Images of SNT-1::GFP are ventral sub-lateral cords. The rest images are dorsal nerve cords. The scale bar represents 10 μm.

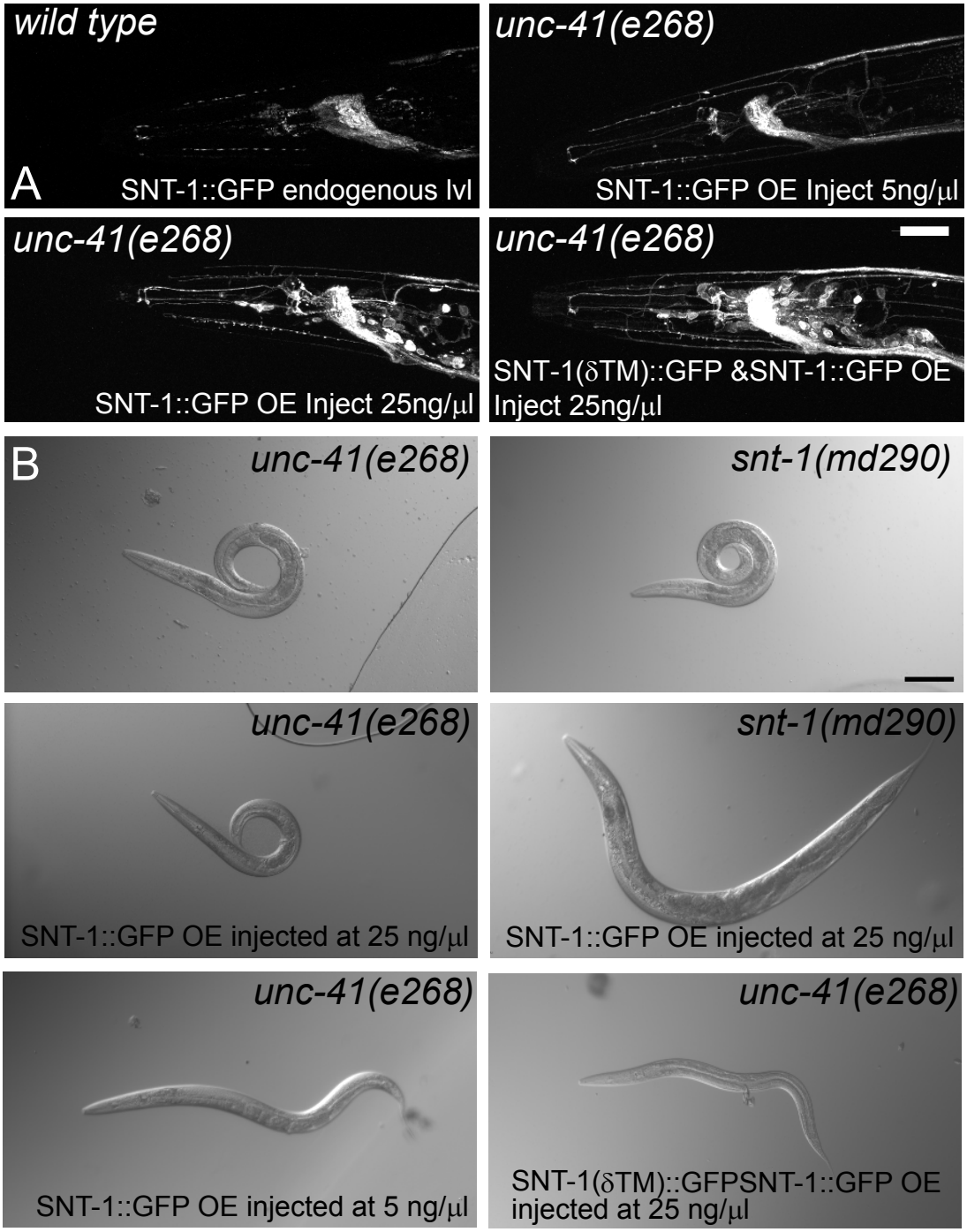

Figure 4.6. Overexpressing synaptotagmin I can not rescue *unc-41* mutants. (A) Representative images of SNT-1::GFP expression level under different overexpression conditions. All images were taken at identical settings. The scale bar represents 20μm. (B) DIC images of *unc-41* mutant, *unc-41* mutants carrying *snt-1::GFP* overexpressing arrays, *snt-1* mutant and *snt-1* mutant carrying *snt-1::GFP* overexpressing array. The scale bar represents 100μm.

deficits as assayed by worm swimming (Figure 4.7). Meanwhile the same extra-chromosomal array overexpressing *snt-1::GFP* was crossed into wild type and *snt-1* null mutant. We found the same array could rescue the body size and posture of *snt-1* mutants (Figure 4.6B) but caused wild- type animals to slow down in worm swimming. It is possible that overexpression of SNT-1::GFP results in retention of protein in the soma that affects the normal transportation process to synapses, so we re-injected the same construct either at lower concentration (5ng/ul) or along with *snt-1::GFP* without a transmembrane domain that has been shown to significantly rescued *snt-1* mutants (data not shown) to alleviate retention. In all of these conditions, no rescue of *unc-41* animals is observed (Figure 4.6 and 4.7). Thus, providing more synaptotagmin I in *unc-41* mutants can not bypass the requirement of UNC-41, suggesting UNC-41 is absolutely required for maintaining the proper sub-cellular localization of synaptotagmin I.

Discussion

In this study, we show that the *unc-41* gene in *C. elegans* encodes two proteins that are members of the STNB/Stonin family. Like other members of the STNB/stonin family, the UNC-41 proteins possess a central stonin-homology domain, and a C-terminal μ-homology domain. The *unc-41* mutant phenotype was significantly rescued by expression of a STNB cDNA under control of the *unc-41A* promoter, we conclude that the UNC-41 proteins are directly orthologous to the *Drosophila* STNB protein.

The two isoforms of UNC-41 are expressed almost exclusively in neurons and are localized to synapses. In our previous study, we found that the synaptotagmin I binding motif in UNC-41 is critical for its synaptic localization (Jung et al., 2007); however missing synaptotagmin I does not disrupt the synaptic localization of UNC-41. After

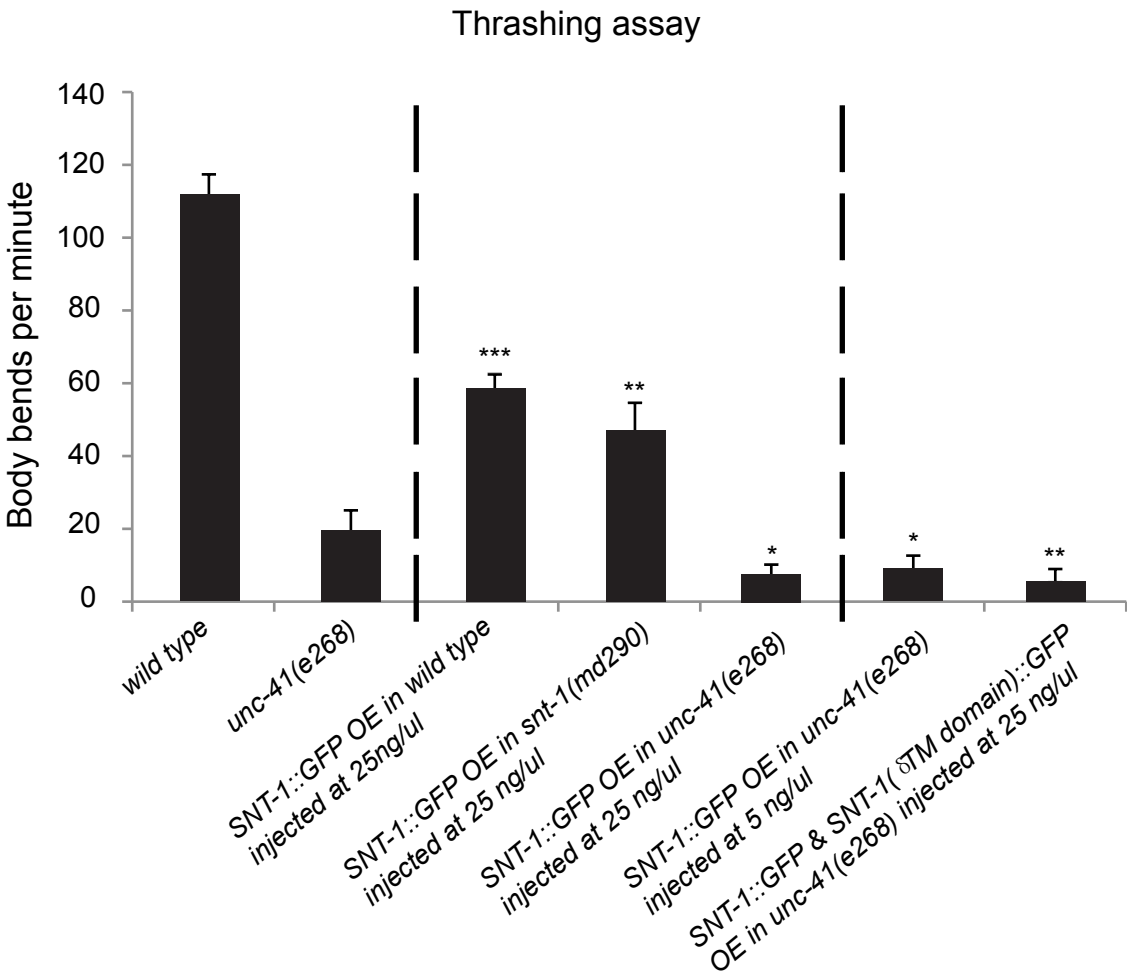

Figure 4.7. Rescue of *unc-41* is assayed by worm swimming. Thrashing rate per minute ± SEM is as follows: wild type 114 ± 3.39, *n* = 7; *unc-41(e268)* 21.43 ± 3.65, *n* = 7; SNT-1::GFP OE in wild type (injected at 25 ng/ul) 60.57 ± 2.26, *n* = 7; SNT-1::GFP OE in *snt-1(md290)* (injected at 25 ng/ul) 49 ± 5.62, *n* = 7; SNT-1::GFP OE in *unc-41(e268)* (injected at 25 ng/ul) 8.83 ± 1.54, *n* = 6; SNT-1::GFP OE in *unc-41(e268)* (injected at 5 ng/ul) 10.5 ± 2.14, *n* = 6; SNT-1::GFP and SNT-1::GFP(δTM) OE in *unc-41(e268)* (injected both at 25 ng/ul) 7.14 ± 1.82, *n* = 7. All *t* tests are compared with the thrashing rate of *unc-41(e268)*. * P<0.05, ** P<0.01, *** P<0.001.

testing UNC-41 localization in synaptotagmin triple mutants, other paralogues of synaptotagmin in *C. elegans* do not play an important role for localizing UNC-41 either. Due to the potential redundancy between synaptotagmins, it might require to knock down all synaptotagmin paralogues simultaneously. On the other hand, besides synaptotagmins, UNC-41 interacts with other endocytic proteins, which can possibly recruit or stabilize UNC-41 at synapses. In *C. elegans*, several endocytic protein mutants exhibit the same phenotypes as those of *unc-41*. These proteins include synaptojanin, endophilin and AP180. So it will be interesting to investigate UNC-41 localization in these mutants.

Based on ultra-structural analysis, *unc-41* mutants have 50% synaptic vesicle reduction, which is similar to the defect observed from the medium subunit mutant of AP2. The *unc-1 apm-2* double mutants have the same amount of vesicles as *unc-41* single mutants suggesting UNC-41 functions in the same endocytic pathway with AP2. Thus UNC-41 and APM-2 do not have functional redundancy consistent with a previous study that the μ-homologous domains from UNC-41 and APM-2 are not interchangeable (Phillips et al., 2010).

One major function of UNC-41 is possibly to re-sort synaptotagmin I into clathrin-coated pit for endocytosis, which is supported by the observation that synaptotagmin I is completely mislocalized from synapses at sub-lateral cords in *unc-41* mutants. Phenotypically, *unc-41* and *snt-1* mutant animals are similar to each other. However the vesicle reduction level in *snt-1* mutants is more severe than that in *unc-41* mutants (personal communication with Rob Hobson, Jorgensen lab), suggesting synaptotagmin I localized at the plasma membrane can still facilitate synaptic vesicle endocytosis. In the future, dendra or tdEOS tagged synaptotagmin I can be crossed into

unc-41 mutants to test if synaptic vesicles left in *unc-41*mutants are lack of synaptotagmin I by fluorescent electron-microscopy.

In *C. elegans*, overexpressing synaptotagmin I does not bypass the requirement of UNC-41, which conflicts with the result from *Drosophila* that overexpression of Synaptotagmin I rescues the lethality and synaptic vesicle recycling deficits associated with StonedB mutations (Fergestad and Broadie, 2001).Thus it suggests that unlike StoneB from *Drosophila,* UNC-41 is essential to maintain synaptotagmin I at the right sub-cellular place in *C. elegans*. In addition, the size of synaptic vesicles is increased 10% in *unc-41* mutants, so UNC-41 involves in regulating the size of synaptic vesicles possibly by affecting the organization of clathrin-coated pits.

Materials and methods

Strains

The wild strain is Bristol N2. The reference strain EG1531 for *unc-41(e268)V* was outcrossed twice before phenotypic analysis. All *oxSi* strains were generated by mosSCI (Frokjaer-Jensen et al., 2008), so the exogenous genes were inserted as a single copy.

The strains used for UNC-41::GFP localization experiment were: EG4775: *snt-1(md290) II; oxEx1072[Punc-41A::GFP::unc-41B Pcc::GFP]* EG4741: *oxEx1050[Punc-41A::GFP::unc-41B Pcc::GFP]* EG6426: *snt-4(ok503)I; snt-1(md290) II; snt-2(tm1711)III; oxEx1528[Punc-41A::GFP::unc-41B Pcc::GFP]* EG6427: *snt-6(tm3686)II snt-1(md290) II; snt-3(tm2426)V; oxEx1529[Punc-41A::GFP::unc-41B Pcc::GFP].*

The strain used for electron microscopy was EG4216 *unc-41(e268)V; apm-2(e840)X.*

The strains used for localization of synaptic vesicle proteins were: EG5882: *snt-*

1(md290)II; oxSi114[snt-1::GFP unc-119(+)] IV EG6428 *oxSi114[snt-1::GFP unc-119(+)]IV; unc-1(e268)V* EG5717: *unc-119(ed3)III; oxSi36[unc-47::GFP unc-119(+)]IV* EG6429 *oxSi36[unc-47::GFP unc-119(+)]IV; unc-41(e268)V* MT8247: *lin-15(n765ts)X nIs52[Punc-25::snb::GFP lin-15(+)]X* EG3049: *unc-41(e268)V; lin-15(n765ts)X nIs52[Punc-25::snb::GFP lin-15(+)]X*

The strains used for UNC-41 overexpression experiment were EG6430: *oxEx1534[snt-1::GFP(25ng) Pcc::GFP]* EG6431: *md290II; oxEx1534[snt-1::GFP(25ng) Pcc::GFP]* EG6432: *unc-41(e268)V oxEx1534[snt-1::GFP(25ng) Pcc::GFP]* EG6433: *unc-41(e268)V; oxEx1535[snt-1::GFP (5ng) Pcc::GFP]* EG6434: *unc-41(e268)V; oxEx1536[snt-1::GFP (25ng) snt-1::GFP(δTM 25ng) Pcc::GFP].*

Origin of *unc-41* mutants

The mutants with *md* allele designations were isolated in the Rand laboratory as spontaneous mutants resistant to the acetylcholinesterase inhibitor aldicarb (Miller et al., 1996; Nguyen et al., 1995). They were identified as *unc-41* alleles by genetic mapping and complementation, and were outcrossed at least six times. All of the *unc-41* alleles with *e* allele designations were isolated at MRC, Cambridge, and were generously provided by Jonathan Hodgkin. The *unc-41* alleles n2163 and n2913 were isolated by Erik Jorgensen and H. R. Horvitz, and *ox63* was isolated by Erik Jorgensen.

Molecular biology, sequence analysis and cloning of *unc-41*

Standard molecular biology techniques were used for preparing *C. elegans* DNA and RNA, screening cDNA and genomic libraries, and performing Northern blot analyses. The *unc-41* gene was cloned by transposon tagging (Moerman et al., 1986). We isolated

several spontaneous unc-41 mutations in screens for aldicarb-resistant mutants in a mutator background. We then probed genomic DNA from these mutant strains, along with isogenic revertants, with Tc1 sequences. We identified a Tc1-hybridizing SacI fragment that was present in strains containing the *unc-41(md1175)* allele, and absent in a spontaneous revertant of *md1175*. This SacI fragment was subcloned, and the sequences flanking the Tc1 transposon were used to probe genomic and cDNA libraries. The genomic phage RM#231L was isolated from a *C. elegans* genomic library prepared by Heidi Browning and Tom Blumenthal. It contains the complete *unc-41* gene plus 3529-bp of upstream sequence. The genomic sequence was determined by "primer walking", using plasmid subclones from phage RM#231L as templates. Sequencing primers were synthesized at the Molecular Biology Resource Facility at the University of Oklahoma Health Sciences Center. Genomic clones and cDNAs were completely sequenced on both strands using the fmol DNA Cycle Sequencing System (Promega, Madison, WI). The larger isoform, UNC-41A, has a predicted mass of 188 kDa, and the smaller isoform, UNC-41B, has a predicted mass of 160 kDa. The *unc-41* gene, which has the cosmid designation C27H6.1, was subsequently sequenced by the *C. elegans* Genome Sequencing Consortium (Genbank Accession number NM073165), with identical results. The cosmid G18K16 (Genbank Accession number AC084520) contains the *C. briggsae* homolog of *unc-41*.

Analysis of mutations

Mutations were analyzed by Southern blot or PCR analysis. Some of the mutants have altered fragment lengths, which allowed us to determine the approximate nature of the rearrangement. Further analysis involved amplification of specific 1-2 kb

unc-41 genomic regions using direct single-worm PCR from individual mutant animals. The precise deletion endpoints or insertion sites were then determined by sequencing purified PCR products using internal primers. PCR products from those mutants without rearrangements were used for Restriction Endonuclease Fingerprinting analysis. Several of the mutations were analyzed by direct sequencing of PCR-amplified genomic DNA. Most of the sequencing of mutants was performed by the DNA Sequencing Center at Oklahoma State University.

Transgenic methods for determining UNC-41 expression pattern

Expression plasmids for transformation utilized the pPD49.26 vector, or derivatives (gifts of Andy Fire, Stanford School of Medicine). Putative promoter regions from the *unc-41* gene were cloned into the first multiple cloning site of pPD49.26. The cDNA to be expressed was cloned into the second multiple cloning site: CFP or YFP reporter gene carrying a nuclear localization signal (gift of Andy Fire, Stanford School of Medicine).

DNA transformation methods for *C. elegans* were essentially as described by Mello et al. (Mello et al., 1991) except that a plasmid containing the wild-type *pha-1* cDNA (gift of Heinke and Ralf Schnabel, Max-Plank-Institute fur Biochemie, Martinsried) was used as a transformation marker. The *pha-1(e2123)* mutation results in a temperature-sensitive embryonic lethal phenotype ; animals homozygous for this mutation will not grow at 25 degree, but are viable and grow normally at 16 degrees. The fluorescent reporter constructs and wild-type *pha-1* cDNA were injected directly into *pha-1* animals; After injection, the recipient animals were transferred to 25 degrees to select for those progeny expressing the wild-type PHA-1 protein.

UNC-41 GFP construct

The GFP–UNC-41B WT (pMG13) *C. elegans* expression plasmid consisted of the 2.5-kb *unc-41* promoter (from RM536), 0.85-kb GFP fragment (from fire lab vector 95.77), and 5.4-kb *unc-41b* cDNA plus 3′UTR (from RM 536) inserted into the EcoRI–SalI restriction sites of pGEM-3zf(+) using the following primers: 5′-AGGAGAATTCCTCCCGGCAATTCGTAATACGTC-3′; 5′-GGGTCCTGAAAATGTTCTATG-3′; 5′-ACATTCCCGGGATGGAACAAGCAGAAAAAGCA-3′; 5′-ACTTGTCGACCATGTGTCAGAGGTTTTCACCGTC-3′; 5′-AGATCCCGGGAGAACCTCCGCCTCCTTTGTATAGTTCATCCATGCCATG-3′; and 5′-ACCGCCCGGGATGAGTAAAGGAGAAGAACTTTTC-3′.

Microinjection

The final DNA concentration of each injection mix is 100 ng/ul. This target concentration was obtained with the addition of Fermentas 1kb DNA ladder (#SM0311).

pMG13 was injected at 1ng/ul in all strains in UNC-41::GFP experiments. The coinjection marker *Pcc:GFP* was injected at 50 ng/ul.

pRH353 *snt-1::GFP* was injected at 25ng/ul, 5 ng/ul or 25 ng/ul along with 25 ng/ul pRH426 *snt-1::GFP(δTM)* respectively in synaptotagmin I over-expression experiment. The coinjection marker *Pcc:GFP* was injected at 50 ng/ul.

Microscopy and imaging

Images of UNC-41 expression pattern. Confocal images were collected on a Leica TCS NT confocal microscope. Images were collected with a 40x magnification

objective, at 1024x1024 pixels, with 0.5 micron Z-steps. Images were cropped to size, assembled, and annotated using Adobe Photoshop CS2. All images within a given experiment were collected in the same session using identical settings and were processed identically.

All other images. Worms are immobilized by using 2% phenoxy propanol and imaged on a Pascal LSM5 confocal microscope using a Zeiss plan-Neofluar 10x 0.3 NA or Zeiss plan-apochromat 63x 1.4NA oil objectives.

Electron microscopy

Wild type (N2), *unc-41(e268)* and *unc-41(e268) dpy-23(e840)* adult nematodes were prepared in parallel for transmission electron microscopy (Rostaing et al., 2004; Adler et al., 2006). All animals were raised at room temperature (22.5°C). After high-pressure freezing, chemical fixation and substitution, and embedding, mutant and control blocks were blinded, and ribbons of ultrathin (33 nm) serial sections were collected using an Ultracut 6 microtome (Leica). 250 contiguous ultrathin sections were cut from two animals from each genotype. Images were collected on a Hitachi H-7100 125keV electron microscope using a Gatan slow scan digital camera. Image analysis was performed using ImageJ software (v1.38 NIH). Axonal processes in the ventral nerve cord were reconstructed for the VA and VB acetylcholine motor neurons and the VD γ-aminobutyric (GABA) motor neurons. Neuromuscular synapses were identified by the presence of a varicosity containing synaptic vesicles surrounding a dense projection oriented toward the muscle. The total number of neuromuscular junctions analyzed was 19 synapses (10 acetylcholine and 9 GABA) for *unc-41* and 18 synapses (9 acetylcholine and 9 GABA) for *unc-41 dpy-23* double mutants. Vesicles were analyzed only in sections

containing a dense projection. The numbers of synaptic vesicles (~30nm), dense-core vesicles (~40nm) and large vesicles (>40nm) at each synapse were counted, and their distances from presynaptic specialization and plasma membrane were determined, as well as their diameters. The average number of synaptic vesicles and docked vesicles per profile were calculated for each set of images containing a part of the presynaptic dense projection. The numbers for each profile were averaged to obtain the final value.

Acknowledgements

We thank Andre Jones and Gunther Hollopeter for kindly providing UNC-47::GFP strain

References

Diril, M.K., M. Wienisch, N. Jung, J. Klingauf, and V. Haucke. 2006. Stonin 2 is an AP-2-dependent endocytic sorting adaptor for synaptotagmin internalization and recycling. *Dev Cell*. 10:233-44.

Dittman, J., and T.A. Ryan. 2009. Molecular circuitry of endocytosis at nerve terminals. *Annu Rev Cell Dev Biol*. 25:133-60.

Fergestad, T., and K. Broadie. 2001. Interaction of stoned and synaptotagmin in synaptic vesicle endocytosis. *J Neurosci*. 21:1218-27.

Fergestad, T., W.S. Davis, and K. Broadie. 1999. The stoned proteins regulate synaptic vesicle recycling in the presynaptic terminal. *J Neurosci*. 19:5847-60.

Frokjaer-Jensen, C., M.W. Davis, C.E. Hopkins, B.J. Newman, J.M. Thummel, S.P. Olesen, M. Grunnet, and E.M. Jorgensen. 2008. Single-copy insertion of transgenes in Caenorhabditis elegans. *Nat Genet*. 40:1375-83.

Grigliatti, T.A., L. Hall, R. Rosenbluth, and D.T. Suzuki. 1973. Temperature-sensitive mutations in Drosophila melanogaster. XIV. A selection of immobile adults. *Mol Gen Genet*. 120:107-14.

Gu, M., K. Schuske, S. Watanabe, Q. Liu, P. Baum, G. Garriga, and E.M. Jorgensen. 2008. Mu2 adaptin facilitates but is not essential for synaptic vesicle recycling in Caenorhabditis elegans. *J Cell Biol*. 183:881-92.

Harada, S., I. Hori, H. Yamamoto, and R. Hosono. 1994. Mutations in the unc-41 gene cause elevation of acetylcholine levels. *J Neurochem*. 63:439-46.

Harris, T.W., E. Hartwieg, H.R. Horvitz, and E.M. Jorgensen. 2000. Mutations in synaptojanin disrupt synaptic vesicle recycling. *J Cell Biol*. 150:589-600.

Jorgensen, E.M., E. Hartwieg, K. Schuske, M.L. Nonet, Y. Jin, and H.R. Horvitz. 1995. Defective recycling of synaptic vesicles in synaptotagmin mutants of Caenorhabditis elegans. *Nature*. 378:196-9.

Jung, N., M. Wienisch, M. Gu, J.B. Rand, S.L. Muller, G. Krause, E.M. Jorgensen, J. Klingauf, and V. Haucke. 2007. Molecular basis of synaptic vesicle cargo recognition by the endocytic sorting adaptor stonin 2. *J Cell Biol*. 179:1497-510.

Maritzen, T., J. Podufall, and V. Haucke. 2010. Stonins--specialized adaptors for synaptic vesicle recycling and beyond? *Traffic*. 11:8-15.

Martina, J.A., C.J. Bonangelino, R.C. Aguilar, and J.S. Bonifacino. 2001. Stonin 2: an adaptor-like protein that interacts with components of the endocytic machinery. *J Cell Biol*. 153:1111-20.

McIntire, S.L., E. Jorgensen, and H.R. Horvitz. 1993. Genes required for GABA function in Caenorhabditis elegans. *Nature*. 364:334-7.

Mello, C.C., J.M. Kramer, D. Stinchcomb, and V. Ambros. 1991. Efficient gene transfer in C.elegans: extrachromosomal maintenance and integration of transforming sequences. *EMBO J*. 10:3959-70.

Miller, K.G., A. Alfonso, M. Nguyen, J.A. Crowell, C.D. Johnson, and J.B. Rand. 1996. A genetic selection for Caenorhabditis elegans synaptic transmission mutants. *Proc Natl Acad Sci U S A*. 93:12593-8.

Moerman, D.G., G.M. Benian, and R.H. Waterston. 1986. Molecular cloning of the muscle gene unc-22 in Caenorhabditis elegans by Tc1 transposon tagging. *Proc Natl Acad Sci U S A*. 83:2579-83.

Nguyen, M., A. Alfonso, C.D. Johnson, and J.B. Rand. 1995. Caenorhabditis elegans mutants resistant to inhibitors of acetylcholinesterase. *Genetics*. 140:527-35.

Nonet, M.L., A.M. Holgado, F. Brewer, C.J. Serpe, B.A. Norbeck, J. Holleran, L. Wei, E. Hartwieg, E.M. Jorgensen, and A. Alfonso. 1999. UNC-11, a Caenorhabditis elegans AP180 homologue, regulates the size and protein composition of synaptic vesicles. *Mol Biol Cell*. 10:2343-60.

Phillips, A.M., M. Ramaswami, and L.E. Kelly. 2010. Stoned. *Traffic*. 11:16-24.

Phillips, A.M., M. Smith, M. Ramaswami, and L.E. Kelly. 2000. The products of the Drosophila stoned locus interact with synaptic vesicles via synaptotagmin. *J Neurosci*. 20:8254-61.

Rand, J.B., and R.L. Russell. 1985. Molecular basis of drug-resistance mutations in C. elegans. *Psychopharmacol Bull*. 21:623-30.

Robinson, M.S., and J.S. Bonifacino. 2001. Adaptor-related proteins. *Curr Opin Cell Biol*. 13:444-53.

Walther, K., M.K. Diril, N. Jung, and V. Haucke. 2004. Functional dissection of the interactions of stonin 2 with the adaptor complex AP-2 and synaptotagmin. *Proc Natl Acad Sci U S A*. 101:964-9.

Zhang, B., Y.H. Koh, R.B. Beckstead, V. Budnik, B. Ganetzky, and H.J. Bellen. 1998. Synaptic vesicle size and number are regulated by a clathrin adaptor protein required for endocytosis. *Neuron*. 21:1465-75.

CHAPTER 5

PRELIMINARY CHARACTERIZATION OF THE EPSIN ORTHOLOGUE IN *C. ELEGANS*

My contribution to this work includes the following:

1. Balancing and outcrossing *epn-1(tm3357)* allele.
2. Investigating the expression pattern of *epn-1*.
3. Building constructs and rescuing *epn-1* in tissue-specific manner.

Abstract

Epsin, as the representative ENTH domain protein, functions in clathrin-mediated endocytosis presumably for membrane bending. In the absence of Epsin, clathrin-coated pits lack membrane curvature, suggesting an early but critical role in endocytosis. Studies from *Drosophila* and lamprey show conflicting results regarding the function of Epsin in neurotransmission. In this chapter, we investigated the Epsin ortholog *epn-1* in *C. elegans* and its potential role in synaptic vesicle recycling. To our surprise, EPN-1 is not a synaptic protein in worms. When EPN-1 is specifically expressed in neurons, it is not localized to presynaptic terminals, which suggests EPN-1 is not required for synaptic vesicle endocytosis in *C. elegans.*

Introduction

Epsin is a well-studied endocytic protein involved in clathrin-coated pit formation. It was first discovered as a binding partner of another accessory protein Eps15 in clathrin-mediated endocytosis (Chen et al., 1998). Therefore it is named as Eps15 Interacting protein or Epsin (Horvath et al., 2007). This protein has potential roles in both membrane bending and cargo recruitment. One of the important characteristics of Epsin is that it has a well-conserved protein module at its N-terminus called the ENTH domain. The ENTH domain stands for Epsin N-terminal homologous domain. It is present in a protein family required for membrane trafficking throughout eukaryotes (De Camilli et al., 2002).

The ENTH domain is a globular structure composed of 7 α-helices (helix1-7) and an unstructured 14-residue region at its N-terminus (Koshiba et al., 2002). Upon binding with PI(4,5)P2 or Ins(1,4,5)P3, the disordered N-terminal region will fold into an

amphipathic α-helix, called helix 0 (Ford et al., 2002). Helix 0 was proposed to insert into the cytosolic leaflet of lipid bilayer to drive membrane bending. In addition, the concaved surface formed by the newborn helix 0 and the rest of ENTH domain can sense the membrane curvature (Itoh and De Camilli, 2006). Thus ENTH-domain proteins bind specifically to PI(4,5)P2 enriched membranes and likely provide the driving force for membrane invagination.

Outside the ENTH domain, Epsin has several conserved binding motifs for interacting with different binding partners. The type and number of these motifs varies between Epsin homologs. Generally, the ENTH domain of Epsin is followed by two ubiquitin interacting motifs (UIM), which can fulfill the function of Epsin as an adaptor protein to recruit ubiquitinated cargo proteins into clathrin-coated pits (Kazazic et al., 2009). Next to the UIMs are multiple repeats of DPF/W motifs for interacting with the appendage domain of α adaptin from the AP2 complex. The DPF/W motifs are always flanked by clathrin boxes, which are responsible for clathrin interaction (Legendre-Guillemin et al., 2004; Owen et al., 1999). At the C-terminus of Epsin, there are NPF repeats for interacting with EH domain proteins, such as Eps15 and intersectin (De Camilli et al., 2002).

Epsin can stimulate clathrin cage assembly from soluble clathrin triskelia (Kalthoff et al., 2002). In vitro, Epsin recruits clathrin to a PI(4,5)P2 monolayer to form an invaginated clathrin-coated pit. If Epsin is changed to AP180, another clathrin adaptor that can also facilitate clathrin-cage formation, the coated pit is flat (Ford et al., 2002). This result demonstrates the importance of Epsin for the acquisition of membrane curvature, suggesting that Epsin functions at the onset of clathrin-mediated endocytosis.

Even though the roles of Epsin in clathrin-mediated endocytosis have been studied for a decade, the function of this protein in synaptic vesicle recycling is still not clear. In *Drosophila,* the loss of Epsin in neurons does not cause neurotransmission defects and the total number of synaptic vesicles is wild-type (Bao et al., 2008). However in lamprey, the active synapses show dramatic loss of vesicles and coated-pits after blocking Epsin function by antibody injection (Jakobsson et al., 2008). In order to enhance our knowledge of Epsin's function in neurotransmission, we investigated the Epsin ortholog in *C. elegans*, *epn-1*. Our data suggest that EPN-1 is not required for synaptic vesicle recycling in worms.

Results

epn-1 encodes the only Epsin ortholog in *C. elegans*

A mutant allele (*tm3357)* of *epn-1* was successfully isolated by the Mitani lab. It contains a 329 bp deletion from the second intron to the fourth exon. Right at the deletion junction, there is a 7 bp insertion of the sequence GATATAT, according to the coding strand of *epn-1* (Figure 5.1A, B). This gene is located on chromosome X. *epn-1(tm3357)* makes the worm embryonic lethal so this allele is balanced by szT1 which is a translocation between chromosome I and X.

Phylogenetic analysis of the ENTH domain shows that *epn-1* is grouped in the same clade with *Drosophila* liquid facets and human epsin 1-3 (Legendre-Guillemin et al., 2004), suggesting this gene encodes the only ortholog of Epsin in *Caenorhabditis elegans*. The protein structure of EPN-1 is shown in Figure 5.1 C. It contains the well-conserved ENTH domain at its N-terminus. Immediately adjacent are two UIM motifs for binding ubiquitinated protein cargoes. In the middle of the protein three DPF/W motifs are

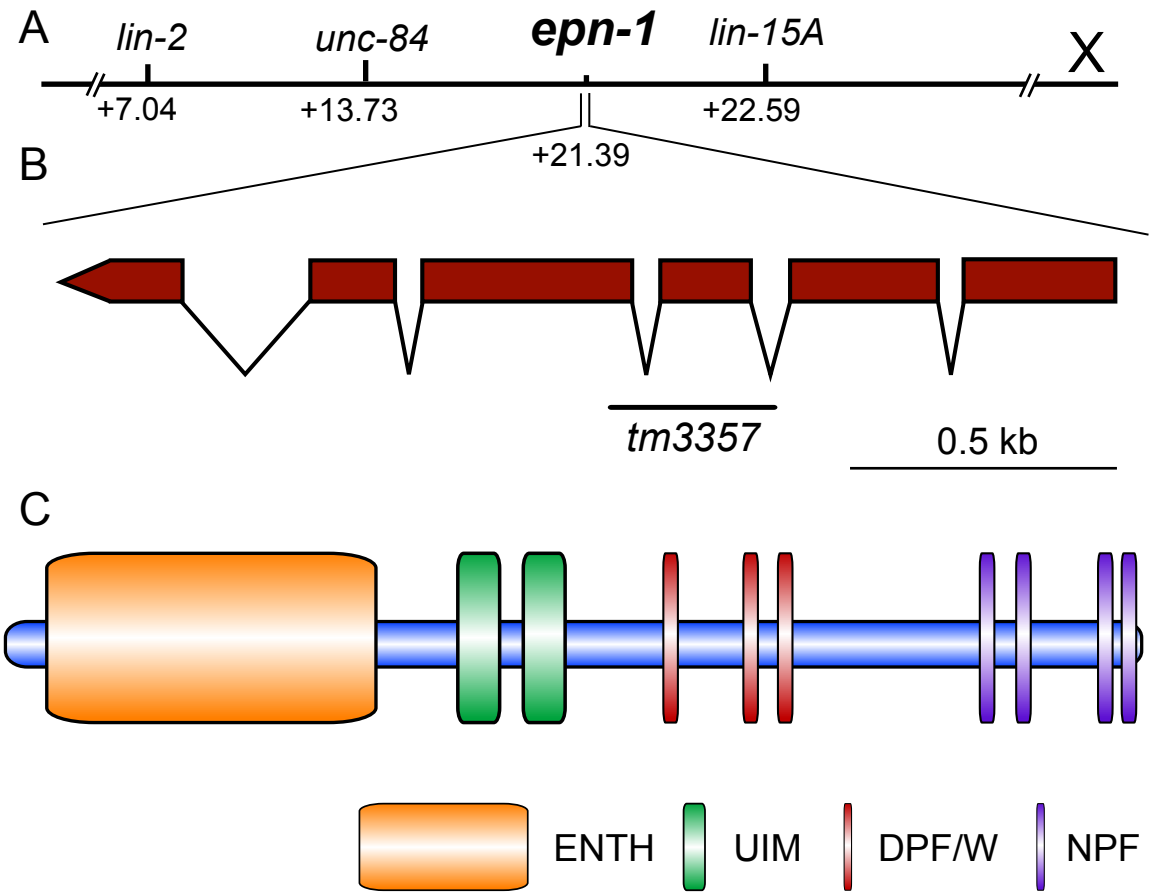

Figure 5.1. The gene and protein structure of the Epsin ortholog in *C. elegans*. (A) Genetic map position of *epn-1* on chromosome X. (B) Genomic structure of the *epn-1* gene. The deleted region from allele *tm3357* is indicated by the black bar. The first exon is on the right hand side. (C) The protein domain and motif cartoon of EPN-1. The protein N-terminus is on the left hand side.

identified as the potential binding sites for α adaptin, which are flanked by three clathrin binding motifs (DLL) (Morgan et al., 2000). At the C-terminus of EPN-1, four NPF motifs interact with EH domain proteins, such as Eps15.

epn-1 expression pattern

EPN-1 is predicted to be required in almost every living cell for cell-surface endocytosis. To better understand where *epn-1* is expressed, we made a construct fusing GFP to the C-terminus of the *epn-1* coding sequence. This construct is driven by the endogenous promoter for *epn-1* and can fully rescue *epn-1(tm3357)* mutants. After making transgenic worms, fluorescence is observed in hypodermis (Figure 5.2A, B tail), spermatheca (Figure 5.2A), head nerve ring (Figure 5.2B, head), pharyngeal muscle (Figure 5.2B head), vulva (Figure 5.2B, body) and coelomocytes (Figure 5.2C). Intestine expression is also observed (data not shown). Interestingly, GFP signal is not detected in any motor neuron synapses along both the ventral and dorsal sides of the worm (Figure 5.2 C). Thus, *epn-1* is expressed in all tissues examined and the protein is likely enriched at the plasma membrane as suggested by the expression pattern in coelomocytes.

EPN-1 is not a synaptic protein

Based on previous studies, Epsin is likely to function at the beginning of clathrin mediated endocytosis to acquire membrane curvature and recruit clathrin for coat formation. If this is true, eliminating EPN-1 in neurons will block clathrin-mediated endocytosis for synaptic vesicle recycling. However, the lack of synaptic expression of the *epn-1::GFP* fusion construct suggests that EPN-1 is not even a synaptic protein in *C. elegans*. It is also possible that the expression level of EPN-1 driven by its own promoter

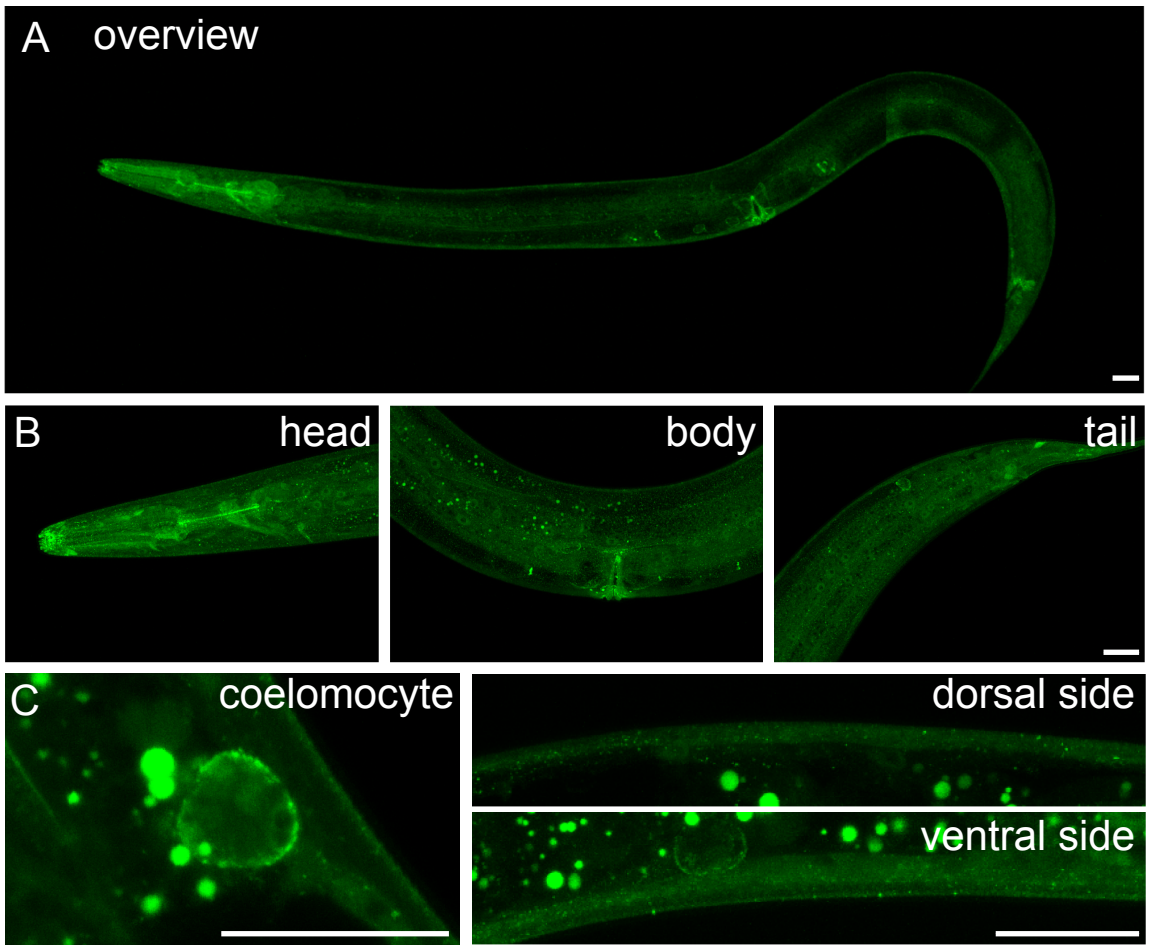

Figure 5.2. *epn-1* translational GFP expression pattern. (A) A single worm overview of EPN-1::GFP under a 20X objective. (B) Closer view of EPN-1::GFP in the head, mid-body and tail region under a 40X objective. (C) EPN-1::GFP localization in coelomocytes and the hypodermal ridge under a 63X objective. The scale bar represents 20 μm.

is very low at synapses, which is difficult to detect when GFP is also expressed in the hypodermis. Therefore we used the pan-neuronal promoter *Prab-3* to drive *epn-1::GFP* expression. Fluorescence from these transgenic worms is observed exclusively in the nervous system; but surprisingly, EPN-1::GFP fusion proteins diffuse throughout the axon and are not specific to synapses (Figure 5.3 A, B). This result indicates that EPN-1 is not functioning at synapses in *C. elegans.* The same construct was also used to rescue *epn-1(tm3357)* mutants. The rescued worms are still lethal. The best-rescued worms grow to adulthood but have skin problems, an infertile gonad and in general are very ill. Thus the lethality of *epn-1* mutants is not exclusively due to a lack of EPN-1 function in neurons.

To further explore which tissue contributes to the lethality phenotype of *epn-1*, we did skin- specific rescue by using the *dpy-7* promoter. The rescued F1 worms from the balanced strain can grow into adults but are sick and egg-laying defective. In the F2 generation, almost all worms are dead as L2 larvae. In rare cases they become adults. Taken together, our data show that the lethality of *epn-1* mutants is likely caused by the lack of EPN-1 activity from multiple tissues, suggesting a broad requirement of EPN-1 during the worm life cycle. However, the lack of EPN-1 synaptic expression is consistent with the results from *Drosophila* Epsin and indicates that EPN-1 is not involved in synaptic vesicle recycling in *C. elegans.*

Discussion

In this chapter we investigated the expression pattern and synaptic localization of *epn-1,* the Epsin ortholog in *C. elegans.* The gene *epn-1* is expressed in almost every tissue and the loss of EPN-1 causes worm embryonic lethal. Failure to rescue *epn-1*

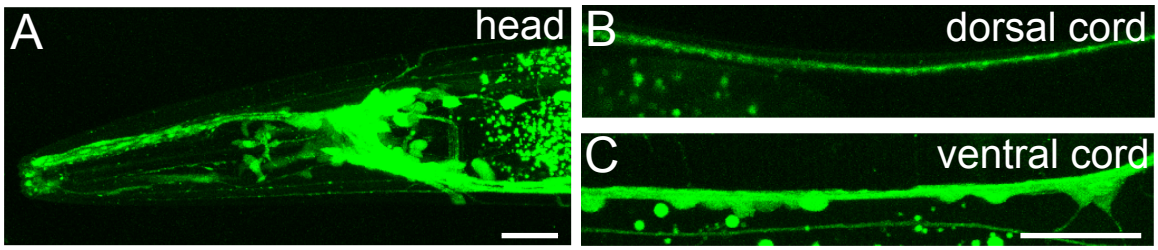

Figure 5.3. Pan-neuronal EPN-1::GFP diffues throughout the axon. (A) EPN-1::GFP localization in the head nerve ring. (B) EPN-1::GFP localization in the dorsal nerve cord. (C) EPN-1::GFP localization in the ventral nerve cord. The scale bar represents 20 μm.

mutants in a single tissue suggests its broad requirement in worms. Considering that extrachromosomal arrays are silenced in the worm germline, it is quite surprising that EPN-1::GFP can fully rescue *epn-1* mutants. It is possible that EPN-1 is not required for oocyte maturation. But due to the high rate of endocytosis in a growing oocyte , there likely exists a functionally redundant protein with EPN-1 in worm gonads.

Based on previous studies, Epsin functions at the clathrin-coated pit to acquire membrane curvature and also binds AP2 and clathrin. If clathrin-mediated endocytosis is the major mechanism for synaptic vesicle recycling, disrupting *epn*-1 will likely cause a profound effect on neurotransmission. However when *epn-1::GFP* is expressed exclusively in neurons, it diffuses throughout the axon, which is in contrast to the punctate distribution pattern seen for μ2 and α adaptins. All three of these proteins are primarily localized on the plasma membrane through interactions with PI(4,5)P2; thus, it is interesting that only EPN-1 is excluded from the cell surface at synapses. This result suggests at least two possibilities. First, PIP2 is not sufficient to recruit EPN-1 to the plasma membrane and requires assistance from another protein that is not expressed in neurons. Second, during clathrin-mediated endocytosis, the spatial and temporal protein-protein interactions for synaptic vesicle recycling are distinct from the well-studied transfferin and EGFR endocytosis. EPN-1 might not be involved in endocytosis at presynaptic terminals. Since AP2 is responsible for the majority of synaptic vesicle recycling, as suggested in Chapter 3, there may exist a neuronal specific BAR domain or ENTH domain protein to fulfill the role of EPN-1 in curvature acquisition. On the other hand, the expression of *epn-1* in the nerve ring suggests that EPN-1 does in fact function in neurons. Studies from *Drosophila* indicate that Epsin functions in ubiquitin pathways

to regulate synapatic plasticity and structure (Bao et al., 2008), In *C. elegans*, Epsin is present in the head nerve ring but is absent from synapses and cell bodies of motor neurons suggesting if Epsin plays a similar role in worms, this function is only required in subset of neurons.

Materials and methods

Strains

The wild strain is Bristol N2. The reference allele *tm3357* was nicely provided by the *C. elegans* gene knockout consortium and was outcrossed four times before phenotypic analysis.

The strain used for the EPN-1 translational GFP analysis was *unc-119(ed3)III; oxEx1424[Pepn-1::epn-1::GFP unc-119(+)]*.

The strains used for *epn-1* tissue-specific rescue were: *epn-1(tm3357)X; oxEx1399[Pepn-1::epn-1::GFP Punc-122::GFP]* and *epn-1(tm3357)X; oxEx1406[Prab-3::epn-1::GFP Pcc::GFP] oxEx1413[epn-1(+) Pmyo-2::mCherry]*.

GFP construct

The Multisite Gateway three fragment construction system was used (Invitrogen catalog no.12537-023) to generate all *epn-1::GFP* constructs. A 1.5 kb genomic fragment before the ATG of *epn-1* was cloned into the pENTRY4-1 donor vector. ATGless, *Prab-3* and *Pdpy7* 4-1 entry vectors are the same as those described in Chapter *3*. The *epn-1* genomic coding sequence of about 1.9 kb was cloned into the pENTRY 1-2 donor vector. The 3' UTR entry vector pENTRY2-3 GFP::*unc-54* 3'UTR was made and used in the LR reaction to generate the *epn-1*::GFP fusion gene driven by different promoters.

Microinjection

The total DNA concentration of the injection mixes were 100 ng/ul. All *epn-1::GFP* related constructs were injected at 1ng/ul. Different coinjection markers were injected at the following concentrations: *Punc-122::GFP* (50 ng/ul); *unc-119(+)* (50 ng/ul); *Pmyo-2::mCherry* (2.5 ng/ul). Fermentas 1kb DNA ladder (#SM0311) was used to bring the final concentration to 100 ng/ul.

Confocal microscopy

Worms were immobilized with 2% phenoxy propanol and imaged on a Pascal LSM5 confocal microscope using a Zeiss plan-Neofluar 10x 0.3 NA, 20x 0.5 NA, 40x 1.3 NA oil or Zeiss plan-apochromat 63x 1.4NA oil objectives.

References

Bao, H., N.E. Reist, and B. Zhang. 2008. The Drosophila epsin 1 is required for ubiquitin-dependent synaptic growth and function but not for synaptic vesicle recycling. *Traffic*. 9:2190-205.

Chen, H., S. Fre, V.I. Slepnev, M.R. Capua, K. Takei, M.H. Butler, P.P. Di Fiore, and P. De Camilli. 1998. Epsin is an EH-domain-binding protein implicated in clathrin-mediated endocytosis. *Nature*. 394:793-7.

De Camilli, P., H. Chen, J. Hyman, E. Panepucci, A. Bateman, and A.T. Brunger. 2002. The ENTH domain. *FEBS Lett*. 513:11-8.

Ford, M.G., I.G. Mills, B.J. Peter, Y. Vallis, G.J. Praefcke, P.R. Evans, and H.T. McMahon. 2002. Curvature of clathrin-coated pits driven by epsin. *Nature*. 419:361-6.

Horvath, C.A., D. Vanden Broeck, G.A. Boulet, J. Bogers, and M.J. De Wolf. 2007. Epsin: inducing membrane curvature. *Int J Biochem Cell Biol*. 39:1765-70.

Itoh, T., and P. De Camilli. 2006. BAR, F-BAR (EFC) and ENTH/ANTH domains in the regulation of membrane-cytosol interfaces and membrane curvature. *Biochim Biophys Acta*. 1761:897-912.

Jakobsson, J., H. Gad, F. Andersson, P. Low, O. Shupliakov, and L. Brodin. 2008. Role of

epsin 1 in synaptic vesicle endocytosis. *Proc Natl Acad Sci U S A*. 105:6445-50.

Kalthoff, C., J. Alves, C. Urbanke, R. Knorr, and E.J. Ungewickell. 2002. Unusual structural organization of the endocytic proteins AP180 and epsin 1. *J Biol Chem*. 277:8209-16.

Kazazic, M., V. Bertelsen, K.W. Pedersen, T.T. Vuong, M.V. Grandal, M.S. Rodland, L.M. Traub, E. Stang, and I.H. Madshus. 2009. Epsin 1 is involved in recruitment of ubiquitinated EGF receptors into clathrin-coated pits. *Traffic*. 10:235-45.

Koshiba, S., T. Kigawa, A. Kikuchi, and S. Yokoyama. 2002. Solution structure of the epsin N-terminal homology (ENTH) domain of human epsin. *J Struct Funct Genomics*. 2:1-8.

Legendre-Guillemin, V., S. Wasiak, N.K. Hussain, A. Angers, and P.S. McPherson. 2004. ENTH/ANTH proteins and clathrin-mediated membrane budding. *J Cell Sci*. 117:9-18.

Morgan, J.R., K. Prasad, W. Hao, G.J. Augustine, and E.M. Lafer. 2000. A conserved clathrin assembly motif essential for synaptic vesicle endocytosis. *J Neurosci*. 20:8667-76.

Owen, D.J., Y. Vallis, M.E. Noble, J.B. Hunter, T.R. Dafforn, P.R. Evans, and H.T. McMahon. 1999. A structural explanation for the binding of multiple ligands by the alpha-adaptin appendage domain. *Cell*. 97:805-15.

CHAPTER 6

SUMMARY AND FUTURE DIRECTION

To support the fast rate of neurotransmission, synaptic vesicles need to be locally recycled and reloaded with neurotransmitters after exocytosis. Clathrin-mediated endocytosis is widely accepted to be involved in this process. Here we investigated its role for synaptic vesicle recycling in *C. elegans*. The basic approach is to disrupt clathrin-mediated endocytosis by knocking out endocytic accessory proteins in the same pathway which, in this thesis, include the major adaptor complex AP2, the synaptotagmin adaptor UNC-41 and a membrane bending protein Epsin.

AP2 is required for synaptic vesicle recycling

AP2 recruits transmembrane cargoes to the endocytic site and nucleates clathrin to initiate growth of the clathrin-coat. In addition, the two big subunits of AP2 can interact with a variety of endocytic accessory proteins, such as other adaptors, membrane-bending proteins and the pinchase, dynamin (Owen et al., 2000; Praefcke et al., 2004). Because of AP2's central role, removal of the medium subunit μ2 in mice (Mitsunari et al., 2005) or the big subunit α in flies (Gonzalez-Gaitan and Jackle, 1997) causes embryonic lethality. However, *C. elegans* are still viable after knocking out either μ2 or α adaptin. The subcellular localization of α adaptin is normal in μ2 adaptin mutants in *C. elegans* (Gu et al., 2008) and the reciprocal experiment gives the same result (Figure 3.4), suggesting

AP2 might still partially function in single adaptin mutants. When these two adaptin mutants are crossed together, worms exhibit a high dead rate, which recapitulates the phenotypes from mice and flies. Based on the crystal structure, μ2 adaptin forms half of the AP2 complex with one of the big subunits β2 and α adaptin forms the other half of the AP2 complex with the small subunit σ2 (Collins et al., 2002b). This suggests that AP2 is required for worm viability. Eliminating the entire AP2 complex requires knocking out at least μ2 and α adaptins simultaneously.

We rescued the adaptin double mutant back to a maintainable strain by introducing the μ2 and α subunits specifically back to the hypodermis. Ultrastructural analysis indicates that the number of synaptic vesicles is reduced by 70% in the skin-rescued double mutants. However their locomotion is fairly normal with just a mild defect in the worm thrashing assay. These results indicate that AP2 is responsible for the majority of synaptic vesicle recycling in *C. elegans*. On the other hand, AP2 independent endocytosis clearly exists. In the absence of α adaptin, synapses accumulate large vesicles that are likely to be endosomal intermediates. Disruption of clathrin-mediated endocytosis via AP2 elimination likely stresses the synapse. It is possible that under these conditions endocytosis at the cell surface leans more heavily on the AP2-independent bulk endocytosis. A recent study suggests that AP1 is involved in generating vesicles from endosomal intermediates (Glyvuk et al., 2010). And from an older point of view, this method of vesicle recycling could also depend on AP3 (Danglot and Galli, 2007). Further studies on the function of AP1 and AP3 in synaptic vesicle endocytosis will improve our understanding of vesicle recycling through endosomal intermediates. Mutants for the μ subunits of each AP complex are currently available in *C. elegans*.

Because AP-dependent endocytosis also requires clathrin, the vesicle-recycling defect observed in a μ1-3 triple mutant would also indicate the role of clathrin in synaptic vesicle recycling.

UNC-41 is the absolute synaptotagmin recruiter in *C. elegans*

In clathrin-mediated endocytosis, different transmembrane cargoes require specific adaptors for recruitment into clathrin-coated pits. However, the mechanism for re-sorting vesicle proteins into clathrin-coated pits is still poorly understood. AP180 is the specific adaptor for synaptobrevin in *C. elegans*. In AP180 mutants, synaptobrevin is not clustered at synaptic varicosities but diffuses throughout the axon (Nonet et al., 1999). The specific adaptor for synaptotagmin is stonin2 in mammals or stoned in *Drosophila* (Fergestad and Broadie, 2001; Jung et al., 2007). The orthologue of stonin2 is encoded by the gene *unc-41* in *C. elegans.* We found that the synaptotagmin binding site on UNC-41 is essential for UNC-41 synaptic localization. In the absence of UNC-41, synaptotagmin I diffuses away from synapses suggesting that in *C. elegans,* the mechanism for recycling synaptotagmin is similar to human and *Drosophila*. However in contrary to the previous StonedB result from *Drosophila* (Fergestad and Broadie, 2001), overexpressing synaptotagmin I can not by pass the requirement of UNC-41, which suggests UNC-41 is absolutely required for maintaining the proper sub-cellular localization of synaptotagmin I. Compared to stonin2 and stoned, UNC-41 is conserved at its C-terminus including the stonin homologous domain and the μ homologous domain. But its N-terminus is quite different and contains the DPF motif for interaction with AP2. Therefore this part of the protein could confer some novel functions.

Epsin is not required for curvature acquisition at synapses

Membrane invagination is one of the critical steps in clathrin-mediated endocytosis. So far, proteins containing N-BAR domains or ENTH domains have been shown to generate membrane curvature (Itoh and De Camilli, 2006). Epsin is one of the well-known ENTH proteins. It is a potential adaptor for ubiquitinated cargoes and can bind clathrin, AP2 and EH domain containing proteins. More importantly, this protein facilitates clathrin coat formation on the invaginated membrane. In vitro, clathrin coated pits are flat in the absence of Epsin (Ford et al., 2002), suggesting Epsin functions at the onset of clathrin-mediated endocytosis. Therefore the absence of Epsin should cause all clathrin-mediated endocytosis to stall at the plasma membrane. In *C. elegans*, the absence of Epsin causes embryonic lethality, suggesting the early requirement of this protein during worm development. However, Epsin shows a low level of neuronal expression and is not expressed at worm synapses, indicating it is not involved in synaptic vesicle recycling. A study from *Drosophila* Epsin illustrates a similar result (Bao et al., 2008). Since clathrin-mediated endocytosis is clearly involved in synaptic vesicle recycling in *C. elegans*, some other membrane bending protein must acquire membrane curvature at synapses. One potential candidate is the N-BAR domain protein, endophilin. In lamprey, blocking endophilin at synapses causes the accumulation of shallow clathrin-coated pits (Andersson et al., 2010). In *C. elegans*, endophilin mutants show a severe synaptic vesicle recycling defect (Schuske et al., 2003). Another candidate is the N-BAR domain protein, amphiphysin. However, it is more likely to function at the end of clathrin-mediated endocytosis by sensing the membrane curvature at the fission neck and recruiting dynamin and actin skeleton for vesicle scission from the plasma membrane

(Dawson et al., 2006). In the future, it will be interesting to do an in vitro assay on liposome tubulation by adding these synaptic enriched BAR domain or ENTH domain proteins. A screen for other BAR domain protein mutants will also be important.

References

Andersson, F., P. Low, and L. Brodin. 2010. Selective perturbation of the BAR domain of endophilin impairs synaptic vesicle endocytosis. *Synapse*. 64:556-60.

Bao, H., N.E. Reist, and B. Zhang. 2008. The Drosophila epsin 1 is required for ubiquitin-dependent synaptic growth and function but not for synaptic vesicle recycling. *Traffic*. 9:2190-205.

Collins, B.M., A.J. McCoy, H.M. Kent, P.R. Evans, and D.J. Owen. 2002. Molecular architecture and functional model of the endocytic AP2 complex. *Cell*. 109:523-535.

Danglot, L., and T. Galli. 2007. What is the function of neuronal AP-3? *Biol Cell*. 99:349-61.

Dawson, J.C., J.A. Legg, and L.M. Machesky. 2006. Bar domain proteins: a role in tubulation, scission and actin assembly in clathrin-mediated endocytosis. *Trends Cell Biol*. 16:493-8.

Fergestad, T., and K. Broadie. 2001. Interaction of stoned and synaptotagmin in synaptic vesicle endocytosis. *J Neurosci*. 21:1218-27.

Ford, M.G., I.G. Mills, B.J. Peter, Y. Vallis, G.J. Praefcke, P.R. Evans, and H.T. McMahon. 2002. Curvature of clathrin-coated pits driven by epsin. *Nature*. 419:361-6.

Glyvuk, N., Y. Tsytsyura, C. Geumann, R. D'Hooge, J. Huve, M. Kratzke, J. Baltes, D. Boening, J. Klingauf, and P. Schu. 2010. AP-1/sigma1B-adaptin mediates endosomal synaptic vesicle recycling, learning and memory. *EMBO J*. 29:1318-30.

Gonzalez-Gaitan, M., and H. Jackle. 1997. Role of Drosophila alpha-adaptin in presynaptic vesicle recycling. *Cell*. 88:767-76.

Gu, M., K. Schuske, S. Watanabe, Q. Liu, P. Baum, G. Garriga, and E.M. Jorgensen. 2008. Mu2 adaptin facilitates but is not essential for synaptic vesicle recycling in Caenorhabditis elegans. *J Cell Biol*. 183:881-92.

Itoh, T., and P. De Camilli. 2006. BAR, F-BAR (EFC) and ENTH/ANTH domains in the

regulation of membrane-cytosol interfaces and membrane curvature. *Biochim Biophys Acta*. 1761:897-912.

Jung, N., M. Wienisch, M. Gu, J.B. Rand, S.L. Muller, G. Krause, E.M. Jorgensen, J. Klingauf, and V. Haucke. 2007. Molecular basis of synaptic vesicle cargo recognition by the endocytic sorting adaptor stonin 2. *J Cell Biol*. 179:1497-510.

Mitsunari, T., F. Nakatsu, N. Shioda, P.E. Love, A. Grinberg, J.S. Bonifacino, and H. Ohno. 2005. Clathrin adaptor AP-2 is essential for early embryonal development. *Mol Cell Biol*. 25:9318-23.

Nonet, M.L., A.M. Holgado, F. Brewer, C.J. Serpe, B.A. Norbeck, J. Holleran, L. Wei, E. Hartwieg, E.M. Jorgensen, and A. Alfonso. 1999. UNC-11, a Caenorhabditis elegans AP180 homologue, regulates the size and protein composition of synaptic vesicles. *Mol Biol Cell*. 10:2343-60.

Owen, D.J., Y. Vallis, B.M. Pearse, H.T. McMahon, and P.R. Evans. 2000. The structure and function of the beta 2-adaptin appendage domain. *EMBO J*. 19:4216-27.

Praefcke, G.J., M.G. Ford, E.M. Schmid, L.E. Olesen, J.L. Gallop, S.Y. Peak-Chew, Y. Vallis, M.M. Babu, I.G. Mills, and H.T. McMahon. 2004. Evolving nature of the AP2 alpha-appendage hub during clathrin-coated vesicle endocytosis. *EMBO J*. 23:4371-83.

Schuske, K.R., J.E. Richmond, D.S. Matthies, W.S. Davis, S. Runz, D.A. Rube, A.M. van der Bliek, and E.M. Jorgensen. 2003. Endophilin is required for synaptic vesicle endocytosis by localizing synaptojanin. *Neuron*. 40:749-62.